(1)

Main Search Page

EXHIBIT D

Results of your search : **from 3 [1 and 2] keep 1-2,4,13,18,27-28,42-43**
Citations available: **9**
Citations displayed: **1-9**

Go to ... Help | Logoff

Citation 1

Authors
Morgan D. Holcomb L. Saad I. Gordon M. Maines M.

Title
IMPAIRED SPATIAL NAVIGATION LEARNING IN TRANSGENIC MICE OVER-EXPRESSING HEME OXYGENASE-L

Source
Brain Research. 808(1):110-112, 1998 Oct 12.

Abstract
Transgenic mice expressing heme oxygenase-1 (HO-1) using the **neuron-specific enolase** promoter were impaired in learning the Morris water maze compared to non**transgenic** littermates. The memory of the HO-1 mice for the location of the platform was similarly impaired when tested using a probe trial after 7 training blocks, but performance on visible platform trials was similar for both groups of mice. Importantly, both HO-1 and non**transgenic** mice had normal sensorimotor function, and performed the same on a Y-maze alternation task, highlighting the **specificity** of memory deficit in the spatial navigation task. These results suggest that carbon monoxide, one product of HO-1 activity, interferes in the development of spatial navigation memory, and may play a role in normal memory function. [References: 10]

Go to ... Help | Logoff

Citation 2

Authors
Chen JS. Kelz MB. Zeng GQ. Sakai N. Steffen C. Shockett PE. Picciotto MR. Duman RS. Nestler EJ.

Title
TRANSGENIC ANIMALS WITH INDUCIBLE, TARGETED GENE EXPRESSION IN BRAIN

Source
Molecular Pharmacology. 54(3):495-503, 1998 Sep.

Abstract
Several inducible gene expression systems have been developed in vitro in recent years to overcome limitations with traditional **transgenic** mice. One of these, the tetracycline-regulated system, has been used successfully in vivo. Nevertheless, concerns remain about the ability of this system to direct high levels of transgene expression in vivo and to enable such expression to be turned on and off effectively. We report here the generation, using a modified tetracycline-regulated system under the control of the **neuron-specific enolase** promoter, of several lines of mice that direct transgene expression to **specific** brain regions, including the striatum, cerebellum CA1 region of the hippocampus, or deep layers of cerebral neocortex. Transgene expression in these mice can be turned off completely with low doses of doxycycline (a tetracycline derivative) and driven to very high levels in the absence of doxycycline. We demonstrate this tissue-**specific**, inducible expression for three transgenes: those that encode luciferase (a reporter protein) or Delta FosB or the cAMP-response element binding protein (CREB) (two transcription factors). The various lines of **transgenic** mice demonstrate an inducible system that generates high levels of transgene expression in **specific** brain regions and represent novel and powerful tools with which to study the functioning of these (or potentially any other) genes in the brain. [References: 37]

Go to ... Help | Logoff

Citation 3

Authors
Offen D. Beart PM. Cheung NS. Pascoe CJ. Hochman A. Gorodin S. Melamed E. Bernard R. Bernard O.

Title
TRANSGENIC MICE EXPRESSING HUMAN BCL-2 IN THEIR NEURONS ARE RESISTANT TO 6-HYDROXYDOPAMINE AND 1-METHYL-4-PHENYL-1,2,3,6-TETRAHYDROPYRIDINE NEUROTOXICITY

Source

Proceedings of the National Academy of Sciences of the United States of America. 95(10):5789-5794, 1998 May 12.

Abstract

The protooncogene bcl-2 inhibits **neuronal** apoptosis during normal brain development as well as that induced by cytotoxic drugs or growth factor deprivation. We have previously demonstrated that **neurons** of mice deficient in Bcl-2 are more susceptible to neurotoxins and that the dopamine (DA) level in the striatum after systemic 1-methyl-4-phenyl-1,2,3,6 tetrahydropyridine (MPTP) administration was significantly lower than in wild-type mice, In the present study we have used **transgenic** mice overexpressing human Bcl-2 under the control of **neuron-specific enolase** promoter (NSE-hbcl-2) to test the effects of the neurotoxins 6-hydroxy-dopamine (6-OHDA) and MPTP on **neuronal** survival in these mice. Primary cultures of neocortical **neurons** from normal and **transgenic** mice were exposed to these dopaminergic neurotoxins, Addition of 6-OHDA resulted in cell death of essentially all **neurons** from normal mice. In contrast, in cultures generated from heterozygous NSE-hbcl-2 **transgenic** mice, only 69% of the cells died while those generated from homozygous **transgenic** mice were highly resistant and exhibited only 34% cell death. A similar effect was observed with **neurons** treated with MPP+. Moreover, while the striatal dopamine level after MPTP injections was reduced by 32% in the wild type, the concentration remained unchanged in the NSE-hbcl-2 heterozygous mice. In contrast levels of glutathione-related enzymes were unchanged. In conclusion, overexpression of Bcl-2 in the **neurons** provided protection, in a dose-dependent manner, against neurotoxins known to selectively damage dopaminergic **neurons**. This study provides ideas for inhibition of **neuronal** cell death in neurodegenerative diseases and for the development of efficient neuroprotective gene therapy. [References: 42]

Go to ... Help | Logoff

Citation 4

Authors

Bosse P. Bernex F. Desepulveda P. Salaun P. Panthier JJ.

Title

MULTIPLE NEUROENDOCRINE TUMOURS IN **TRANSGENIC** MICE INDUCED BY C-KIT-SV40 T ANTIGEN FUSION GENES

Source

Oncogene. 14(22):2661-2670, 1997 Jun 5.

Abstract

Transgenic mice carrying either a 1.008 or a 4.225 kb of the mouse c-kit 5'-flanking sequences linked to the oncogenic large T antigen (TAg) region of the sinian virus 40 (SV40) genome were generated to test if the c-kit promoter could be used to develop useful mouse models. Both constructs promote tumourigenesis in the pituitary and the thyroid with high efficiency. The cell types from which each of these tumours derives were identified. Tumours of the pituitary derive from alpha-MSH-expressing cells located in the intermediate lobe, Transformed cells of the thyroid were calcitonin-positive, implying that the tumours derive from C cells or their precursors, Chromogranin A and **neuron-specific enolase**, general neuroendocrine cell markers, were expressed in both tumour types. Furthermore a variety of tumours appeared in the **transgenic** mice. Several of them stained positively for chromogranin A and/or **neuron-specific enolase**, This suggests a previously unsuspected tissue-**specificity** of the c-kit 5' flanking sequences for neuroendocrine cells. The Kit-TAg **transgenic** mouse Lines may represent a valuable model for the study of the development and the biology of neuroendocrine tumours. [References: 53]

Go to ... Help | Logoff

Citation 5

Authors

Twyman RM. Jones EA.

Title

SEQUENCES IN THE PROXIMAL 5' FLANKING REGION OF THE RAT **NEURON-SPECIFIC ENOLASE** (NSE) GENE ARE SUFFICIENT FOR CELL TYPE-**SPECIFIC** REPORTER GENE EXPRESSION

Source

Journal of Molecular Neuroscience. 8(1):63-73, 1997 Feb.

Abstract

We investigated the regulation of the rat **neuron-specific enolase** gene using a transient transfection approach. Recent **transgenic** mouse studies have shown that a 1.8-kb segment of the rat NSE gene 5' flanking region, including the first (noncoding) exon but not the first intron, is able to drive expression of a reporter gene in parallel with endogenous NSE. These data suggest that cis-acting elements responsible for the spatial and temporal pattern of NSE gene expression are located within the proximal 1.8 kb of the 5' flanking sequence. To further investigate this region, we joined the 1.8-kb regulatory cassette to the cat reporter gene and generated a number of constructs in which the flanking sequence was

progressively deleted from the 5' end. These constructs were tested by transient transfection into **neuronal** and **nonneuronal** cells, followed by an assay for CAT activity. We found that as little as 255 bp of 5' flanking sequence was able to confer cell type-**specificity** on the reporter gene. Further truncation to 120 bp of 5' sequence resulted in a sharp downregulation of reporter activity in PC12 cells but a significant rise in both Neuro-2A neuroblastoma cells and **nonneuronal** Ltk- cells, indicating that cis-acting elements controlling the regulation of NSE in Ltk-, Neuro-2A, and PC12 cells may lie within the 135 bp region covered by this deletion. This region contains an AP-2 site and an element similar in sequence and position to a motif identified in the proximal promoter region of the **neuron-specific** peripherin gene. Reduction to 95 bp of 5' sequence resulted in a slight downregulation of CAT activity in all cell lines tested, and further truncation to 65 bp of 5' sequence caused a universal reduction to background levels of CAT activity, concomitant with the disruption of the basal NSE promoter. Our results show that the 5' flanking region of the NSE gene is capable of conferring cell type-**specificity** on a heterologous gene in transfected cells and that elements responsible for this are located within the proximal 255 bp. [References: 33]

Go to ... Help | Logoff

Citation 6

Authors

Coluccidamato GL. Santelli G. Dalessio A. Chiappetta G. Mineo A. Manzo G. Vecchio G. Defranciscis V.

Title

DBL EXPRESSION DRIVEN BY THE **NEURON SPECIFIC ENOLASE** PROMOTER INDUCES TUMOR FORMATION IN **TRANSGENIC** MICE WITH A P53(+/-) GENETIC BACKGROUND

Source

Biochemical & Biophysical Research Communications. 216(3):762-770, 1995 Nov 22.

Abstract

The dbl oncogene, generated by the truncation of the amino-terminal portion of the proto-oncogene sequence, encodes a guanine-nucleotide-releasing factor. The transforming activity of this oncogene has never been demonstrated in vivo or in vitro except in the NIH 3T3 mouse fibroblast cell line. The expression of the proto-dbl transcript is confined to tissues and tumors of neuroectodermal derivation. Therefore, to study the transforming activity of the dbl oncogene in vivo. we have generated **transgenic** mice that express this oncogene in neuroepithelial tissues. Mice carrying the dbl oncogene did not develop a tumor. Successively, to establish whether dbl interacts with the tumor suppressor gene p53 in tumorigenesis, we have used a p53 deficient mouse strain. The results reported here indicate that dbl is capable of causing tumor formation in vivo when its expression is driven in an appropriate cellular and genetic environment. (C) 1995 Academic Press, Inc. [References: 19]

Go to ... Help | Logoff

Citation 7

Authors

Race RE. Priola SA. Bessen RA. Ernst D. Dockter J. Rall GF. Mucke L. Chesebro B. Oldstone MBA.

Title

NEURON-SPECIFIC EXPRESSION OF A HAMSTER PRION PROTEIN MINIGENE IN **TRANSGENIC** MICE INDUCES SUSCEPTIBILITY TO HAMSTER SCRAPIE AGENT

Source

Neuron. 15(5):1183-1191, 1995 Nov.

Abstract

To study the effect of cell type-restricted hamster PrP expression on susceptibility to the hamster scrapie agent, we generated **transgenic** mice using al kb hamster cDNA clone containing the 0.76 kb HPrP open reading frame under control of the **neuron-specific enolase** promoter. In these mice, expression of HPrP was detected only in brain tissue, with highest levels found in **neurons** of the cerebellum, hippocampus, thalamus, and cerebral cortex. These **transgenic** mice were susceptible to infection by the 263K strain of hamster scrapie with an average incubation period of 93 days, compared to 72 days in normal hamsters. In contrast, non**transgenic** mice were not susceptible to this agent. These results indicate that **neuron-specific** expression of the 1 kb HPrP minigene including the HPrP open-reading frame is sufficient to mediate susceptibility to hamster scrapie, and that HPrP expression in non**neuronal** brain cells is not necessary to overcome the TSE species barrier. [References: 61]

Go to ... Help | Logoff

Citation 8

Authors

Alouani S. Ketchum S. Rambosson C. Eistetter HR.

Title

TRANSCRIPTIONAL ACTIVITY OF THE
NEURON-SPECIFIC ENOLASE
(NSE) PROMOTER IN MURINE EMBRYONIC STEM (ES) CELLS AND PREIMPLANTATION EMBRYOS

Source

European Journal of Cell Biology. 62(2):324-332, 1993 Dec.

Abstract

Mouse embryonic stem (ES) cells were transfected with a plasmid composed of an E. coli lacZ gene fused to 1.8 kb of rat **neuron-specific enolase** (NSE) promoter sequences. While this reporter construct had been shown previously to function exclusively in postmitotic **neurons** and neuro-endocrine cells of **transgenic** mice, stably transfected ES cell clones unexpectedly displayed beta-galactosidase (beta-Gal) activity in the undifferentiated state. This transcriptional activity of the heterologous NSE promoter was confirmed by the identification of endogenous NSE mRNA in undifferentiated ES cells, mouse morulae and blastocysts. NSE protein, however, could not be found in undifferentiated ES cells. Interestingly, in ES cells which were cultured for 7 days under differentiation conditions in vitro, beta-Gal activity decreased to basal levels consistent with the parallel down-regulation of endogenous NSE mRNA. In contrast, prolonged culture of ES cells under differentiation conditions led to the reappearance of NSE mRNA and beta-Gal activity after 17 days. Significant increases in beta-Gal activity were also observed in ES cells which were cultured either on dishes coated with attachment factors such as laminin and gelatin or in the presence of nerve growth factor (NGF). These results suggest that i) transcriptional control mechanisms regulating **neuron**al gene expression are present at early developmental stages in the mouse and ii) ES cells provide a useful in vitro model system for the analysis of developmentally regulated cellular and molecular events coupled to **neuron-specific enolase** promoter activity. [References: 42]

Go to ... Help | Logoff

Citation 9

Authors

Andersen JK. Frim DM. Isacson O. Breakefield XO.

Title

HERPESVIRUS-MEDIATED GENE DELIVERY INTO THE RAT BRAIN -
SPECIFICITY AND EFFICIENCY OF THE
NEURON-SPECIFIC ENOLASE
PROMOTER

Source

Cellular & Molecular Neurobiology. 13(5):503-515, 1993 Oct.

Abstract

1. Herpesvirus infection with genetically engineered vectors is a way to deliver foreign gene products to various cell populations in culture and in vivo. Selective **neuron**al gene expression can be achieved using the **neuron-specific enolase** (NSE) promoter regulating expression of a transgene placed in and delivered by a herpesvirus vector. 2. We sought to determine the anatomical **specificity** and efficiency of herpesvirus-mediated gene transfer into the rat brain following placement of virus particles carrying a transgene (lacZ) under control of the NSE promoter. The virus utilized was thymidine kinase (TK) deficient and therefore replication deficient in the brain. 3. Infusion of 10(6) plaque-forming units of virus into the striatum caused a limited number of striatal **neurons** to express the lacZ transgene mRNA and protein product 7 days postinfection. In addition, small numbers of **neurons** expressing the transgene mRNA and protein were found ipsilateral to the viral injection in the frontal cortex, substantia nigra pars compacta, and thalamus. **Neurons** at these anatomic loci project directly to the striatal injection site. No other cells within the brains of injected animals expressed the lacZ gene. 4. While this herpesvirus NSE vector was capable of introducing novel functional genetic information into postmitotic **neurons** within defined neuroanatomic constraints, the numbers of **neurons** expressing detectable levels of beta-galactosidase was minimal. The calculated efficiency of delivery and transgene expression at 7 days postinfection was 1 **transgenic neuron** per 10(4) virus particles infused. 5. We conclude that NSE probably is not an optimal promoter for use in gene delivery to CNS **neurons** in herpesvirus vectors and that the efficacy of gene delivery using other **neuron-specific** promoters placed at various sites in the herpes viral genome needs to be explored. [References: 47]

Main Search Page

Obesity, diabetes, and neoplasia in yellow A^{vy}/- mice: ectopic expression of the *agouti* gene

TERENCE T. YEN*,[1] ANNE M. GILL*, LUCIANO G. FRIGERI,[†] GREGORY S. BARSH,[‡] AND GEORGE L. WOLFF[§,2]

*Lilly Research Laboratories, Eli Lilly & Co., Lilly Corporate Center, Indianapolis, Indiana 46285, USA; [†]Department of Molecular and Experimental Medicine, Scripps Research Institute, La Jolla, California 92037, USA; [‡]Department of Pediatrics and Howard Hughes Medical Institute, Stanford University School of Medicine, Stanford, California 94305-5428, USA; [§]Division of Nutritional Toxicology, National Center for Toxicological Research, Food and Drug Administration, U.S. Department of Health and Human Services, Jefferson, Arkansas 72079-9590, USA; and Departments of Biochemistry/Molecular Biology and Pharmacology/Toxicology, University of Arkansas for Medical Sciences, Little Rock, Arkansas 72205, USA

ABSTRACT The *viable yellow* A^{vy} mutation results in a mottled yellow mouse that is obese, slightly larger than its nonyellow sibs, and more susceptible to tumor formation in those tissues sensitized by the strain genome. The mutation exhibits variable expressivity resulting in a continuum of coat color phenotypes, from clear yellow to pseudoagouti. The mouse *agouti* protein is a paracrine signaling molecule that induces hair follicle melanocytes to switch from the synthesis of black pigment to yellow pigment. Molecular cloning studies indicate that the obesity and growth effects of the A^{vy} mutation result from ectopic expression of the normal *agouti* gene product. This review seeks to summarize the current state of knowledge regarding the obesity, stimulation of somatic growth, and enhancement of tumor formation caused by the A^{vy} mutation, and to interpret these pleiotropic effects in terms of the normal function of the *agouti* protein.—Yen, T. T., Gill, A. M., Frigeri, L. G., Barsh, G. S., and Wolff, G. L. Obesity, diabetes, and neoplasia in yellow A^{vy}/- mice: ectopic expression of the *agouti* gene. *FASEB J.* 8: 479-488; 1994.

Key Words: obesity · diabetes · neoplasia · yellow mouse · agouti locus

HISTORY OF THE A^{vy} MUTATION AT THE *AGOUTI* LOCUS IN THE MOUSE

The *viable yellow* (A^{vy}) mutation arose spontaneously in 1960 from the agouti (A) allele at the *agouti* locus in the C3H/HeJ strain (1). The *agouti* locus is located between loci *Hck-1* (hematopoietic cell kinase-1) and *Src-1* (Rous sarcoma virus proto-oncogene) in a section of mouse chromosome 2 that contains many mouse genes that have homologs (conserved synteny) on human chromosome 20q.

This locus determines the relative amounts of black (eumelanin) and yellow (phaeomelanin) pigment in the hairs. The species-type hair color pattern, "agouti," is common among mammals and is characterized by a subapical yellow band in black or brown hair; in mice heterozygous or homozygous for A^{vy} (hereafter A^{vy}/-), there is usually an excess of yellow pigment (see below). A^{vy} is one of four dominant *agouti* mutations associated with pleiotropic effects, the most prominent of which are obesity and increased somatic growth. In addition, A^{vy} and at least one other obesity-associated *agouti* allele, *lethal yellow* (A^{y}), are associated with increased susceptibility to diabetes (2) and to endogenously and exogenously induced hyperplasia, preneoplastic lesions, and neoplasms (3).

Most data reviewed here have been obtained with yellow VY/Wf-A^{vy}/*a* mice, in which case black *a/a* littermates served as non-A^{vy} controls. Alternatively, F_1 hybrids from matings of VY/Wf-A^{vy}/*a* mice with mice of another inbred strain, e.g., BALB/c-*A/A*, produce A^{vy}/*A* and agouti (*A/a*) mice, the latter serving as the non-A^{vy} controls.

The VY/Wf strain was developed at The Institute for Cancer Research, Philadelphia, from A^{vy}/*a* males and females of the first and third generations of backcrossing of C3H/HeJ- A^{vy} onto C57BL/6J and were obtained from The Jackson Laboratory, Bar Harbor, Maine, in 1962; thus, the strain includes 6.25%–25% C3H/HeJ genome and 75%–93.75% C57BL/6J genome. Breeding stock of the VY/Wf strain was provided to one of us (T.T.Y.) at Eli Lilly & Co., Inc. in 1970, rederived by cesarean section in 1985, and maintained as strain VY/WfL. Strain VY/Wf was brought to the National Center for Toxicological Research by G.L.W. in 1972. Litters were derived by cesarean section and fostered on C3H-MTV$^-$ dams in the NCTR breeding colony in 1977. The resulting VY/WffC3Hf/Nctr- A^{vy} strain is maintained in a SPF barrier-sustained environment.

THE *AGOUTI* GENE AND ITS ACTION

The *agouti* gene has recently been cloned (4, 5). It is normally expressed in the skin, the testes, and during embryonic development. The encoded protein is 131 amino acids in length and consists of a signal sequence, a central region that is highly basic, and a cysteine-rich carboxyl terminus. Multiple isoforms differ by the nature of their promoters and associated 5' untranslated exons and range in size from 697 nucleotides (nt)[3] to 792 nt, not including the polyA tail (Fig. 1*A*, Fig. 1*B*) (6).

---

[1]Present address: Department of Biochemistry and Molecular Biology, Indiana University School of Medicine, Indianapolis, IN 46202-5122, USA.

[2]To whom correspondence should be addressed, at: National Center for Toxicological Research, 3900 NCTR Rd., Jefferson, AR 72079, USA.

[3]Abbreviations: α-MSH, α-melanocyte stimulating hormone; IAP, intracisternal A particle; HF, high fat; HS, high sucrose; GTT, glucose tolerance test; MNNG, N-methyl-N'-nitro-N-nitrosoguanidine; nt, nucleotides.

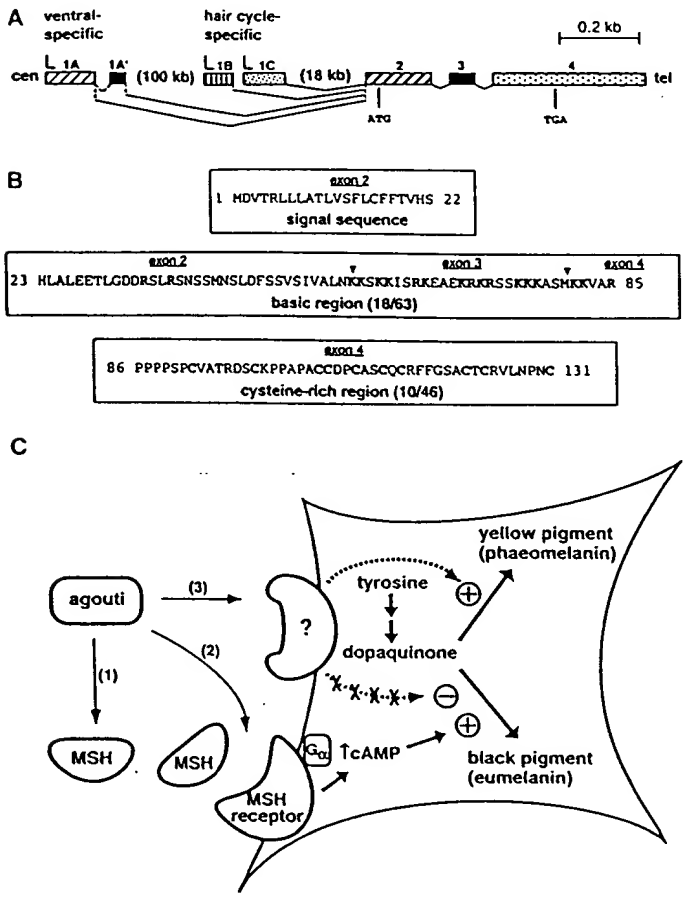

Figure 1. *Agouti* gene structure and action. *A)* Exon and intron structure reveal that the protein coding sequence is contained within exons 2, 3, and 4. Multiple isoforms of *agouti* mRNA differ in their 5' untranslated region and result from the use of different promoters and/or alternative splicing (6). A ventral-specific promoter results in isoforms that contain exon 1A or exons 1A and 1A', whereas a hair cycle-specific promoter results in isoforms that contain exon 1B or 1C. *B)* The amino acid sequence of the *agouti* protein contains a signal sequence, an amino-terminal basic domain with a high proportion of arginine and lysine residues, and a cysteine-rich carboxyl terminus. *C)* Possible mechanisms for *agouti* gene action, based on a secreted protein with a limited radius of action. Because the actions of α-MSH oppose and override those of *agouti* resulting in the synthesis of black pigment, the *agouti* protein may act by reducing the amount of active α-MSH available to the melanocyte; by interfering with activation of the melanocortin receptor; or by binding to its own receptor leading to an intracellular block to melanocortin receptor activation.

The *agouti* protein induces melanocytes within hair follicles to switch from synthesis of eumelanin (black pigment) granules to synthesis of phaeomelanin (yellow) granules, which become incorporated into a growing hair. A series of elegant transplantation studies (7; reviewed in ref 8) indicated that the gene product is produced by nonpigment cells and acts in a paracrine fashion, as it does not affect melanocytes in adjacent follicles or melanocytes in the interfollicular epidermis. These observations are consistent with recent studies which demonstrate that *agouti* expression within the hair follicle occurs only during the time of yellow pigment synthesis (4, 5). Although *agouti* RNA is also expressed in the testes and during embryonic development (6), there is no known function for the gene in these tissues; even null mutations in *agouti* have detectable effects only on coat color (4, 9).

The mechanism by which the *agouti* protein alters the function of melanocytes is not yet clear, although there are two different hypotheses (Fig. 1*C*) based on the opposing interactions between *agouti* and the 13 amino acid peptide α-melanocyte stimulating hormone (α-MSH). α-MSH causes melanocytes to switch from the synthesis of phaeomelanin to eumelanin (10), an effect that is mediated through a G_s-coupled seven transmembrane domain receptor that has recently been cloned (11). The α-MSH receptor on melanocytes is encoded by the *extension* (*E*) locus (12), and appears to be one member of a family of melanocortin receptors that also includes the ACTH receptor and at least two additional receptors expressed in the central nervous system (12–14). As expected, introduction of the α-MSH receptor into heterologous cells results in the stimulation of adenylate cyclase (11, 12). Exogenous α-MSH or exogenous dibutyryl-cAMP can override the effects of local agouti protein production (15), whereas loss-of-function mutations in the α-MSH receptor (*e*) result in the production of phaeomelanin regardless of the level of *agouti* expression (13, reviewed in ref 7). Therefore, it is possible that the *agouti* protein acts as an antagonist of the receptor to prevent α-MSH-induced stimulation of adenylate cyclase (16). Lack of a functional α-MSH receptor in *e/e* mice (13) failed to prevent A^y-induced obesity (17), indicating that this receptor is not required for *agouti*-associated obesity. Development of obesity in yellow mice is also independent of yellow pigment synthesis as demonstrated by complete inhibition of the latter by a gain-of-function mutation [*somber* (E^{so})] at the *extension* locus; totally black $A^y/a^c/E^{so}/E^+$ mice still become obese (18).

A second hypothesis proposes that *agouti* protein binds to its own receptor and interferes with the action of α-MSH at an intracellular level (19). A putative *agouti* receptor might couple to another G protein that inhibits adenylate cyclase, or affects other intracellular messengers such as calcium or phosphoinositol. Distinguishing between these two hypotheses for *agouti* gene action has important implications for understanding the molecular pathogenesis of A^{vy}-induced obesity and increased tumor susceptibility.

THE A^{vy} PHENOTYPE

Obese yellow $A^{vy}/-$ mice can be identified visually as early as 2–3 days after birth and, in contrast to mice homozygous for the recessive obesity mutations *ob* and *db*, have somewhat heavier muscles and longer bones than their non-A^{vy} sibs (reviewed in ref 20). No phenotypic differences between A^{vy}/a and A^{vy}/A^{vy} mice have been described.

Mottled $A^{vy}/-$ mice exhibit variegation with agouti and black patches or continuous and discontinuous transverse stripes on a yellow background. The pattern of transverse stripes is similar to that observed in animals that are mosaic or chimeric for a coat color mutation whose effects are mediated via the dermis (21). This suggests that A^{vy}-associated expression of *agouti* is unstable during early embryonic development, but stabilizes and is clonally propagated before the allocation of progenitor cells to dermal segments.

In general, effects of A^{vy} on nonpigment cells vary more or less concordantly with the coat color phenotype. Thus, yellow mice are obese and hyperinsulinemic, whereas pseudoagouti mice are lean and normoinsulinemic; however, the relative proportions of yellow pigment in mice with different degrees of mottling are *not* correlated with body weight. Even a small yellow area on an otherwise completely "pseudoagouti" mouse is often sufficient to predict that the animal likely will become obese and hyperinsulinemic, and thus will

not fit the definition of pseudoagouti (G. L. Wolff, unpublished observations).

MOLECULAR BASIS OF THE A^{vy} MUTATION

Northern analyses of tissues from adult yellow A^{vy}/a mice, using an *agouti* cDNA as probe, demonstrate expression of an RNA indistinguishable in size from the normal *agouti* RNAs, but in every tissue of the body rather than just in the skin and testes. This RNA is not detectable by Northern analysis in tissues of pseudoagouti A^{vy}/a mice (Fig. 2).

One of the most interesting aspects of A^{vy} is its variable expressivity with regard to coat color pattern, which is strongly influenced by the strain genome of the mother and by her *agouti* locus phenotype (22). Corresponding to the proportions of hair follicle melanocytes in which the *agouti* gene is expressed, $A^{vy}/-$ animals may be completely yellow (highest proportion), mottled (intermediate proportion), or pseudoagouti (lowest proportion). The phenotype of pseudoagouti animals is similar, but not identical, to the nonmutant agouti phenotype; rather than a subapical yellow band, individual hairs may exhibit a disordered arrangement of yellow pigment throughout the entire hair (23).

Molecular cloning studies indicate that the A^{vy}-specific RNA is chimeric, with a foreign 5' sequence derived from an intracisternal A particle (IAP) element (H. Vrieling, D. M. J. Duhl, K. A. Miller, G. T. Wolff, and G. S. Barsh, unpublished results). The 5' sequence is not translated, and is spliced to exons 2, 3, and 4 of the normal *agouti* gene (H. Vrieling et al., unpublished results). Thus, the A^{vy}-specific RNA encodes a normal *agouti* protein expressed in nearly every tissue of the body. These findings explain several genetic and biologic observations regarding A^{vy}.

The variable expressivity of A^{vy} can be explained most easily by epigenetic inactivation of regulatory sequences within the IAP, as germline reversion to A has not been observed. The variegation observed in mottled $A^{vy}/-$ mice indicates that gene inactivation occurs stochastically among precursor cells during embryonic development before hair follicle clones are laid down; after this time it is clonally inherited. This type of clonal inheritance might be maintained either by DNA methylation or by changes in chromatin conformation. Genetic studies (22) suggest that factors that influence A^{vy} gene inactivation depend on both strain background and parental origin.

The pseudoagouti phenotype is most easily explained by early inactivation of IAP regulatory sequences in every cell of the embryo, followed by partial reactivation in a small proportion of cells. An alternative explanation that the pseudoagouti phenotype represents inactivation in most, but not all, cells of the animal seems less likely given that pseudoagouti mice exhibit a fine-grained mosaicism rather than a single yellow stripe on an otherwise agouti animal.

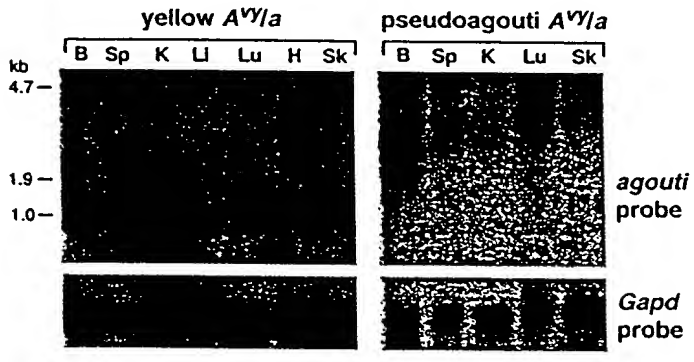

Figure 2. Molecular abnormalities in the A^{vy} mutation. Northern hybridization analysis of *agouti* expression in different tissues of adult yellow and pseudoagouti A^{vy}/a mice. Total RNA (30 μg) was isolated from brain (B), spleen (Sp), kidney (K), liver (Li), lung (Lu), heart (H), or skin (Sk) of yellow or pseudoagouti A^{vy}/a mice, fractionated on a formaldehyde-agarose gel, and transferred to a nylon membrane. The blot was hybridized with a probe that contained agouti coding sequences, stripped, and then rehybridized with a probe for the glyceraldehyde 3-phosphate dehydrogenase (Gapd) gene to control for amount of RNA present. Normally, *agouti* RNA is expressed only in the skin and the testes. Although there is no RNA detectable in pseudoagouti animals, their phenotype suggests a fine-grained mosaicism of *agouti* gene expression (see text).

THE OBESE-DIABETIC SYNDROME IN THE YELLOW $A^{vy}/-$ MOUSE

Obesity and diabetes are serious health hazards, not only by themselves, but also especially as risk factors for cardiovascular and respiratory diseases (24). In the U.S. 80% of type II diabetics are obese and about 20% of obese individuals are diabetic (25). Genetic rodent models of obesity and/or diabetes are important tools for elucidating the pathophysiology of these conditions and for testing new therapeutic approaches (26). The abnormalities in yellow $A^{vy}/-$ mice are markedly different from those caused by the recessive mouse obesity mutations *ob* (obese) and *db* (diabetes) and are reviewed in some detail.

Parabiosis of strain YS/Wf (27) yellow A^{y}/a with black *a/a* littermates of the same sex between 4 and 28 weeks of age failed to affect the body weight or fat content of either partner (28). These data indicate that the *agouti* protein does not circulate, at least not in sufficient quantity to induce obesity. This is in accord with the autocrine/paracrine mode of action of the *agouti* protein as suggested by its effects on hair follicle melanocytes and on cultured cells.

In contrast, parabiosis of fat *db/db* with lean nonmutant mice caused the lean partner to lose weight, become hypoglycemic, and die within 50 days of the surgery (29). When *ob/ob* mice were parabiosed with *db/db* partners, the *ob/ob* mice became hypoglycemic, lost weight, and died of starvation. Parabiosis of *ob/ob* with lean nonmutant mice decreased the food intake and slowed the weight gain of the *ob/ob* partners compared with these parameters in *ob/ob:ob/ob* parabionts (30). These results are interpreted as indicating that *ob/ob* mice are unable to produce enough of a postulated circulating satiety factor to regulate their food intake, whereas *db/db* mice produce sufficient satiety factor but cannot respond to it because of a defective satiety center.

In yellow A^{vy}/a or A^{y}/a mice, plasma corticosterone levels are not elevated above those in their nonyellow sibs, and adrenalectomy does not prevent development of obesity (reviewed in ref 3). In contrast, plasma corticosterone levels in *ob/ob* and *db/db* mice are elevated compared with their lean littermates (reviewed in ref 3).

Neither thyrotrophin, growth hormone, nor prolactin is involved in the development of obesity in either yellow or obese mice as the absence of these hormones in yellow dwarf (A^{y}/a *dw/dw*) mice and obese dwarf (*ob/ob dw/dw*) mice

failed to prevent adiposity (reviewed in ref 3). Indeed, the effects of the *agouti* protein in increasing lean body mass, as well as fat deposition, are still expressed in yellow hypophysectomized mice, even though to a lesser degree than in sham-operated mice (31, 32).

Hyperphagia

Yellow A^{vy}/- mice eat 10–36% more than their non-A^{vy} sibs, depending on genetic strain background (33–36). However, as in other genetic obesities in rodents, the degree of hyperphagia alone does not account for the fourfold increase of carcass triglyceride content of yellow A^{vy}/a mice (26%) compared with *a/a* controls (6%) (33). The results of the diet restriction experiment (34) discussed in a later section suggest that increased efficiency of calorie utilization also plays a role in the development of obesity. This was confirmed by measurements demonstrating a threefold greater efficiency in female yellow A^{vy}/A than in female agouti *A/a* (BALB/c × VY)F1 hybrid mice (35).

The effects of A^{vy} on body weight are apparent in mice fed a standard diet (4–6% fat), one with 10% fat (HF), and one with a high proportion of sucrose (HS). However, the effects of A^{vy} on insulin resistance and glucose metabolism are more pronounced with the HF and HS diets.

Both the HF and HS diets were more diabetogenic in female A^{vy}/A mice, as measured by an impaired glucose tolerance test (GTT), than the control diet. GTT impairment in A^{vy}/A mice was detected after 3 weeks of feeding; in contrast, the GTT of female *A/a* control mice was minimally affected (35).

Although hyperphagia in yellow A^{vy}/- mice is not necessary or sufficient to account for obesity, an intriguing observation, regarding a possible cause of hyperphagia is based on the effects of α-MSH compared with desacetyl-α-MSH. Bray et al. (36) found that the pituitary of yellow A^{vy}/a mice had a reduced α-MSH:desacetyl-α-MSH ratio. Because desacetylated α-MSH was more potent than α-MSH in stimulating food intake (37), reduced acetylation of α-MSH may play a role in A^{vy}-associated hyperphagia. Studies of adrenalectomized yellow mice showed that the effects of MSH peptides on food intake, weight gain, and fat storage were independent of, but interacted with, the effects of corticosterone (38). It will be interesting to determine whether desacetyl-α-MSH has an altered affinity for melanocortin receptors that may be involved in eating behavior.

Carcass triglyceride content

At 6 to 10 weeks of age, yellow A^{vy}/- mice exhibited twice the amount of carcass triglycerides per unit body weight compared with non-A^{vy} controls (33). By 5 months of age when their weights began to plateau, the carcass triglyceride content in yellow A^{vy}/a mice was about 26% of the body weight, 4.4-fold the amount compared with black *a/a* controls (33).

These observations are in contrast to C57BL/6J-*ob/ob* and C57BL/KsJ-*db/db* mice, which have a greater degree of obesity and an earlier onset. At 5 weeks of age, *db/db* and *ob/ob* mice already exhibited carcass triglyceride contents 3- and 4.5-fold those of their corresponding lean controls, and plateaued with triglyceride contents of 42% and 52%, respectively (33). These observations, in combination with morphometric data on adipocytes (39), led to the proposal that obesity of yellow A^{vy}/a mice is mostly hypertrophic, whereas the obesities of *ob/ob* and *db/db* mice are mostly hyperplastic (33).

Lipogenesis and lipolysis

One reason for the difference in the development of obesity between A^{vy}/a mice and *ob/ob* or *db/db* mice is the rate of hepatic lipogenesis (33). Although the lipogenic rate of A^{vy}/a mice was twice that of age-matched young black *a/a* mice and sixfold that of age-matched adult black *a/a* mice, the rates of A^{vy}/a mice were much lower at either age than those of *ob/ob* and *db/db* mice at corresponding ages (33). This may explain why yellow mice were more sensitive than *ob/ob* and *db/db* mice to antiobesity agents such as LY79771 (40). When treated with LY79771, body weights of yellow mice decreased, whereas those of *ob/ob* and *db/db* mice plateaued but were not reduced.

Regardless of its mechanism, an antiobesity agent perturbs the balance between energy intake and energy output until a new balance is established. In *ob/ob* and *db/db* mice and fatty *fa/fa* rats, antiobesity compounds arrest the development of obesity, but the very high hepatic lipogenic rate maintains the existing obesity and, hence, high body weight. In yellow mice, the hepatic lipogenic rate is higher than normal. However, in contrast to the rate in *ob/ob* and *db/db* mice and fatty *fa/fa* rats, it is not high enough to maintain the obesity during administration of LY79771, and thus drug treatment results in weight loss.

The sensitivity of yellow mice to antiobesity compounds is not restricted to β-agonists such as LY79771 and LY104119 (34). Other antiobesity compounds such as fluoxetine (41), a serotonin reuptake inhibitor that suppresses appetite, and ephedrine (42), which both suppresses appetite and stimulates thermogenesis, also reduced the body weight of yellow mice.

With regard to lipolysis, studies of isolated adipose tissue in vitro indicated that the basal lipolytic rate of adipose tissue from yellow A^{vy}/a mice was about half that of *a/a* mice (43), possibly due to the difference in the density of adipocytes as a function of different adipocyte size (39). Therefore, the response to lipolytic agents between yellow and black mice was normalized according to the respective basal rates. Measured by the release of free fatty acid and glycerol, the response of A^{vy}/a adipose tissue to epinephrine (43), theophylline (43), and the β agonists LY79771 (44) and LY104119 (34) was lower than normal. However, the response of A^{vy}/a adipose tissue to dibutyryl cyclic AMP was normal (43).

These observations suggest that yellow A^{vy}/a mice have a defect in the signaling mechanisms responsible for generating and/or maintaining intracellular cyclic AMP in adipocytes. This was confirmed by measuring total cyclic AMP concentrations in the adipose tissue and incubation medium in the presence of LY79771 (44) and LY104119 (34). This signaling deficiency in adipose tissue provides a striking parallel to the effect of *agouti* in pigment cells. Although the cyclic AMP-coupled lipolytic defect is a contributing factor to the obesity of yellow A^{vy}/a mice, it may not result from the direct action of the mutation as it is also present in obese *ob/ob* and *db/db* mice (45) and in obese A^{y}/a mice (43).

Thermogenesis

An important determinant of energy balance and regulation of body weight is nonshivering thermogenesis, which occurs in brown adipose tissue under the control of the sympathetic nervous system (46). The accumulation of tissue dopamine resulting from the inhibition of dopamine β-hydroxylase by 1-cyclohexyl-2-mercaptoimidazole is one method of measuring sympathetic tone that reflects the relative level of nonshivering thermogenesis (47).

Normally, heart, liver, and interscapular brown adipose tissue exhibit a marked diurnal rhythm of dopamine accumulation, reaching a peak just before the initiation of the light cycle. In A^{vy}/a mice this rhythm was dampened in the liver and brown adipose tissue but not in the heart (48). Concordantly, whole body thermogenesis of yellow A^{vy}/a mice, measured with a gradient layer calorimeter, was about 75% that of *a/a* mice (34). As in the case of lipogenesis and lipolysis, changes in thermogenesis are also present in rodent obesity caused by other single gene mutations (46).

When yellow A^{vy}/a mice were forced to lose weight by restricting food intake to 80% of the ad libitum level, whole body thermogenesis decreased, presumably as a compensatory mechanism (34). Subsequently, thermogenesis increased to its preweight loss rate, but no further weight loss ensued. However, a subsequent 20% diet restriction (64% of ad libitum) caused further weight loss, but no change in thermogenesis, before the weight stabilized for the second time. These observations suggest that the change in thermogenesis is insufficient to account for the changes in body weight, and instead suggest that alterations in fuel efficiency account for the observed regulation of body weight.

It seems likely that fuel efficiency increased after the first weight loss experience and thus the same level of thermogenesis was maintained in spite of lower energy intake. Regulation, leading to increased fuel efficiency, could occur by a variety of different mechanisms and may be integrated by the hypothalamus (49). The fact that yellow mice are able to stabilize their weights at different levels of energy intake indicates that their hypothalamic control of energy homeostasis is intact but the set point for the equilibrium is high.

The reduced thermogenesis could be corrected by β-agonists such as LY79771 (50) and LY104119 (34). This, together with the ability of these compounds to stimulate lipolysis in these mice (34, 44, 50), resulted in weight loss.

Hyperinsulinemia and pancreatic islet hyperplasia and hypertrophy

Unlike *db/db* mice that are hyperinsulinemic at 10 days of age (51) and *ob/ob* mice in which hyperinsulinemia is detectable by 4 weeks of age (52), A^{vy}/A (BALB/c × VY)F_1 mice did not become hyperinsulinemic until about 6 weeks of age (53) and exhibited a sexual dimorphism in this characteristic as well as in the degree of hyperglycemia. By 2 months of age, plasma insulin concentrations in female yellow A^{vy}/a mice were 4-fold those of controls, whereas those in comparable male mice were 10-fold those of *a/a* control mice (2). By the time the obesity of A^{vy}/a mice peaked at 6 months of age, both male and female mice had plasma insulin levels more than 20-fold those of male and female black *a/a* mice, with female A^{vy}/a mice usually having the highest concentrations (2, 54).

Plasma insulin data from strain VY/WfL yellow A^{vy}/a and black *a/a* mice younger than 5 weeks of age are not available. However, longitudinal studies of pancreatic insulin and glucagon contents and pancreatic islet morphometrics have been performed in two separate experiments. In one study, pancreatic islets of strain VY/WfL male and female A^{vy}/a and *a/a* mice were measured and counted at 21 days and at 3, 6, and 12 months of age (T. T. Yen and G. Williams, unpublished data). No hyperplasia or hypertrophy of islets was observed in either male or female yellow mice at 21 days, but both were present at 3 months. In another study, the number of β cells was higher in male A^{vy}/A (BALB/c × VY)F1 hybrid mice than in male *A/a* mice at 21 days of age; however, neither the insulin or glucagon contents per unit weight of pancreas nor the mean total islet areas differed between A^{vy}/A and *A/a* mice (55). These data suggest that morphological changes precede biochemical changes in pancreatic islets.

A gender difference existed in islet size. At 6 months of age, the mean islet size of female *a/a* mice was 10-fold that of comparable male mice (2). Regardless of the gender difference, 6-month-old male and female A^{vy}/a mice had islet sizes approximately twice as large as the corresponding *a/a* mice (T. T. Yen and G. Williams, unpublished data). Although quantitative mouse to mouse correlations are not available, it appears that female A^{vy}/a mice are more hyperinsulinemic and have a higher degree of islet hyperplasia and hypertrophy than male A^{vy}/a mice.

Hyperinsulinemia and lipogenesis

To define the temporal interactions among obesity, hyperinsulinemia, and the activities of six hepatic lipogenic enzymes (glucose-6-phosphate dehydrogenase, 6-phosphogluconate dehydrogenase, malic enzyme, citrate cleavage enzyme, acetyl CoA carboxylase, fatty acid synthetase), a developmental study was conducted in A^{vy}/a and *a/a* mice at 2, 3, 5, and 8 months of age (56). Yellow $A^{vy}/-$ mice are especially suitable for dissecting the temporal relationships among these parameters because their obesity develops relatively slowly.

In yellow mice, the specific activity of malic enzyme correlated positively with body weight, liver weight, plasma insulin level, and age. The specific activities of citrate cleavage enzyme and 6-phosphogluconate dehydrogenase correlated positively with age, body weight, and liver weight. However, when adjusted for insulin level, correlations between other parameters disappeared, indicating that elevated plasma insulin level was a common factor that correlated with the increase of body and liver weight and with specific activities of malic enzyme and citrate cleavage enzyme. Correlation does not prove that hyperinsulinism is the cause of obesity in yellow $A^{vy}/-$ mice, but does suggest that it plays a central role in its development.

Hyperglycemia

Although obesity poses an increased risk for diabetes, not all obese people develop diabetes and not all diabetics are obese (25). This suggests that development of obesity and diabetes can be influenced by independent factors (57). Many obese human subjects exhibit only impaired glucose tolerance (58) and do not progress to a diabetic state (59) because both insulin resistance and β cell defects are required to precipitate type II diabetes (60). This is also true for the genetic rodent obesities (61), including A^{vy} (2). Yellow $A^{vy}/-$ mice exhibit hyperinsulinism and insulin resistance, but the development of overt hyperglycemia depends on physiological factors that differ with strain background, gender, and diet.

A case in point is that male and female yellow A^{vy}/a mice with identical strain background are obese, hyperinsulinemic, insulin resistant, and glucose intolerant; however, only the males are hyperglycemic. Most female yellow mice are normoglycemic or, if their blood glucose levels are elevated, the elevation is slight. Administration of dexamethasone induces hyperglycemia in female yellow mice (62), reminiscent of the diabetogenic effects of glucocorticoids in humans (63). It can be reversed by ciglitazone, a compound that improves insulin sensitivity (62). The induction of hyperglycemia in female A^{vy}/a mice is concomitant with the induction of hepatic estrone sulfotransferase (64), an enzyme that inactivates estrogens, supporting the hypothesis that estrogens confer protection against the development of diabetes (61).

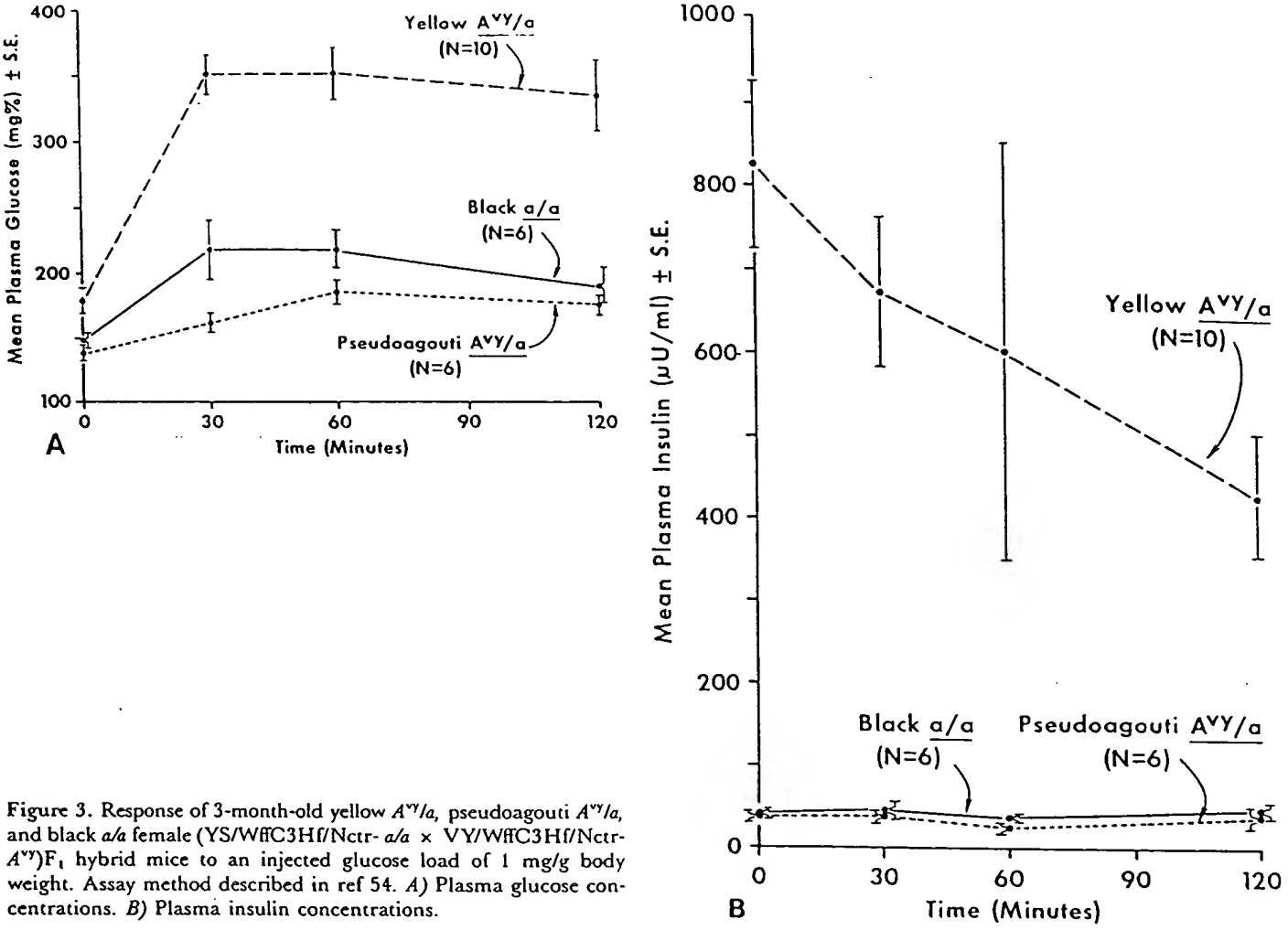

Figure 3. Response of 3-month-old yellow A^{vy}/a, pseudoagouti A^{vy}/a, and black *a/a* female (YS/WffC3Hf/Nctr-*a/a* × VY/WffC3Hf/Nctr-A^{vy})F_1 hybrid mice to an injected glucose load of 1 mg/g body weight. Assay method described in ref 54. *A)* Plasma glucose concentrations. *B)* Plasma insulin concentrations.

Insulin resistance

The insulin resistance of yellow $A^{vy}/-$ mice has been quantitated directly in vivo and in vitro. The former was measured by the ability of exogenous insulin to lower fasting blood glucose or to improve glucose tolerance (2). The latter was determined in isolated adipose tissue by the ability of insulin to stimulate glucose metabolism (2) or to suppress hormone-stimulated lipolysis (65). In general, both types of measurements show increased insulin resistance in 6- to 7-month-old yellow $A^{vy}/-$ mice compared with *a/a* mice (2). The degree of resistance is relatively greater in males compared with females, and parallels the sexual dimorphism in hyperglycemia. Maximal responses to insulin could not be elicited in either in vivo or in vitro systems, suggesting that insulin resistance in these mice is due to postreceptor defects (2, 53). Direct assays of insulin resistance in vivo in yellow mice younger than 6–7 months have not yet been performed; however, glucose metabolism in adipose tissue showed some insulin resistance in 2-month-old male yellow A^{vy}/a mice; this coincided with the earliest age at which hyperinsulinemia was observed (2). To discern the cause and effect relationship between hyperinsulinemia and insulin resistance will require analyses in even younger mice.

Compounds that improve insulin sensitivity without decreasing body weight, such as ciglitazone (54) and Tanabe-174 (66), were able to normalize blood glucose and plasma insulin without causing weight loss. This suggests that hyperinsulinism and insulin resistance are not required to maintain obesity in yellow A^{vy}/a mice. Although insulin is lipogenic, antilipolytic, and thermogenic, hyperinsulinism and insulin resistance may play only a permissive, rather than a primary, role in the maintenance of obesity. On the other hand, insulin resistance does play a pivotal role in the expression of hyperglycemia.

PLEIOTROPY AND THE LEAN PSEUDOAGOUTI A^{vy}/a PHENOTYPE

As noted earlier, *agouti* mRNA could not be detected by Northern analysis in tissues of pseudoagouti A^{vy}/a mice. These mice are similar in body weight to control black *a/a* mice. They also have normal glucose and insulin levels, and respond normally to a glucose load (Fig. 3*A*, Fig. 3*B*). Their rates of glucose oxidation and conversion of glucose to lipid are higher than those in the obese yellow A^{vy}/a mice and resemble those of the *a/a* mice (67). However, these mice do not represent a complete reversion to the nonmutant phenotype, as indicated by detailed analysis of their hair color pattern (23) and by their response to the tumor promoter lindane (see next section).

Comparison of the responses of the pseudoagouti with the yellow A^{vy}/a and black *a/a* mice makes it possible to discriminate between those physiologic, pathologic, and metabolic responses to particular agents associated with obesity

and those that are modulated by a presumed very low or mosaic expression of the *agouti* gene (68). For example, lung and liver tumor formation occurred in the lindane-treated pseudoagouti as well as in the yellow A^{vy}/a mice, but *not* in the black *a/a* littermates. In contrast, A^{vy}/a mice differ in some components of immunocompetence from pseudoagouti A^{vy}/a and black *a/a* mice, but the pseudoagouti and black mice do not differ from each other (69). Likewise, in the lindane study (70, see below) the yellow A^{vy}/a females experienced 50% mortality between 17 and 24 months of age, regardless of treatment group, whereas the pseudoagouti and black females experienced only half as great mortality, i.e., 24% and 23%.

GROWTH REGULATION, HYPERPLASIA, AND NEOPLASIA

Enhancement of somatic growth by the A^{vy} and A^{y} genes and their influence on development of hyperplasia, preneoplastic lesions, and neoplasms were reviewed previously (20), as was utilization of these characteristics in carcinogenicity/toxicity bioassays (71). In general, the effects of A^{vy} on tumor development are rather subtle compared with other oncogenes. Endogenously ("spontaneous") or exogenously induced tumors or hyperplastic precursor lesions may develop in a wide variety of epithelial and mesenchymal tissues in yellow $A^{vy}/-$ and $A^{y}/-$ animals, depending on the strain background and treatment with specific carcinogens (W. E. Heston and co-workers, reviewed in ref 3 and 20).

Specific effects of A^{vy} on tumor incidence in mice with genomes susceptible or resistant to liver tumor formation are illustrated by the results of two studies. In one study yellow A^{vy}/A and agouti *A/a* male mice with a *susceptible* (C3H × VY)F1 genome were fed a phenobarbital-supplemented diet for 1 year (72). No difference in the incidence (18%) of single hepatocellular adenomas was observed between the genotypes. However, *multiple* adenomas appeared in 36% of the yellow mice, but in only 5% of the agouti sibs.

In the second study yellow A^{vy}/a, pseudoagouti A^{vy}/a, and black *a/a* female mice with the (YS × VY)F1 genome, which is relatively *resistant* to liver tumor development, were fed a diet supplemented with lindane (γ-hexachlorocyclohexane) for 24 months (70). The black *a/a* females were completely resistant to the compound, no formation of hepatocellular tumors or lung tumors above the background incidence (<5%) being observed. In contrast, hepatocellular adenoma incidence in treated yellow mice was increased 27% above background and 6% above background in treated pseudoagouti females. Lung tumor incidence was increased 15% above background in the yellow mice and 7% in the pseudoagouti mice.

Increased somatic growth in yellow mice indicates an effect of the *agouti* protein on an unknown process (or processes) of growth regulation in the animal. The cumulative data from chronic bioassays of the response of A^{vy}/a mice to various toxicants suggest that the presence of *agouti* protein in susceptible tissues also affects growth regulation at the cellular level and appears to potentiate/facilitate processes involved in cell transformation to hyperplasia and neoplasia. In addition, the anabolic tissue environments in yellow mice stimulate tumor growth.

The effects of A^{vy} on cell transformation in vitro have been examined in two different studies with apparently opposite results. In one study, established cell lines from A^{vy}/a fibroblasts exhibited elevated levels of spontaneous focus formation compared with cell lines from *a/a* mice of the same strains (73). In another study, primary fibroblasts from A^{vy}/a mice exhibited lower levels of spontaneous and N-methyl-N'-nitro-N-nitrosoguanidine (MNNG)-induced transformation compared with control fibroblasts from *a/a* mice (74). The apparent difference between the results of the two studies may reflect the different experimental protocols and/or the use of primary fibroblasts vs. established cell lines.

In summary, expression of A^{vy} results in increased tumor susceptibility by itself and in combination with classical tumor promoters, both in genetically susceptible as well as in genetically resistant strain backgrounds. It is significant that, even though *agouti* expression could not be detected by Northern analysis in pseudoagouti mice, there is nonetheless a slight increase in tumor formation in this phenotype.

POSSIBLE MECHANISMS FOR A^{vy}-INDUCED OBESITY AND FUTURE DIRECTIONS

The A^{vy}-specific RNA codes for a normal *agouti* protein. Similarly, three other obesity-associated *agouti* mutations also result from the ubiquitous expression of chimeric RNAs, which each encode a normal *agouti* protein (H. Vrieling et al., unpublished results). These observations suggest that A^{vy}-induced obesity results from ectopic activation of a signaling pathway that is used normally by hair follicle melanocytes, and leads to two alternative hypotheses (16, 19) based on possible mechanisms for *agouti* signaling in hair follicles (Fig. 4*A*).

If the *agouti* protein normally antagonizes the action of α-MSH at its melanocyte receptor (melanocortin-1 receptor) (Fig. 4*B*), then ectopic *agouti* expression is likely to antagonize the effects of α-MSH and related compounds at other melanocortin receptors, of which three have been cloned. None of the four cloned melanocortin receptors is expressed in the liver, in the pancreas, or in adipocytes. Therefore, if *agouti*-induced obesity is caused by melanocortin antagonism, A^{vy}-associated defects in lipolysis, lipogenesis, insulin sensitivity, and insulin overproduction are all likely to be consequences, rather than causes, of A^{vy}-induced obesity. Under this scenario, likely targets for *agouti* in nonpigment cells are expression of the melanocortin-3 and 4 receptors in the hypothalamus, which might lead to alterations in thermogenesis, eating behavior, and/or release of corticotrophic releasing factor. As described above, alterations in each of these components characterize all the rodent genetic obesities including A^{vy}. However, in no case does the magnitude of a particular alteration appear to be sufficient to account for the degree of obesity observed (reviewed in ref 26).

A second hypothesis proposes that *agouti* binds to its own receptor in melanocytes, and that the same or a similar receptor is present on nonpigment cells in most tissues, including brain, and can account for the plethora of physiologic derangements observed in yellow $A^{vy}/-$ mice (Fig. 4*C*). This hypothesis is attractive given the parallels between adenylate cyclase metabolism in adipocytes and melanocytes of A^{vy}/a animals. It could also explain why morphologic alterations in pancreatic islets apparently precede biochemical and physiologic derangements (55), assuming that *agouti* receptors are present on islet cells or their precursors.

Two avenues of research are likely to be helpful in distinguishing between these alternatives. The construction of transgenic animals in which *agouti* is placed under the control of tissue-specific promoters should indicate whether obesity can be induced by expression of *agouti* in potential target organs such as adipocytes or the pancreas. Development of an

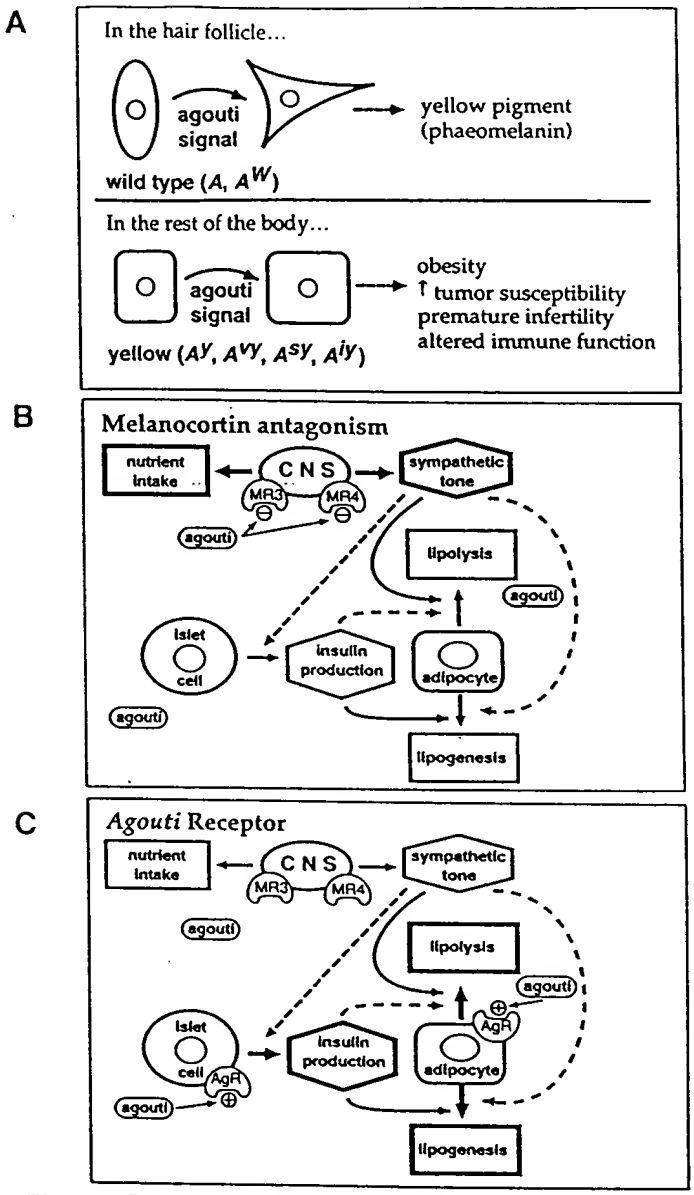

Figure 4. Possible mechanisms of *agouti*-induced obesity. *A)* Ectopic expression of the *agouti* protein in nearly every tissue explains similarities in the pleiotropic effects of A^{vy} and A^{y}. *Agouti* is also expressed ectopically in the dominant *agouti* mutants *sienna yellow* (A^{sy}) and *intermediate yellow* (A^{iy}) (24). A^{sy} and A^{iy} produce obesity but have not been characterized with regard to tumor susceptibility, immune abnormalities, or glucose metabolism. *B)* If *agouti* acts by antagonizing the effects of melanocortins, the MR3 and MR4 receptors in the hypothalamus and other portions of the brain are likely target sites to explain A^{vy}-associated obesity. In this case, alterations in nutrient intake and a reduction in sympathetic tone may be primary events (indicated in boldface). Adrenergic agonists generally produce decreased insulin production and lipogenesis (indicated by the dotted lines) and increased lipolysis (indicated by solid line); therefore, changes in energy balance, hyperinsulinism, and insulin resistance that occur in *agouti*-induced obesity would be secondary to a reduction in adrenergic tone. None of the four melanocortin receptors is expressed at significant levels in adipocytes, although low levels of the MR3 receptor can be detected in rat pancreas. *C)* If *agouti* acts by binding to an as yet unidentified receptor (AgR) expressed in islet cells and/or adipocytes, a direct and primary effect on insulin production and adipocyte metabolism would parallel the effects of *agouti* on G protein-coupled signal transduction in pigment cells. In this case, hyperphagia and altered thermogenesis would be a secondary response. A putative *agouti* receptor might also be expressed in the central nervous system.

in vitro assay for a soluble *agouti* protein should allow testing for antagonism to melanocortin receptor activation and/or to identify an agouti receptor using cell biologic approaches.

CONCLUSION

After almost 50 years of attempts to understand the physiologic/metabolic bases of the "yellow mouse syndrome," cloning and sequencing of the *agouti* gene and definition of the regulation of its expression have made conceptual and experimental integration of the molecular and physiologic aspects of the function of the *agouti* locus a practical possibility. Such studies should lead to a better understanding of the cellular metabolic dysregulations that give rise to obesity, diabetes, and neoplasia. FJ

This review is dedicated to the memory of Margaret M. Dickie who first described the A^{vy} mutation and provided the breeding stock from which Strain VY was developed. We thank K. B. Delclos and D. L. Greenman for constructive critiques of the manuscript.

REFERENCES

1. Dickie, M. M. (1962) A new viable yellow mutation in the house mouse. *J. Hered.* 53, 4-86
2. Yen, T. T., Bue, J. M., and Gill, A. M. (1990) The obese-diabetic syndrome of the viable yellow mouse and pharmacological interventions. In *Frontiers in Diabetes Research. Lessons from Animal Diabetes III.* (Shafrir, E., ed) pp. 294-299
3. Wolff, G. L., Roberts, D. W., and Galbraith, D. B. (1986) Prenatal determination of obesity, tumor susceptibility, and coat color pattern in viable yellow (A^{vy}/a) mice. *J. Hered.* 77, 151-158
4. Bultman, S. J., Michaud, E. J., and Woychik, R. P. (1992) Molecular characterization of the mouse agouti locus. *Cell* 71, 1195-1204
5. Miller, M. W., Duhl, D. M. J., Vrieling, H., Cordes, S. P., Ollmann, M. M., Winkes, B. M., and Barsh, G. S. (1993) Cloning of the mouse *agouti* gene predicts a secreted protein ubiquitously expressed in mice carrying the *lethal yellow* mutation. *Genes & Dev.* 7, 454-467
6. Vrieling, H., Duhl, D. M. J., Millar, S. E., Miller, K. A., and Barsh, G. S. (1994) Differences in dorsal and ventral pigmentation result from temporal- and region- specific expression of alternative isoforms of the mouse *agouti* gene. *Proc. Natl. Acad. Sci. USA* In press
7. Silvers, W. K. (1958) An experimental approach to action of genes at the *agouti* locus in the mouse. III. Transplants of newborn A^{W}-, *A*-, and a^{l}-*skin to* A^{y}-, A^{w}-, *A*-, and *aa* hosts. *J. Exp. Zool.* 137, 189-196
8. Silvers, W. K. (1979) The agouti and extension series of alleles, umbrous, and sable. In *The Coat Colors of Mice,* pp. 6-44, Springer Verlag, New York
9. Barsh, G. S., and Epstein, C. J. (1989) Physical and genetic characterization of a 75-kilobase deletion associated with a^{l}, a recessive lethal allele at the mouse *agouti* locus. *Genetics* 121, 811-818
10. Geschwind, I. (1966) Change in hair color in mice induced by injection of αMSH. *Endocrinology* 79, 1165-1167
11. Mountjoy, K. G., Robbins, L. S., Mortrud, M. T., and Cone, R. D. (1992) The cloning of a family of genes that encode the melanocortin receptors. *Science* 257, 1248-1251.
12. Robbins, L. S., Nadeau, J. H., Johnson, K. R., Kelly, M. A., Roselli-Rehfuss, L., Baack, E., Mountjoy, K. G., and Cone, R. D. (1993) Pigmentation phenotypes of variant extension locus alleles result from point mutations that alter MSH receptor function. *Cell* 72, 827-834
13. Gantz, I., Konda, Y., Tashiro, T., Shimoto, Y., Miwa, H., Munzert, G., Watson, S. J., Delvalle, J., and Yamada, T. (1993) Molecular cloning of a novel melanocortin receptor. *J. Biol. Chem.* 268, 8246-8250
14. Gantz, I., Miwa, H., Konda, Y., Shimoto, Y., Tashiro, T., Watson, S. J., Delvalle, J., and Yamada, T. (1993) Molecular cloning, expression, and gene localization of a 4th melanocortin receptor. *J. Biol. Chem.* 268, 15174-15179
15. Tamate, H. B., and Takeuchi, T. (1964) Action of the *e* locus of mice in the response of phaeomelanic hair follicles to alpha-melanocyte stimulating hormone in vitro. *Science* 224, 1241-1242
16. Jackson, I. (1993) Molecular genetics. Colour-coded switches. *Nature (London)* 362, 587-588
17. Lamoreaux, M. L. (1973) A study of gene interactions using coat color mutants in the mouse and selected mammals. Ph.D. thesis, University of Maine, Orono

18. Wolff, G. L., Galbraith, D. B., Domon, O. E., and Row, J. M. (1978) Phaeomelanin synthesis and obesity in mice: interaction of the viable yellow (A^{vy}) and sombre (e^{so}) mutations. *J. Hered.* 69, 295-298
19. Conklin, B. R., and Bourne, H. R. (1993) Mouse coat color reconsidered. *Nature (London)* 364, 110
20. Wolff, G. L. (1987) Body weight and cancer. *Am. J. Clin. Nutr.* 45, 168-180
21. Mintz, B. (1970) Gene expression in allophenic mice. In *Control Mechanisms in the Expression of Cellular Phenotypes* (Padykula, H. A., ed) pp. 15-42, Academic, New York
22. Wolff, G. L. (1978) Influence of maternal phenotype on metabolic differentiation of agouti locus mutants in the mouse. *Genetics* 88, 529-539
23. Galbraith, D. B., and Wolff, G. L. (1974) Aberrant regulation of the agouti pigment pattern in the viable yellow mouse. *J. Hered.* 65, 137-140
24. Turner, R. C. (1992) The role of obesity in diabetes. *Int. J. Obesity* 16 (Suppl. 2) S43-S46
25. Salan, L. B. (1987) Obesity and non-insulin-dependent diabetes mellitus. In *Recent Advances in Obesity Research: V* (Berry, E. H., Blondheim, S. H., Blondhjeim, H. E., and Shafrir, E., eds) pp. 26-32, John Libbey, London
26. Johnson, P. R., Greenwood, M. R. C., Horwitz, B. A., and Stern, J. S. (1991) Animal models of obesity: genetic aspects. *Annu. Rev. Nutr.* 11, 325-353
27. Wolff, G. L., and Pitot, H. C. (1973) Influence of background genome on enzymatic characteristics of yellow ($A^{y}/-$, $A^{vy}/-$) mice. *Genetics* 73, 109-123
28. Wolff, G. L. (1963) Growth of inbred yellow ($A^{y}a$) and non-yellow (aa) mice in parabiosis. *Genetics* 48, 1041-1058
29. Coleman, D. L., and Hummel, K. P. (1969) Effects of parabiosis of normal with genetically diabetic mice. *Am. J. Physiol.* 217, 1298-1304
30. Coleman, D. L. (1973) Effects of parabiosis of obese with diabetes and normal mice. *Diabetologia* 9, 294-298
31. Plocher, T. A., and Powley, T. L. (1976) Effect of hypophysectomy on weight gain and body composition in the genetically obese yellow (A^{y}/a) mouse. *Metabolism* 25, 593-602
32. Salem, M. A. M., Lewis, U. J., Haro, L. S., Kishi, K., McAllister, D. L., Seavey, B. K., Bee, G., and Wolff, G. L. (1989) Effects of hypophysectomy and the insulin-like and anti-insulin pituitary peptides on carbohydrate metabolism in yellow A^{vy}/A (BALB/c × VY)F_1 hybrid mice. *Proc. Soc. Exp. Biol. & Med.* 191, 408-419
33. Yen, T. T., Allan, J. A., Yu, P. L., Acton, M. A., and Pearson, D. V. (1976) Triacylglycerol contents and in vivo lipogenesis of *ob/ob*, *db/db*, and A^{vy}/a mice. *Biochim. Biophys. Acta* 441, 213-220
34. Yen, T. T., McKee, M. M., and Stamm, N. B. (1984) Thermogenesis and weight control. *Int. J. Obesity* 8 (Suppl. 1) 65-78
35. Frigeri, L. G., Wolff, G. L., and Teguh, C. (1988) Differential responses of yellow A^{vy}/A and agouti A/a (BALB/c × VY) F-1 hybrid mice to the same diets: glucose tolerance, weight gain, and adipocyte cellularity. *Int. J. Obesity* 12, 305-320
36. Bray, G. A., Shimizu, H., Retzios, A. D., Shargill, N. S., and York, D. A. (1988) Reduced acetylation of melanocyte stimulating hormone (MSH): a biochemical explanation for the yellow obese mouse. In *Obesity in Europe 88* (Bjorntorp, P., and Rossner, S., eds) pp. 259-270, John Libbey, London
37. Shimizu, H., Shargill, N. S., Bray, G. A., Yen, T. T., and Geselichen, P. D. (1989) Effects of MSH on food intake, body weight and coat color of the yellow obese mouse. *Life Sci.* 45, 543-552
38. Shimizu, H., Shargill, N. S., and Bray, G. A. (1989) Adrenalectomy and response to corticosterone and MSH in the genetically obese yellow mice. *Am. J. Physiol.* 256, R494-R500
39. Johnson, P. R., and Hirsch, J. (1972) Cellularity of adipose depots in six strains of genetically obese mice. *J. Lipid Res.* 13, 2-11
40. Shaw, W. N., Schmiegel, K. K., Yen, T. T., Toomey, R. E., Meyers, D. B., and Mills, J. (1981) LY79771: a novel compound for weight control. *Life Sci.* 29, 2091-2101
41. Yen, T. T., Wong, D. T., and Bemis, K. G. (1987) Reduction of food consumption and body weight of normal and obese mice by chronic treatment with fluoxetine: a serotonin reuptake inhibitor. *Drug. Dev. Res.* 10, 37-45
42. Yen, T. T., McKee, M. M., and Bemis, K. G. (1981) Ephedrine reduces weight of viable yellow obese mice (A^{vy}/a). *Life Sci.* 28, 119-128
43. Yen, T. T., Steinmetz, J., and Wolff, G. L. (1970) Lipolysis in genetically obese and diabetes-prone mice. *Horm. Metab. Res.* 2, 200-203
44. Yen, T. T., McKee, M. M., Stamm, N. B., and Bemis, K. G. (1983) Stimulation of cyclic AMP and lipolysis in adipose tissue of normal and obese A^{vy}/a mice by LY79771, a phenethanolamine, and stereoisomers. *Life Sci.* 32, 1515-1522
45. Steinmetz, J., Lowry, L., and Yen, T. T. T. (1969) An analysis of the lipolysis in vitro of obese-hyperglycemic and diabetic mice. *Diabetologia* 5, 373-378
46. Himms-Hagen, J. (1989) Brown adipose tissue thermogenesis and obesity. *Prog. Lipid Res.* 28, 67-115
47. Fuller, R. W., and Perry, K. W. (1982) Dopamine accumulation after dopamine β-hydroxylase inhibition in rat hearts as an index of norepinephrine turnover. *Life Sci.* 31, 563-570
48. Yen, T. T., Fuller, R. W., Hemrick-Luecke, S., and Dininger, N. B. (1988) Effects of LY104119, a thermogenic weight-reducing compound, on norepinephrine concentrations and turnover in obese and lean mice. *Int. J. Obesity* 12, 59-67
49. Anderson, G. H., Li, E. T. S., and Glanville, N. T. (1984) Brain mechanisms and the quantitative and qualitative aspects of food intake. *Brain Res. Bull.* 12, 167-173
50. Yen, T. T. (1984) The antiobesity and metabolic activities of LY79771 in obese and normal mice. *Int. J. Obesity* 8, 69-78
51. Coleman, D. L., and Hummel, K. P. (1974) Hyperinsulinemia in preweaning diabetes (*db*) mice. *Diabetologia* 10, 607-610
52. Joosten, H. F. P., and van der Kroon, P. H. W. (1974) Enlargement of epididymal adipocytes in relation to hyperinsulinemia in obese hyperglycemic mice (*ob/ob*). *Metabolism* 23, 59-66
53. Frigeri, L. G., Wolff, G. L., and Robel, G. (1983) Impairment of glucose tolerance in yellow (A^{vy}/A) (BALB/c × VY) F-1 hybrid mice by hyperglycemic peptide(s) from human pituitary glands. *Endocrinology* 113, 2097-2105
54. Gill, A. M., and Yen, T. T. (1991) Effects of ciglitazone on endogenous plasma islet amyloid polypeptide and insulin sensitivity in obese-diabetic viable yellow mice. *Life Sci.* 48, 703-710
55. Warbritton, A., Gill, A. M., Yen, T. T., Bucci, T., and Wolff, G. L. (1994) Pancreatic islet cells in pre-obese yellow $A^{vy}/-$ mice: relation to adult hyperinsulinemia and obesity. *Proc. Soc. Exp. Biol. & Med.* In press
56. Yen, T. T., Greenberg, M. M., Yu, P., and Pearson, D. V. (1976) An analysis of the relationship among obesity, plasma insulin, and hepatic lipogenic enzymes in "viable yellow obese" mice (A^{vy}/a). *Horm. Metab. Res.* 8, 159-166
57. Barrett-Connor, E. (1989) Epidemiology, obesity, and non-insulin-dependent diabetes mellitus. *Epidemiol. Rev.* 11, 172-181
58. Lillioja, S., Mott, D. M., Howard, B. V., Bennett, P. H., Yki-Jarvinen, H., Freymond, D., Nyomba, B. L., Zurlo, F., Swinburn, B., and Borgardus, C. (1988) Impaired glucose tolerance as a disorder of insulin action. *New Engl. J. Med.* 318, 1217-1225
59. Shuman, C. R. (1988) Diabetes mellitus: definition, classification, and diagnosis. In *Diabetes Mellitus* (Galloway, J. A., Potvin, J. H., and Shuman, C. R., eds) pp. 2-13, Eli Lilly, Indianapolis
60. DeFronzo, R. A., Bonadonna, R. C., and Ferrannini, E. (1992) Pathogenesis of NIDDM. A balanced review. *Diabetes Care* 15, 318-368
61. Leiter, E. H. (1993) Obesity genes and diabetes induction in the mouse. *Crit. Rev. Food Sci. Nutr.* 33, 333-338
62. Yen, T. T., Gill, A. M., Powell, J. G., and Sampson, B. M. (1992) Ciglitazone prevents and reverses dexamethasone-induced hyperglycemia in female viable yellow mice. *Int. J. Obesity* 16, 923-933
63. Wajngot, A. S., Giacca, A., Grill, V., Vranic, M., and Efendic, S. (1992) The diabetogenic effects of glucocorticoids are more pronounced in low- than in high-insulin responders. *Proc. Natl. Acad. Sci. USA* 89, 6035-6039
64. Gill, A. M., Leiter, E. H., Powell, J. G., Chapman, H. D., and Yen, T. T. (1994) Dexamethasone-induced hyperglycemia in obese A^{vy}/a (viable yellow) female mice entails preferential induction of hepatic estrogen sulfotransferase. *Diabetes* In press
65. Yen, T. T., and Steinmetz, J. A. (1972) Lipolysis of genetically obese and/or hyperglycemic mice with reference to insulin response of adipose tissue. *Horm. Metab. Res.* 4, 331-337
66. Yen, T., Bue-Valleskey, J., Burkhart, D., Dininger, N., Gill, A., Gold, G., Johnson, T., Myers, S., Shaw, W., Short, W., Tinsley, F., Williams, G., Williams, V., and Yakubu-Madus, F. (1993) The efficacy and adverse effects of a potent insulin sensitivity enhancer: LY282449 (Tanabe-174). *Proc. Eur. Assn. Study Diabetes* 698 (abstr.)
67. Yen, T. T. T., Lowry, L., Steinmetz, J., and Wolff, G. L. (1970) Physiologic and genetic influences on regulation of glucose metabolism in adipose tissue of mice. *Horm. Metab. Res.* 2, 161-165
68. Wolff, G. L. (1991) Obesity, cancer and the viable yellow (A^{vy}/a) mouse: discrimination among pathophysiologic effects of the expression of the A^{vy}/a genotype in obese and lean mice. In *Progress in Obesity Research 1990*, Chap. 70, pp. 445-448
69. Roberts, D. W., Wolff, G. L., and Campbell, W. L. (1984) Differential effects of the mottled yellow and pseudoagouti phenotypes on immunocompetence in A^{vy}/a mice. *Proc. Natl. Acad. Sci. USA* 81, 2152-2156
70. Wolff, G. L., Roberts, D. W., Morrissey, R. L., Greenman, D. L., Allen, R. R., Campbell, W. L., Bergman, H., Nesnow, S., and Frith, C. H. (1987) Tumorigenic responses to lindane in mice: potentiation by a

dominant mutation. *Carcinogenesis* 8, 1889-1897
71. Wolff, G. L. (1993) Multiple levels of response in carcinogenicity bioassays: regulational variation among viable yellow (A^{vy}/-) mice. *J. Exp. Anim. Sci.* 35, 221-231
72. Wolff, G. L., Morrissey, R. L., and Chen, J. J. (1986) Amplified response to phenobarbital promotion of hepatotumorigenesis in obese yellow A^{vy}/A (C3H × VY) F-1 hybrid mice. *Carcinogenesis* 7, 1895-1898
73. Hsiao, W. L., Wendy, Barsh, G. S., Wolff, G. L., and Fan, H. (1991) High level of spontaneous transformation in newly established mouse cell lines carrying the viable yellow mutation (A^{vy}). *Proc. Am. Assn. Cancer Res.* 32, 160
74. Furst, A. S., and Becker, F. F. (1991) Suppression of in vitro chemical transformation by the carcinogenesis-promoting, viable yellow gene A^{vy} *Carcinogenesis* 12, 1157-1160

Antagonism of Central Melanocortin Receptors in Vitro and in Vivo by Agouti-Related Protein

Michael M. Ollmann,* Brent D. Wilson,* Ying-Kui Yang, Julie A. Kerns, Yanru Chen, Ira Gantz, Gregory S. Barsh†

Expression of Agouti protein is normally limited to the skin where it affects pigmentation, but ubiquitous expression causes obesity. An expressed sequence tag was identified that encodes Agouti-related protein, whose RNA is normally expressed in the hypothalamus and whose levels were increased eightfold in *ob/ob* mice. Recombinant Agouti-related protein was a potent, selective antagonist of Mc3r and Mc4r, melanocortin receptor subtypes implicated in weight regulation. Ubiquitous expression of human *AGRP* complementary DNA in transgenic mice caused obesity without altering pigmentation. Thus, Agouti-related protein is a neuropeptide implicated in the normal control of body weight downstream of leptin signaling.

Analysis of mouse obesity mutations has helped define regulatory circuits that govern energy expenditure (*1*). In mice carrying certain alleles of the *Agouti* coat color gene such as *lethal yellow* (A^y) or *viable yellow* (A^{vy}), pleiotropic effects including a yellow coat, obesity, and increased body length are caused by ubiquitous expression of chimeric transcripts encoding a normal Agouti protein (*2–4*). Agouti is a paracrine signaling molecule (*5*) that affects pigmentation by antagonism of the melanocortin 1 receptor (Mc1r) (*6*, *7*), one of five related heterotrimeric GTP-binding protein–coupled receptors named for their ability to respond to α-melanocyte stimulating hormone (α-MSH) and adrenocorticotrophic hormone (ACTH) (*8*). Expression and action of Agouti is normally limited to the skin (*3*, *5*), but recombinant Agouti protein will also antagonize Mc2r and Mc4r (*6*, *9*), expressed primarily in the adrenal gland and the central nervous system (CNS), respectively (*8*, *10*).

Using a characteristic pattern of cysteine spacing from the COOH-terminal region of Agouti to search an expressed sequence tag database, we isolated a gene from 129/sv mice and from humans that encodes a protein nearly identical in size and genomic structure to *Agouti* that we named *Agouti-related protein* (*Agrp*) (Fig. 1A). The same gene was recently described by Shutter *et al.* as *Agouti-related transcript* (*11*). Reverse transcriptase–polymerase chain reaction (RT-PCR) and Northern (RNA) hybridization experiments demonstrated that *Agrp* RNA was expressed primarily in the adrenal gland and the hypothalamus (Fig. 1, B and C). To investigate functional overlap between *Agrp* and *Agouti*, we examined whether the steady-state level of *Agrp* RNA would be altered by ectopic expression of Agouti in A^y/a animals. Northern hybridization analysis of hypothalamic and adrenal gland RNA from A^y/a or coisogenic *a/a* animals revealed an ≈fivefold reduction of *Agrp* RNA in the hypothalamus of A^y/a animals (Fig. 1C). We also measured the levels of hypothalamic *Agrp* RNA in *ob/ob* animals and found an ≈eightfold increase relative to coisogenic controls. In the adrenal gland, levels of *Agrp* RNA in A^y/a and nonmutant animals were below the level of detection, but could easily be detected in *ob/ob* animals.

To determine whether AGRP antagonizes melanocortin signaling, we used the baculovirus expression system to produce conditioned media containing recombinant human AGRP, and measured antagonist activity using a *Xenopus* melanophore cell line developed by Lerner and colleagues (*12*). Melanophores provide a rapid and sensitive bioassay for melanocortin agonists and antagonists because pigment granule dispersion induced by α-

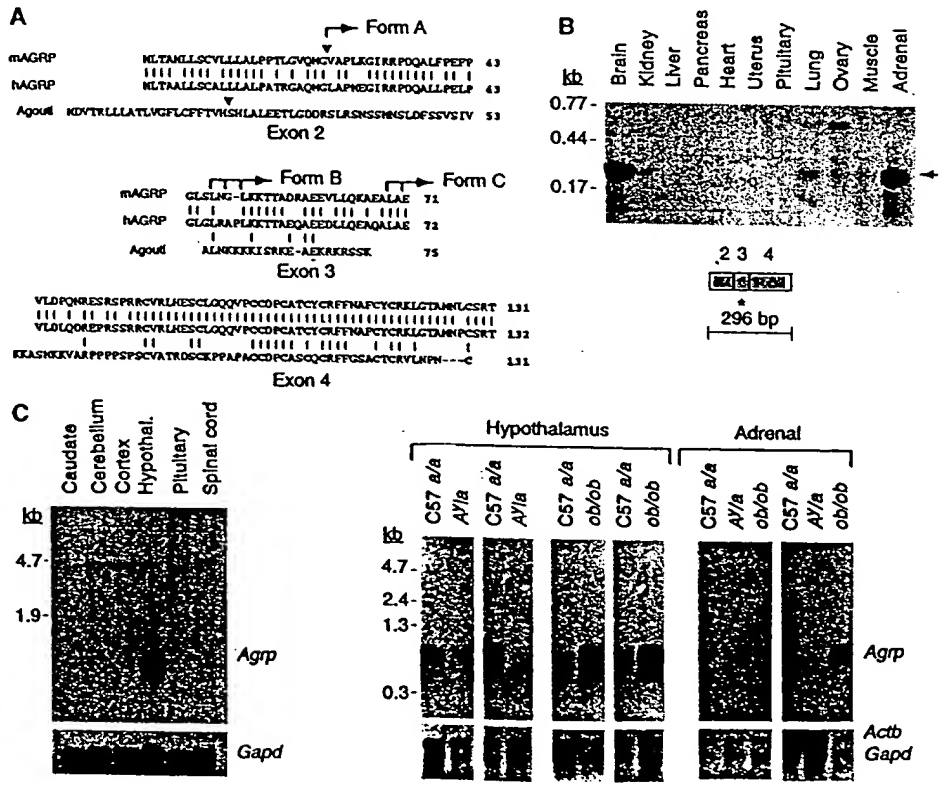

Fig. 1. Structure and expression of *Agrp*. (**A**) Comparison of mouse and human AGRP sequences with that of mouse Agouti. Arrowheads indicate signal sequence cleavage sites; arrows indicate different forms of recombinant AGRP. Abbreviations for the amino acid residues are as follows: A, Ala; C, Cys; D, Asp; E, Glu; F, Phe; G, Gly; H, His; I, Ile; K, Lys; L, Leu; M, Met; N, Asn; P, Pro; Q, Gln; R, Arg; S, Ser; T, Thr; V, Val; W, Trp; and Y, Tyr. Cysteine residues are in bold. (**B**) RT-PCR assay for mouse *Agrp* RNA (*23*). (**C**) Northern hybridization assay for mouse *Agrp* RNA in brain tissues (9 μg, left) or in hypothalamus and adrenal glands of A^y/a and *ob/ob* mice (5 μg, right); each lane represents RNA from a single animal. Relative ratios of *Agrp* RNA determined with a PhosphorImager were based on signal from an exon 4 cDNA probe compared with *Actb* and *Gapd* control probes hybridized to the same blot.

M. M. Ollmann, B. D. Wilson, J. A. Kerns, Y. Chen, G. S. Barsh, Departments of Pediatrics and Genetics and the Howard Hughes Medical Institute, Stanford University School of Medicine, Stanford, CA 94305, USA.
Y.-K. Yang and I. Gantz, Department of Surgery, University of Michigan School of Medicine, Ann Arbor, MI 48109–0682, USA.

*These authors contributed equally to this work.
†To whom correspondence should be addressed at Beckman Center B271A, Stanford University School of Medicine, Stanford, CA 94305-5323, USA. E-mail: gbarsh@cmgm.stanford.edu.

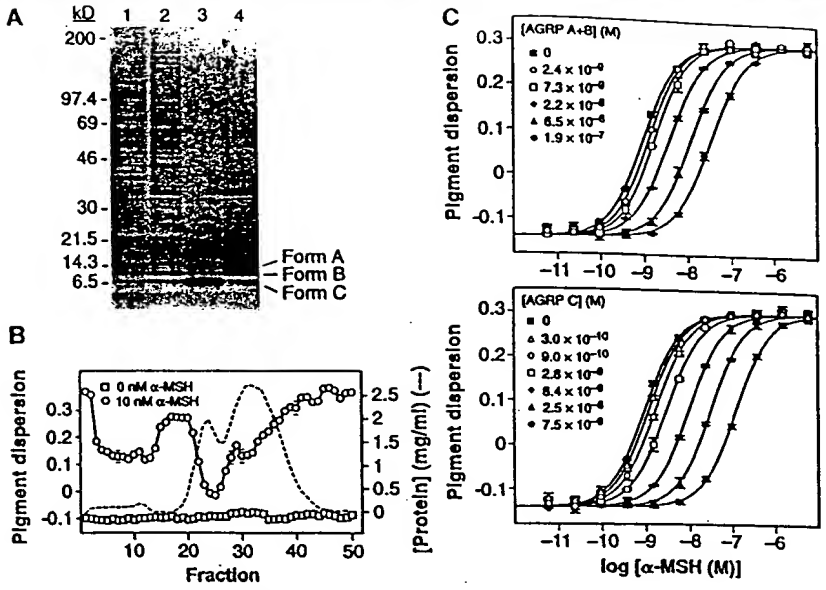

Fig. 2. AGRP activity in *Xenopus* melanophores. (**A**) One microgram of protein from serial steps in the purification procedure analyzed by silver-stained 4 to 20% SDS–polyacrylamide gel electrophoresis. Two liters of conditioned media (lane 1) was applied to a Blue Sepharose Fast Flow Column, then eluted with 40 mM CAPS (pH 10.8), 2.5 M NaCl. Fractions with α-MSH antagonist activity (lane 2) were concentrated (Centriprep 3), buffer-exchanged into 40 mM CAPS (pH 10.8), 20 mM NaCl, applied to a HiTrap Q anion-exchange column, then eluted with a 20 to 800 mM NaCl gradient in 40 mM CAPS (pH 10.8). (**B**) Major peaks of α-MSH antagonist activity in the flow-through (fractions 2 to 13, lane 3) and in fractions 20 to 26 (lane 4) were dialyzed into storage buffer [20 mM Pipes (pH 6.8), 50 mM NaCl]. NH_2-terminal sequencing of the two predominant bands in each peak revealed mature AGRP and two heterogeneous smaller forms as indicated. AGRP purity, estimated by densitometry of a 10-μg sample loaded on a 10% Tricine gel stained with ProBlue, was used to calculate effective concentrations of 40 and 11 μM for form A+B (lane 4) and form C (lane 3), respectively. (**C**) Quantitative α-MSH dose-response analysis of different Agrp forms measured at equilibrium conditions 180 min after addition of AGRP and α-MSH. In the 96-well melanophore assay (*12*), pigment dispersion is calculated as (A_{650} final − A_{650} initial)/A_{650} final, where A_{650} is the absorbance at 650 nm. Data points represent mean ± SEM of triplicate samples.

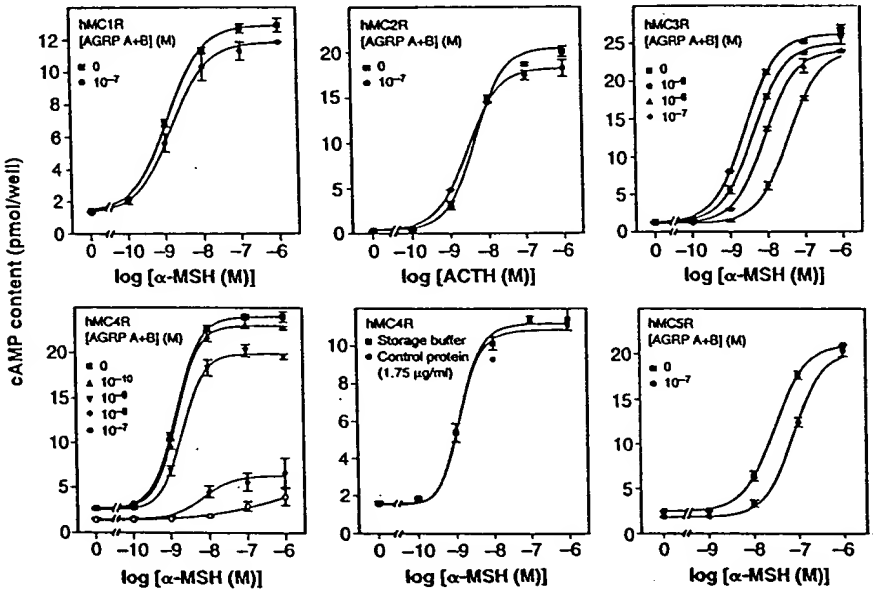

Fig. 3. Effects of AGRP on human melanocortin receptors. 293 cells (hMC1R, hMC3R, hMC4R, or hMC5R) or OS3 cells (hMC2R) stably transfected with the indicated receptor were preincubated with the indicated amounts of AGRP for 30 min; various amounts of α-MSH or ACTH were added for 30 min in the presence of 0.2 mM isobutylmethylxanthine, and total cAMP accumulation was determined on duplicate wells (*9*). Data points represent the mean ± SEM of 2 to 3 independent experiments. As a control for proteins other than AGRP, conditioned media from insect cells infected with an unrelated baculovirus were loaded and eluted from a Blue Sepharose column with conditions identical to those used for AGRP, dialyzed into storage buffer (490 μg/ml), then used at a dilution identical to that used to prepare 100 nM AGRP form A+B. Nanomolar concentrations of AGRP form A+B antagonize the hMC3R and hMC4R but do not meet criteria for competitive antagonism (*15*); therefore, K_B values cannot be calculated.

MSH can be measured in microtiter plates as a change in optical density (*12*). Using the ability of conditioned media to inhibit α-MSH–induced pigment dispersion, we partially purified multiple forms of AGRP that cofractionate with α-MSH antagonist activity by Blue Sepharose and anion-exchange chromatography (Fig. 2). One peak of α-MSH antagonist activity contained mature AGRP with the signal sequence removed (form A) and a mixture of three AGRP fragments cleaved after residues 46, 48, or 50 (form B). The second major peak contained AGRP fragments cleaved after residues 69 or 71 (form C).

Partially purified AGRP forms A+B and form C are potent, specific antagonists of α-MSH–induced pigment dispersion in *Xenopus* melanophores, with calculated antagonist dissociation constant (K_B) values of 7.0 and 1.2 nM, respectively (Fig. 2C). AGRP did not inhibit pigment granule dispersion in the absence of α-MSH and did not inhibit pigment granule dispersion induced by forskolin, a direct activator of adenylate cyclase (*13*).

To examine the selectivity of AGRP for human melanocortin receptors, we added various concentrations of AGRP form A+B to cell lines that had been stably transfected with each of the five different receptor subtypes, then measured the ability of α-MSH or ACTH to induce adenosine 3′,5′-monophosphate (cAMP) accumulation. At concentrations up to 100 nM, AGRP had no effect on hMC1R or hMC2R, and only slightly inhibited hMC5R (Fig. 3). By contrast, AGRP concentrations of 1 nM or more caused a dose-dependent inhibition of α-MSH–induced cAMP accumulation mediated by hMC3R and hMC4R.

Because AGRP form C can antagonize α-MSH in melanophores (Fig. 2) or in Mc4r-transfected cells (*13*), the COOH-terminal cysteine-rich region is probably sufficient for biologic activity, as is the case for Agouti (*14*). Sequence comparison of AGRP and Agouti highlights a short region of similarity beginning with the third Cys residue, CCDPCAXCXCRFF, that may contain determinants required for melanocortin antagonism (Fig. 1A). Nonetheless, the exact biochemical mechanism by which these proteins act is not clear. Most evidence favors competitive antagonism,

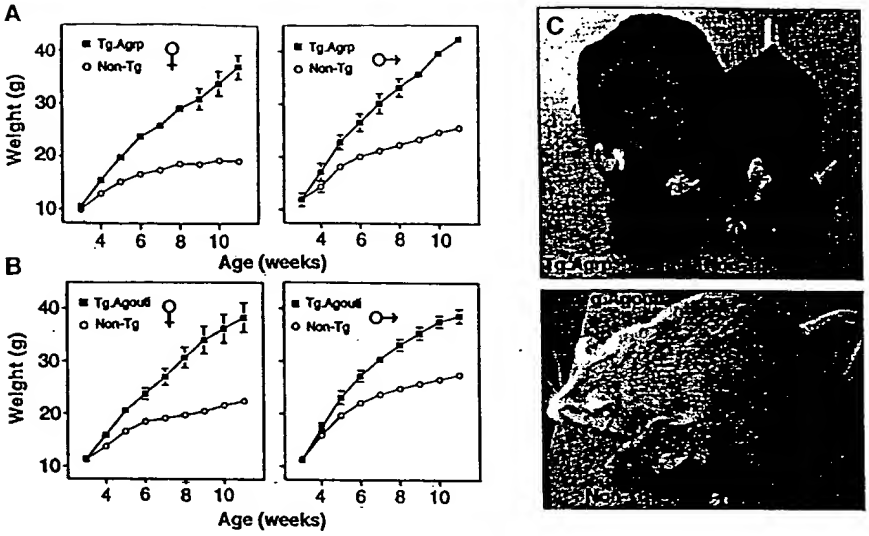

Fig. 4. Effects of AGRP or human Agouti in transgenic mice. A β-actin human *AGRP* cDNA construct nearly identical to one described previously for human Agouti (*24*) was injected into F_2 (C57BL/6J × CBA/J) embryos. One of six F_0 founders (*17*) was bred to C57BL/6J animals. At 11 weeks of age, F_1 transgenic animals (females: $n = 4$; males: $n = 3$) weighed significantly more than nontransgenic littermates (females: $n = 6$, $P = 0.00005$; males: $n = 6$; $P = 0.00002$). The time of onset and level of weight gain caused by the AGRP transgene (**A**) were similar to those caused by the Agouti transgene (**B**), but the AGRP transgene had no effect on pigmentation (**C**). Data points represent the mean ± SEM.

whereby α-MSH and Agouti (or AGRP) bind to mutually exclusive sites on melanocortin receptors (*14*). The effects of AGRP on melanophores are consistent with competitive antagonism, because increasing amounts produced a proportionate and parallel displacement of the α-MSH dose-response curve without affecting maximal signaling (Fig. 2C). For the hMC4R, however, AGRP concentrations of 10 and 100 nM produced a decrease in basal levels of cAMP accumulation, as well as a decrease in the maximal level of α-MSH–induced cAMP accumulation (Fig. 3), neither of which is consistent with competitive antagonism (*15*). It has been proposed that some effects of Agouti are mediated by alterations in calcium flux (*16*), an intriguing finding given the similarity in cysteine spacing between Agouti, AGRP, and certain calcium channel antagonists (*4*). It is possible that Agouti or AGRP does not bind directly to melanocortin receptors or binds to more than one cell surface protein, uncertainties that may be resolved by studies of Agouti and AGRP binding.

To determine whether or not Agouti and AGRP have comparable effects in vivo, we constructed transgenic mice in which the human AGRP cDNA was controlled by the ubiquitously expressed β-actin promoter. Weight gain of six independent transgenic founders was significantly increased over nontransgenic littermates (*17*), and a transgenic line was established. Among F_1 animals carrying the β-actin AGRP transgene, increased weight gain was detectable at 4 weeks of age, reached levels 100 or 70% above that of nontransgenic females or males, respectively, and was nearly indistinguishable from that caused by a β-actin Agouti transgene (Fig. 4). Body length and food consumption were also increased by the AGRP transgene (*17*). By contrast, none of 15 animals carrying the AGRP transgene exhibited a difference in coat color from their nontransgenic littermates (Fig. 4). Thus, although AGRP mimics the effect of Agouti on weight gain, body length, and food consumption, it has no effect on pigmentation.

Given the eightfold increase of hypothalamic expression in *ob/ob* mice, we propose that *Agrp* normally regulates body weight via central melanocortin receptors, analogous to the relation between Agouti and the Mc1r for regulation of pigmentation. Huszar *et al.* (*18*) have shown that Mc4r-deficient animals develop obesity and metabolic derangements that mimic those in $A^y/-$ mice, which suggests that obesity caused by ubiquitously expressed *Agrp* or *Agouti* is mediated largely by Mc4r. However, AGRP may also be a physiologic ligand of Mc3r (Fig. 3), which has been implicated in Agouti-induced obesity (*19*) and whose CNS expression (*20*) more closely matches that of *Agrp*. In the brain, *Agrp* RNA is localized primarily to the arcuate nucleus and median eminence (*11*), but unlike Agouti, which has a very small sphere of action in vivo (*3*), AGRP may diffuse more widely, particularly if it is processed to a smaller COOH-terminal form in vivo. AGRP is also produced by the adrenal gland but does not affect hMC2R and therefore may act at a more distant site.

What advantages do endogenous receptor antagonists such as Agouti or AGRP offer for homeostatic regulation? In the case of melanocortins, which activate five receptors to varying extents, an antagonist limited in its tissue distribution or biochemical specificity, or both, allows individual regulation of receptor subtype signaling. Melanocortin receptors were identified on the basis of their response to the agonist α-MSH (*6*), but physiologic signaling via Mc1r is regulated mainly by alterations in levels of the antagonist, Agouti. Similarly, regulation of Mc3r or Mc4r signaling could be mediated primarily by changes in Agrp expression rather than proopiomelanocortin, the precursor of α-MSH and ACTH. Agouti or AGRP, or both, may also transduce a signal via melanocortin receptors independent of melanocortin binding (*21*), consistent with the effects we observed on basal levels of cAMP accumulation.

Leptin deficiency lies upstream of *Agrp* expression, directly or indirectly, but other signaling systems implicated in energy balance (*22*) may also regulate *Agrp* expression. Additional studies based on gene targeting may help to place *Agrp* in a genetic pathway for feeding behavior, which should be useful in understanding and developing treatments for disorders of body weight regulation.

REFERENCES AND NOTES

1. Y. Zhang *et al.*, *Nature* 372, 425 (1994); L. A. Tartaglia *et al.*, *Cell* 83, 1263 (1995); K. Noben-Trauth, J. K. Naggert, M. A. North, P. M. Nishina, *Nature* 380, 534 (1996); J. K. Naggert *et al.*, *Nature Genet.* 10, 135 (1995).
2. D. M. J. Duhl, H. Vrieling, K. A. Miller, G. L. Wolff, G. S. Barsh, *Nature Genet.* 8, 59 (1994); E. J. Michaud *et al.*, *Genes Dev.* 8, 1463 (1994).
3. W. K. Silvers, in *The Coat Colors of Mice* (Springer-Verlag, New York, 1979), pp. 6–44.
4. J. Manne, A. C. Argeson, L. D. Siracusa, *Proc. Natl. Acad. Sci. U.S.A.* 92, 4721 (1995).
5. S. J. Buttman, E. J. Michaud, R. P. Woychik, *Cell* 71, 1195 (1992); M. W. Miller *et al.*, *Genes Dev.* 7, 454 (1993).
6. D. S. Lu *et al.*, *Nature* 371, 799 (1994).
7. L. S. Robbins *et al.*, *Cell* 72, 827 (1993).
8. K. G. Mountjoy, L. S. Robbins, M. T. Mortrud, R. D. Cone, *Science* 257, 1248 (1992).
9. Y. K. Yang *et al.*, *Mol. Endocrinol.* 11, 274 (1997).
10. I. Gantz *et al.*, *J. Biol. Chem.* 268, 15174 (1993); K. G. Mountjoy, M. T. Mortrud, M. J. Low, R. B. Simerly, R. D. Cone, *Mol. Endocrinol.* 8, 1298 (1994).
11. J. R. Shutter *et al.*, *Genes Dev.* 11, 593 (1997).
12. J. M. Quillan, C. K. Jayawickreme, M. R. Lerner, *Proc. Natl. Acad. Sci. U.S.A.* 92, 2894 (1995); N. Potenza and M. R. Lerner, *Pigment Cell Res.* 5, 372 (1992).
13. M. M. Ollmann, Y.-K. Yang, B. D. Wilson, I. Gantz, G. S. Barsh, unpublished observations.
14. D. H. Willard *et al.*, *Biochemistry* 34, 12341 (1995); S. G. Blanchard *et al.*, *ibid.*, p. 10406.
15. T. P. Kenakin, *Can. J. Physiol. Pharmacol.* 60, 249 (1982).
16. M. B. Zemel *et al.*, *Proc. Natl. Acad. Sci. U.S.A.* 92, 4733 (1995); J. H. Kim *et al.*, *FASEB J.* 10, 1646 (1996).

17. Individually caged mice had free access to standard Chow and were treated in accordance with Stanford guidelines. At 11 weeks of age, female F_0 animals weighed 30.5, 35.5, and 41.9 g, and male F_0 animals weighed 32.4, 34.8, and 43 g—significantly more than nontransgenic littermates (females: 21.1 ± 2.0 g, n = 10, P = 0.02; males: 26 ± 2.0 g, n = 5, P = 0.03, student's t test). At 15 weeks of age, body length of F_1 transgenic animals (10.5 ± 0.1 cm, n = 4) was more than that of nontransgenic littermates (9.18 ± 0.2 cm, n = 10, P = 0.0002). Food consumption measured over a 7-day period at 12 weeks of age for F_1 transgenic animals (27.9 ± 5.4 g, n = 4) was more than that of nontransgenic littermates (21.9 ± 2.8 g, n = 5, P = 0.03).
18. D. Huszar *et al.*, *Cell* 88, 131 (1997).
19. W. Fan, B. A. Boston, R. A. Kesterson, V. J. Hruby, R. D. Cone, *Nature* 385, 165 (1997); L. L. Kiefer *et al.*, *Biochemistry* 36, 2084 (1997).
20. L. Roselli-Rehfuss *et al.*, *Proc. Natl. Acad. Sci. U.S.A.* 90, 8856 (1993); I. Gantz *et al.*, *J. Biol. Chem.* 268, 8246 (1993).
21. W. Siegrist *et al.*, *J. Recept. Signal Transd. Res.* 17, 75 (1997); G. Hunt and A. J. Thody, *J. Endocrinol.* 147, R1 (1995); C. Sakai *et al.*, *EMBO J.* 16, 3544 (1997).
22. J. C. Erickson, G. Hollopeter, R. D. Palmiter, *Science* 274, 1704 (1996); D. Qu *et al.*, *Nature* 380, 243 (1996); M. Spina *et al.*, *Science* 273, 1561 (1996).
23. RNA (1 μg) was amplified by RT-PCR with the oligonucleotides 5′-ATGCTGACTGCAATGTTGCTG-3′ and 5′-GGTAC[illegible]CAAGCAG-3′; identity of the 296-base pair product was confirmed by hybridization with a third oligonucleotide, 5′-CTGCAGAAGGCA[illegible]-3′.
24. B. D. Wilson *et al.*, *Nature Genet.* 4, 223 (1995).
25. We thank M. Lerner, T. Graf, T. Gurney, and F. Chehab for advice and reagents. Supported by NIH grants EY07106 and [illegible] M.M.O., J.A.K., and B.D.W. This work was supported in part by a Veterans Administration [illegible] and by grants from the NIH to the University of Michigan (P30DK-34933) and to G.S.B. (D[illegible] and is an Associate Investigator of the Howard Hughes Medical Institute.

16 May 1997; accepted [illegible] August 1997

NF-AT Activation Induced by a CAML-Interacting Member of the Tumor Necrosis Factor Receptor Superfamily

Götz-Ulrich von Bülow and Richard J. Bram*

Activation of the nuclear factor of activated T cells transcription factor (NF-AT) is a key event underlying lymphocyte action. The CAML (calcium-modulator and cyclophilin ligand) protein is a coinducer of NF-AT activation when overexpressed in Jurkat T cells. A member of the tumor necrosis factor receptor superfamily was isolated by virtue of its affinity for CAML. Cross-linking of this lymphocyte-specific protein, designated TACI (transmembrane activator and CAML-interactor), on the surface of transfected Jurkat cells with TACI-specific antibodies led to activation of the transcription factors NF-AT, AP-1, and NFκB. TACI-induced activation of NF-AT was specifically blocked by a dominant-negative CAML mutant, thus implicating CAML as a signaling intermediate.

We identified proteins that can interact with CAML in a two-hybrid screen (*1*, *2*). To determine if any of these CAML-binding proteins affected signaling in T cells, we examined their ability to modulate activity of the Ca^{2+}-dependent transcription factor NF-AT (*3*). Overexpression of the two-hybrid clones in Jurkat T cells revealed that expression of one clone (encoding the TACI protein) led to activation of NF-AT, suggesting that TACI may lie in the same signaling pathway as CAML. The deduced amino acid sequence of TACI (Fig. 1A) (*4*) includes a single hydrophobic region (residues 166 to 186) that has features of a membrane-spanning segment. Analysis of the protein sequence (*5*) predicted extracellular exposure for the NH_2-terminus with a cytoplasmic COOH-terminus. Although TACI lacks an NH_2-terminal signal sequence, the presence of an upstream stop codon indicates that the complete open reading frame is contained within the clone (*6*). The predicted cell-surface location of TACI was confirmed in intact Cos-7 cells transfected with an expression plasmid encoding TACI with an NH_2-terminal FLAG epitope tag. Staining with monoclonal antibody to FLAG revealed TACI localized to the cell surface (Fig. 2A). TACI is therefore a type III transmembrane protein with an extracellular NH_2-terminus in the absence of a cleaved signal sequence (*7*). Inspection of the TACI protein sequence also revealed two repeated regions (residues 33 to 66 and 70 to 104) that are 50% identical. A PROSITE motif search (*8*) identified this repeated region as a cysteine-rich motif characteristic of the tumor necrosis factor receptor (TNFR) superfamily. Comparison of TACI with other members of TNFR superfamily (Fig. 1B) demonstrates the similarity between these domains, with the best match to cysteine-rich domains of DR3 (also known as Wsl-1, Apo-3, or TRAMP) (*9*).

Northern blot analysis of TACI mRNA demonstrated a 1.4-kb transcript expressed in spleen, small intestine, thymus, and peripheral blood lymphocytes, suggesting that a single TACI transcript is present in both T and B lymphocytes (Fig. 2B). Specific antibody staining of peripheral blood cells with a polyclonal antibody to TACI (*10*) revealed the presence of TACI on the surface of B cells, but not resting T cells (Fig. 2C). Because expression of other TNFR members such as [illegible] is increased after activation of T lymphocytes (*11*) and because TACI appears to be expressed in thymocytes, we examined T cells activated with ionomycin and phorbol ester. Such treatment of T cells induced the synthesis of cell-surface TACI in 54% of CD2-positive cells within 48 hours (Fig. 2D). This subset was equally distributed between CD4 and CD8 cells. Stimulation of interleukin-2 (IL-2)–dependent T cells with antibodies to CD3 and CD28 also induced expression of TACI. A reverse transcriptase–polymerase chain reaction assay revealed TACI message in resting B cells but not in T cells, unless they were activated (*6*).

Neither TACI mRNA nor protein could be detected in untransfected Jurkat cells expressing the SV40 large T-antigen (TAg), either unstimulated or treated with phorbol myristyl acetate (PMA) and ionomycin (*6*). To assess the effect of TACI on NF-AT activity in T cells, we transiently expressed the protein in TAg Jurkat cells along with a secreted alkaline phosphatase reporter driven by the NF-AT–binding sequences from the IL-2 promoter (*12*, *13*, *14*). TACI overexpression could partially replace the requirement for PMA and ionomycin in this assay for maximal activation of the NF-AT reporter. The addition of antibodies to TACI to the cells increased NF-AT activation [illegible] to sevenfold (Fig. 3A), demonstrating that TACI responds to cross-linking at the cell surface. This affinity-purified antibody to TACI had no effect on control transfected cells. To further verify the specificity of the response, we transfected cells with an NH_2-terminal FLAG-epitope–tagged TACI expression plasmid and incubated them with the M2-FLAG monoclonal antibody [illegible]. This treatment gave a similar increase in NF-AT activity (Fig. 3A). The degree of NF-AT activation varied among different experiments because of transfection efficiency, but was typically 40 to 100% of the maximal re-

G.-U. von Bülow, Department of Experimental Oncology, St. Jude Children's Research Hospital, 332 North Lauderdale, Memphis, TN 38105, USA.
R. J. Bram, Departments of Experimental Oncology and Hematology/Oncology, St. Jude Children's Research Hospital, 332 North Lauderdale, and Department of Pediatrics, University of Tennessee, Memphis, TN 38105, USA.
*To whom correspondence should be addressed. E-mail: richard.bram@stjude.org

space and periaxonal collar[5,14,16]. In contrast, P_0 ear later, are present in compacted myelin and are myelin compaction[15,17,20]. The *Krox-20* mutation appears to block Schwann cell differentiation after tivation and engulfing of the axon but before spiral- on and activation of P_0 and MBP. This phenotype is very milar to the defect observed when differentiating Schwann cells are exposed to antibodies directed against galactocerebroside[21] (GalC), the major glycolipid of the myelin sheath. It differs, however, from the lesions associated with mutations affecting genes encoding major myelin proteins[19,20,22]. Our data therefore suggest that *Krox-20* is involved directly or indirectly, in the activation of late myelin genes, although it is not clear whether the absence of late myelin proteins constitutes the cause or the consequence of the differentiation block. Finally, this block is likely to be responsible for the augmentation in the number of Schwann cells by increased proliferation and/or survival. □

Received 20 June; accepted 9 September 1994.

1. Lemke, G. *Glia* **7**, 263–271 (1993).
2. Chavrier, P. *et al. EMBO J.* **7**, 29–35 (1988).
3. Chavrier, P. *et al. EMBO J.* **9**, 1209–1218 (1990).
4. Schneider-Maunoury, S. *et al. Cell* **75**, 1199–1214 (1993).
5. Trapp, B. D. & Quarles, R. H. *J. Cell biol.* **92**, 877–882 (1982).
6. Greenfield, S., Brostoff, S., Eylar, E. H. & Morell, P. *J. Neurochem.* **20**, 1207–1216 (1973).
7. Kies, M. W., Murphy, J. B. & Alvord, E. C. in *Chemical Pathology of the Nervous System* (ed. Folch-Pi, J.) 197 (Pergamon, London, 1961).
8. Wilkinson, D., Bhatt, S., Chavrier, P., Bravo, R. & Charnay, P. *Nature* **337**, 461–464 (1989).
9. Jessen, K. R. *et al. Neuron* **12**, 509–527 (1994).
10. Gabe, M. *Techniques histologiques* (ed. Masson) 468 (Masson, Paris, 1968).
11. Uyemura, K., Tobari, C. & Hirano, S. *Biochim. biophys. Acta* **214**, 190–197 (1970).
12. Brockes, J. P., Fields, K. L. & Raff, M. C. *Brain Res.* **165**, 105–118 (1979).
13. Bunge, M. B., Bunge, R. P., Kleitman, N. & Dean, A. C. *Devl Neurosci.* **11**, 348–360 (1989).
14. Trapp, B. D., Quarles, R. H. & Suzuki, K. *J. Cell biol.* **99**, 594–605 (1984).
15. Trapp, B. D. *J. Cell Biol.* **107**, 675–685 (1988).
16. Li, C. *et al. Nature* **369**, 747–750 (1994).
17. Giese, K. P., Martini, R., Lemke, G., Soriano, P. & Schachner, M. *Cell* **71**, 565–576 (1992).
18. Filbin, M. T., Walsh, F. S., Trapp, B. D., Pizzey, J. A. & Tennekoon, G. I. *Nature* **344**, 871–872 (1990).
19. Kirschner, D. A. & Ganser, A. L. *Nature* **283**, 207–210 (1980).
20. Kimura, M. *et al. Proc. natn. Acad. Sci. U.S.A.* **86**, 5661–5665 (1989).
21. Owens, G. C. & Bunge, R. P. *Glia* **3**, 118–124 (1990).
22. Henry, E. W. & Sidman, R. L. *Science* **241**, 344–346 (1988).
23. Levi, G., Crossin, K. & Edelman, G. M. *J. Cell Biol.* **105**, 2359–2372 (1987).
24. Chomczynski, P. & Sacchi, N. *Analyt. Biochem.* **162**, 156–159 (1987).

ACKNOWLEDGEMENTS. P.T. and S.S.-M. contributed equally to this work. We thank B. Trapp for the gift of anti-P_0, anti-MAG and anti-P_2 antibodies, P. Brophy and F. Lachapelle for the gifts of anti-MAG and anti-MBP antibodies, respectively, M. Wassef and C. Sotelo for critical comments on the manuscript, D. Pham-Dinh, P. Cameron-Curry, N. Baumann and B. Zalc for helpful discussions. This work was supported by grants from INSERM, MRT, EEC, ARC, LNFCC, AFM and AISM. The financial support of Telethon (Italy) to the project 'Molecular modulation of cell adhesion and cytoskeletal molecules during neuromuscular development and regeneration' is gratefully acknowledged.

Agouti protein is an antagonist of the melanocyte-stimulating-hormone receptor

Dongsi Lu*, Derril Willard†, Indravadan R. Patel†, Sue Kadwell†, Laurie Overton†, Tom Kost†, Michael Luther†, Wenbiao Chen*, Richard P. Woychik‡, William O. Wilkison†§ & Roger D. Cone*

* Vollum Institute for Advanced Biomedical Research, Oregon Health Sciences University, Portland, Oregon 97201, USA
† Division of Molecular Sciences, Glaxo Research Institute, Research Triangle Park, North Carolina 27709, USA
‡ Biology Division, Oak Ridge National Laboratory, Oak Ridge, Tennessee 37831-8077, USA

THE genetic loci *agouti* and *extension* control the relative amounts of eumelanin (brown–black) and phaeomelanin (yellow–red) pigments in mammals[1]: *extension* encodes the receptor for melanocyte-stimulating hormone (MSH)[2] and *agouti* encodes a novel 131-amino-acid protein containing a signal sequence[3,4]. Agouti, which is produced in the hair follicle[5], acts on follicular melanocytes[6] to inhibit α-MSH-induced eumelanin production, resulting in the subterminal band of phaeomelanin often visible in mammalian fur. Here we use partially purified agouti protein to demonstrate that agouti is a high-affinity antagonist of the MSH receptor and blocks α-MSH stimulation of adenylyl cyclase, the effector through which α-MSH induces eumelanin synthesis. Agouti was also found to be an antagonist of the melanocortin-4 receptor[7,8], a related MSH-binding receptor. Consequently, the obesity caused by ectopic expression of agouti in the lethal yellow (A^y) mouse[9] may be due to the inhibition of melanocortin receptor(s) outside the hair follicle.

Two models have been proposed for the mechanism by which agouti protein inhibits stimulation of melanogenesis by α-MSH: (1) agouti is a negative regulator of the cyclic AMP signalling pathway acting through a unique agouti receptor[10], or (2) agouti is a competitive antagonist of α-MSH[11]. We produced recom-

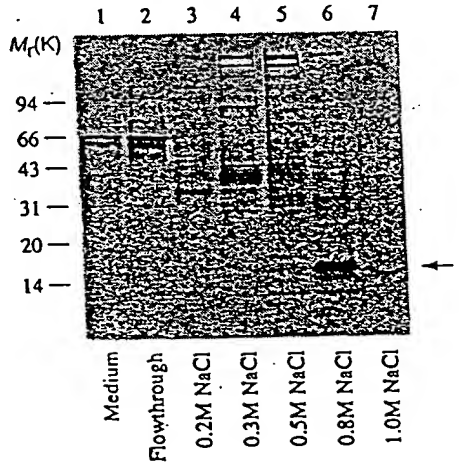

FIG. 1 Production and purification of recombinant agouti polypeptide. A 614-bp *Xbal/Pstl* fragment of the full-length mouse agouti cDNA was subcloned into a *Xbal/Pstl*-digested baculovirus expression vector pAcMP3 (PharMingen, San Diego). Virus was produced using standard methods[22]. 1 μg of each sample was electrophoresed on a 4–20% Tris-glycine gel (Novex, San Diego) and visualized by ProBlue (Integrated Separation Systems, MA) staining. The agouti protein eluted with the 0.8 M-NaCl wash. The 18.5K agouti species (arrow) was not observed in media infected with wild-type virus, and was demonstrated, after elution from the gel, to contain agouti by N-terminal sequencing. Lanes: 1, 48 h post-infection medium from pAcMP3-M.agouti-infected cells; 2, flow-through from Poros-20 HS column; 3–7, NaCl elutions from Poros-20 HS column. Arrow indicates authentic agouti protein.
METHODS. *T. ni* cells were infected at an MOI of 2 with pAcMP3-M.agouti virus or control virus and media were collected 48 h post-infection. This medium was directly loaded onto a Poros-20 HS cation-exchange column (PerSeptive Biosystems, MA) and bound protein eluted with NaCl concentrations from 0.2–1.0 M. The 0.8 M fraction was dialysed into 50 mM NaCl, 20 mM PIPES, pH 6.5, and then diluted for assay. Agouti concentrations were estimated from gel electrophoresis and amino-acid analysis of purified protein. Media controls consisted of unrelated baculovirus supernatants collected 48 h post-infection and purified by NaCl elution of a Poros-20 HS column as for agouti.

§ To whom correspondence should be addressed.

binant agouti protein using the baculovirus expression system in order to test these hypotheses. The band indicated by the arrow in Fig. 1 was absent from *Trichiplusia* cells not infected with the agouti/baculovirus vector, and its identity as the *agouti* gene product was verified by N-terminal sequencing (data not shown). Agouti pooled from the 0.8 M NaCl elution shown in this preparation was estimated to be 75% pure, resulting in an effective agouti concentration of ~0.14 mg ml^{-1}.

Agouti action was examined initially on the B16F10 murine melanoma cell line[12]. Agouti (0.7 nM) shifted the half-maximal effective concentration (EC_{50}) for stimulation of adenylyl cyclase by α-MSH in these cells from 1.7 ± 0.24 nM to 13.4 ± 3.3 nM (data not shown). To characterize agouti action further, we examined the effects of agouti on the MSH receptor (MSH-R) and other G-protein-coupled receptors stably transfected into the human embryonic kidney 293 cell[8,13–15]. α-MSH had no effect on the cAMP pathway in untransfected 293 cells, demonstrating the absence of endogenous melanocortin receptors in this cell line (Fig. 2*a*). Furthermore, addition of agouti (0.7 nM) had no effect on the basal adenylyl cyclase levels. Agouti also had no effect on the ability of thyroid-stimulating hormone (TSH) to bind to its receptor and stimulate adenylyl cyclase in TSH-R-transfected 293 cells (Fig. 2*b*). As the TSH-R couples to the same G protein as do the melanocortin receptors, G_s, this experiment shows that agouti acts upstream of G_s in the cAMP signalling pathway.

In contrast, the same concentration of agouti protein produced a significant shift in the adenylyl cyclase/functional coupling curve of the murine MSH-R expressed in 293 cells (Fig. 3*a*). Control supernatants from baculovirus-infected cells at the same total protein concentration had no effect. Agouti protein (0.7 nM) increased the EC_{50} for activation of adenylyl cyclase from 1.5 ± 1.1 × 10^{-9} to 2.2 ± 1.2 × 10^{-8} M, but did not alter the maximally induced activity of the receptor. The apparent K_i value calculated from four independent experiments was 3.2 ± 2.6 × 10^{-10} M. A dose–response curve demonstrated increasing inhibition of the murine MSH-R by agouti at concentrations from below 10^{-9} M up to 10^{-6} M (Fig. 3*b*). The human MSH receptor was also inhibited by agouti but only at much higher protein concentrations (Fig. 3*c*). It is conceivable that, unlike its murine counterpart, human agouti is antagonist of the human MSH-R. But as the wi… a hi… pigmentation phenotype is not commonly observed …d-ty… possible that agouti no longer antagonizes MSH-R … in the human hair follicle.

The ability of agouti to shift the MSH-R functional cc… curve without affecting maximal receptor activation sug… that agouti was acting as a competitive antagonist. To inve… this further, the ability of the protein to compete with a … melanocortin peptide for binding to the mouse MSH-… examined. Adrenocorticotropic hormone (ACTH), whic… tains the α-MSH peptide in its first 13 amino acids, … radiolabelled at Tyr 23 without loss of potency and binds … same site on the melanocortin receptors as does α-MSH. Competition binding experiments were performed wit… labelled ACTH$_{1-39}$ and the M-3 subclone of the Cloudma… ine melanoma cell line. This cell line was used because of th… density of MSH receptors expressed on the plasma mem… (10,000–50,000), in contrast to the MSH-R-transfected 29… which were estimated to express under 1,000 MSH recepto… cell (data not shown). ACTH bound the MSH-R with … of 6.3 ± 13.3 × 10^{-8} M, within the range of previously re… values[12] (Fig. 3*d*). Using a single-site model, agouti p… blocked 50% of specific ACTH binding to the MSH re… at a concentration of 1.2 ± 0.7 ng ml^{-1} (K_i = IC$_{50}$ (half-m… inhibitory concentration) = 6.6 ± 3.8 × 10^{-10} M) (Fig. 3*e*). … lar results were obtained when a synthetic radiolabelled α-… analogue (Nle$_4$, D-Phe$_7$-α-MSH) was used as the radiola… ligand (data not shown). As a control, baculovirus super… from *T. ni* cells infected with a baculovirus construct cont… an unrelated gene insert was purified as described for a … This protein had no activity in this assay (Fig. 3*e*) or on α-… stimulation of adenylyl cyclase in MSH-R-transfected 29… (data not shown).

So far there are five members of the melanocortin re… family, MC1-R (MSH-R)[14,16], MC2-R (ACTH … MC3-R[15,17], MC4-R[7,8] and MC5-R[18,19]. No functions ha… been described for the latter three members of the famil… the MC3-R and MC4-R are expressed primarily in the c… nervous system in brain nuclei involved in neuroendocrin…

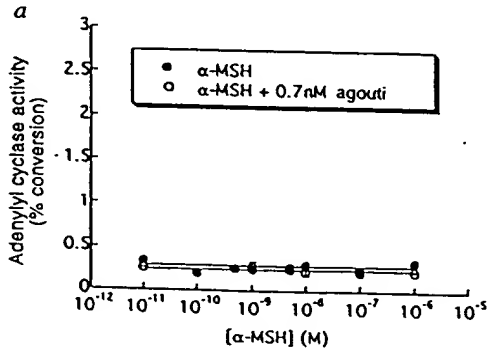

FIG. 2 Agouti does not affect basal or TSH-R-stimulated adenylyl cyclase activity. *a*, Adenylyl cyclase assay showing no effect of agouti on basal levels of this enzyme in untransfected 293 cells. α-MSH treatment also elicits no response, demonstrating the absence of endogenous melanocortin receptors in this cell line. *b*, Adenylyl cyclase assay showing no effect of agouti protein on the cAMP signalling pathway following activation by bovine thyroid-stimulating hormone (TSH) of adenylyl cyclase in 293 cells transfected with human TSH-receptor.

METHODS. Agouti protein was prepared as Fig. 1. Two independent preparations of agouti yielded similar results. 293 cells (5 × 10^5) and 293 cells expressing human TSH-R were preloaded with 5 μCi ^{3}H-aden… ine for 1.5 h at 37 °C in a 5% CO… varying concentrations of α-MSH (*a*) or bovine TSH (*b*) in the pre… or absence of 0.7 nM agouti for 40 min in cyclase assay incu… medium (Dulbecco's modified Eagle's medium containing 0.1 m… bovine serum albumin and 0.1 mM isobutylmethylxanthine). M… was aspirated and 2.5% perchloric acid containing 0.1 mM cAM… used to stop the incubation. Adenylyl cyclase activity was calc… by determining the per cent conversion of ^{3}H-adenine to ^{3}H-cA… described[23,24]. Correlation of cAMP accumulation measured i… assay with actual adenylyl cyclase activity is made under the as… tion that isobutymethylxanthine effectively blocks cAMP degra… Data represent means and standard deviations from triplicat…

autonomic control. Surprisingly, agouti was also found to be a potent antagonist of α-MSH activation of the MC4-R (Fig. 4*a*). Once again, the protein appeared to act like a competitive antagonist, not significantly interfering with maximal activation of the receptor. The same concentration of agouti (0.7 nM) did not antagonize activation of the MC3 or MC5 receptors, and the MC5-R was unaffected even at 100 nM agouti concentrations (Fig. 4*b*, *c*).

Our results show that agouti is a high-affinity antagonist of the MSH-R, and of at least one of the other melanocortin receptors. Agouti appears to function as a competitive antagonist, inhibiting agonist binding to the MSH-R. This unique bifunctional regulation of the MSH-R by α-MSH and agouti allows for fine spatial and temporal regulation of eumelanin and phaeomelanin synthesis. These findings also provide a context for understanding the complex interactions of agouti and extension (MSH-R)

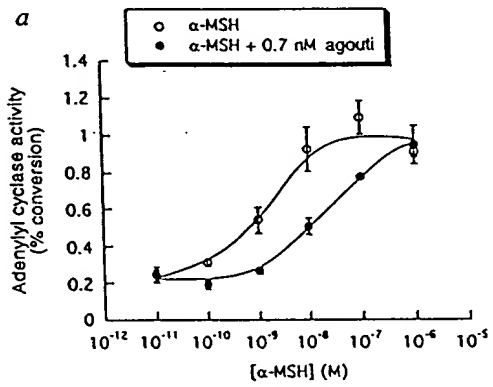

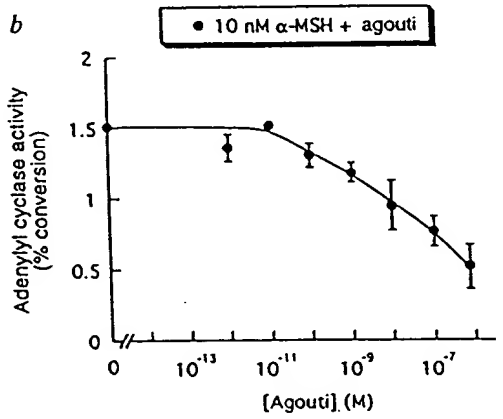

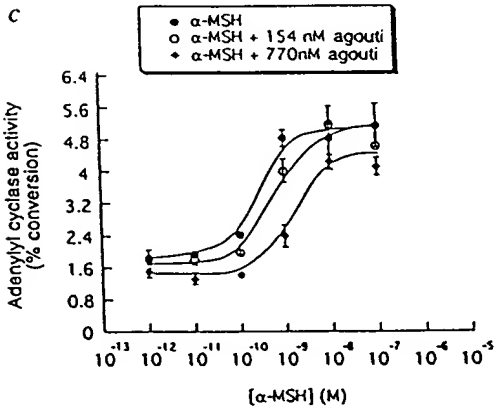

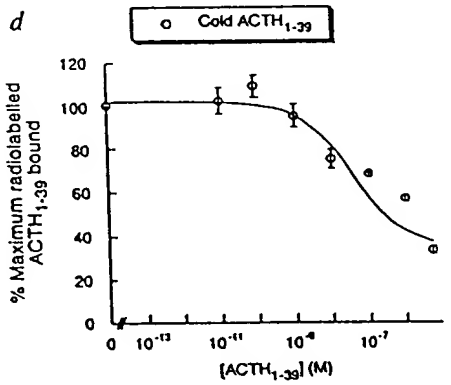

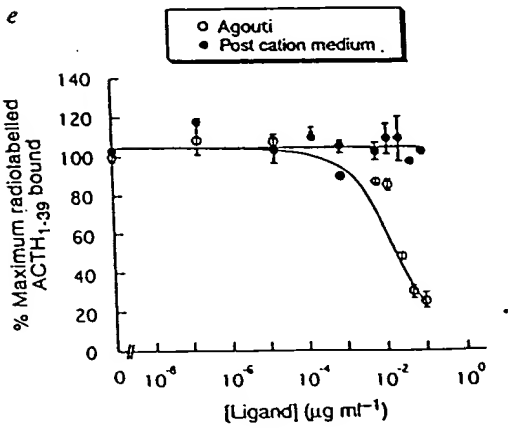

FIG. 3 Agouti is an antagonist of α-MSH at the murine MSH receptor. *a*, Agouti inhibits activation of the mMSH-R by α-MSH in stably transfected 293 cells, as monitored by stimulation of adenylyl cyclase. *b*, Agouti inhibition of murine MSH-R activation is dose-responsive. mMSH-R expressing 293 cells were stimulated with 10 nM α-MSH in the presence of agouti (10^{-12}–7×10^{-7} M). *c*, Agouti inhibits activation of human MSH-R at high protein concentrations. No inhibition of MSH-R activation by 0.7 nM agouti was observed. EC_{50} values were $2.3 \pm 0.8 \times 10^{-10}$ M (no agouti), $8.8 \pm 2.1 \times 10^{-10}$ M (154 nM agouti), and $1.1 \pm 1.5 \times 10^{-9}$ M (770 nM agouti). *d*, Competition binding demonstrates murine MSH-R expression in the Cloudman M-3 melanoma cell line. *e*, Competition binding demonstrates agouti protein blocks ^{125}I-labelled $ACTH_{1-39}$ binding to mouse MSH-R. Baculovirus supernatants from SF9 cells infected with a virus containing an unrelated gene insert were purified in parallel with agouti protein and did not block ^{125}I-labelled $ACTH_{1-39}$ binding to MSH-R up to 0.01 μg ml^{-1}. Values are shown as protein concentrations to compare agouti with control protein. METHODS. *a*–*c*, Adenylyl cyclase activity was measured as for Fig. 2. EC_{50} values were calculated using GraphPad InPlot version 4.0. *d*, *e*, Competition binding with radiolabelled ACTH has been described[25]: 1×10^6 cells were washed twice with binding medium and incubated in binding medium containing 9×10^{-11} M ^{125}I-labelled $ACTH_{1-39}$ (200,000 c.p.m.; Amersham) and different concentrations of agouti, control protein or cold ACTH for 2 h at 22 °C. Cells were then washed, lysed and counted as before[25] and data were analysed using the Kaleidagraph software package. Nonspecific binding, determined as the amount of radioactivity bound at 10^{-5} M cold ACTH, was 10% of the total counts bound.

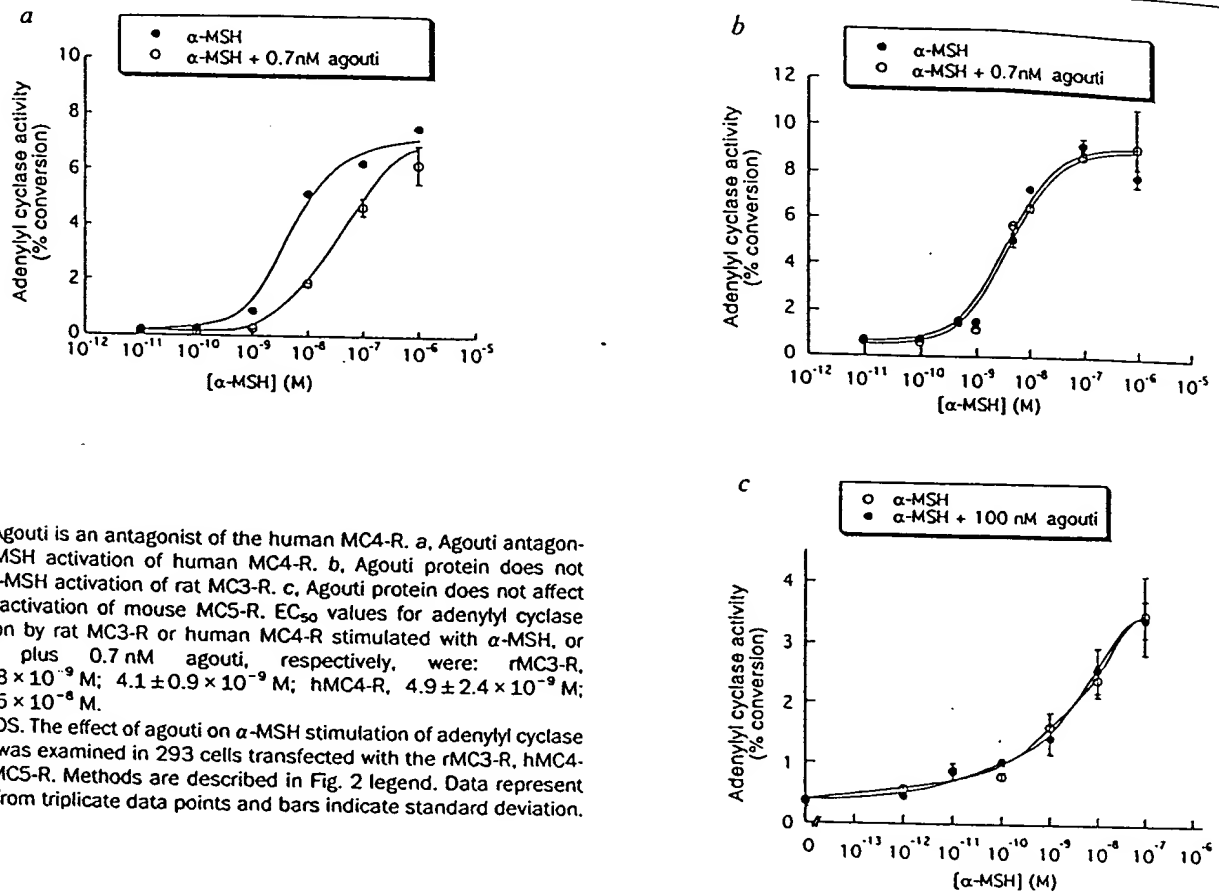

FIG. 4 Agouti is an antagonist of the human MC4-R. *a*, Agouti antagonizes α-MSH activation of human MC4-R. *b*, Agouti protein does not affect α-MSH activation of rat MC3-R. *c*, Agouti protein does not affect α-MSH activation of mouse MC5-R. EC_{50} values for adenylyl cyclase activation by rat MC3-R or human MC4-R stimulated with α-MSH, or α-MSH plus 0.7 nM agouti, respectively, were: rMC3-R, $4.2 \pm 0.8 \times 10^{-9}$ M; $4.1 \pm 0.9 \times 10^{-9}$ M; hMC4-R, $4.9 \pm 2.4 \times 10^{-9}$ M; $3.3 \pm 0.5 \times 10^{-8}$ M.
METHODS. The effect of agouti on α-MSH stimulation of adenylyl cyclase activity was examined in 293 cells transfected with the rMC3-R, hMC4-R or mMC5-R. Methods are described in Fig. 2 legend. Data represent means from triplicate data points and bars indicate standard deviation.

responsible for many mammalian coat colour variants, such as the variable black and tan markings in the German shepherd, resulting from combinations of two *extension* (E^m, E) and three *agouti* (A^y, a^y, a^t) alleles[20].

Because agouti also antagonizes MC4-R function, ectopic overexpression of agouti may lead to obesity in the lethal yellow mouse (A^y) through pathological antagonism of melanocortin receptor(s) expressed outside the hair follicle. Although no agouti pigmentation phenotype has ever been reported in humans, a gene encoding a conserved human agouti protein has been found[21] and so may have a physiological role. □

Received 13 June; accepted 15 September 1994.

1. Silvers, W. K. *The Coat Colors of Mice: A Model for Mammalian Gene Action and Interaction* (Springer, New York, 1979).
2. Robbins, L. S. *et al. Cell* **72**, 827–834 (1993).
3. Buttman, S. J., Michaud, E. J. & Woychik, R. P. *Cell* **71**, 1195–1204 (1992).
4. Miller, M. W. *et al. Genes Dev.* **7**, 454–467 (1993).
5. Silvers, W. K. & Russel, E. S. *J. exp. Zool.* **130**, 199–220 (1955).
6. Lamoreux, M. L. & Mayer, T. C. *Devl Biol.* **46**, 160–166 (1975).
7. Gantz, I. *et al. J. biol. chem.* **268**, 15174–15179 (1993).
8. Mountjoy, K. G. *et al. Molec. Endocr.* **8**, 1298–1308 (1994).
9. Dickerson, G. E. & Gowen, J. W. *Science* **105**, 496–498 (1947).
10. Conklin, B. R. & Bourne, H. R. *Nature* **364**, 110 (1993).
11. Jackson, I. J. *Nature* **362**, 587–588 (1993).
12. Siegrist, W. *et al. J. Rec. Res.* **8**, 323–343 (1988).
13. Frazier, A. L. *et al. Molec. Endocr.* **4**, 1264–1276 (1990).
14. Mountjoy, K. G. *et al. Science* **257**, 543–546 (1992).
15. Roselli-Rehfuss, L. *et al. Proc. natn. Acad. Sci. U.S.A.* **90**, 8856–8860 (1993).
16. Chhajlani, V. & Wikberg, J. E. S. *FEBS Lett.* **309**, 417–420 (1992).
17. Ganz, I. *et al. J. biol. Chem.* **268**, 8246–8250 (1993).
18. Chhajlani, V., Muceniece, R. & Wikberg, J. E. S. *Biochem. biophys. Res. Commun.* **195**, 866–873 (1993).
19. Desamaud, F. *et al. Biochem. J.* **293**, 367–373 (1994).
20. Little, C. C. *The Inheritance of Coat Colors in Dogs* (Macmillan, New York, 1957).
21. Kwon, H. Y. *et al. Proc. natn. Acad. Sci. U.S.A.* (in the press).
22. Summers, M. D. & Smith, G. E. *Texas Agric. exp. St. Bull.* 1555 (1987).
23. Salomon, Y. *Meth. Enz.* **195**, 22–28 (1991).
24. Johnson, R. A. & Salomon, Y. *Meth. Enzym.* **195**, 3–21 (1991).
25. Rainey, W. E., Viard, I. Saez, J. M. *J. biol. Chem.* **264**, 21474–21477 (1989).

ACKNOWLEDGEMENTS. This work was supported by NIH grants (R.D.C.), and by the Office of Health and Environmental Research, US Department of Energy, under contract with Martin Marietta Energy Systems, Inc. (R.P.W.). We thank J. Weiel, P. DeLacey, and K. Lewis for their help and M. Furth and T. Kenakin for discussion.

Inefficient gene transfer by adenovirus vector to cystic fibrosis airway epithelia of mice and humans

Barbara R. Grubb, Raymond J. Pickles, Hong Ye, James R. Yankaskas, Ralph N. Vick, John F. Engelhardt*, James M. Wilson*, Larry G. Johnson & Richard C. Boucher

CF/Pulmonary Research and Treatment Center, University of North Carolina at Chapel Hill, Chapel Hill, North Carolina 27599-7020, USA
* Institute of Human Gene Therapy, University of Pennsylvania, Philadelphia, Pennsylvania 19104-4268, USA

THE success of adenoviral vectors for gene therapy of lung disease in cystic fibrosis (CF) depends on efficient transfer of the complementary DNA encoding the correct version of the cystic fibrosis transmembrane regulator (CFTR) to the affected columnar epithelial cells lining the airways of the lung. Pre-clinical studies *in vitro* suggest that low doses of adenovirus vectors carrying the CFTR cDNA can correct defective Cl^- transport in cultured human CF airway epithelia[1]. Here we use mice carrying the disrupted CF gene[2] to test the efficacy of this transfer system *in vivo*. We find that even repeated high doses can only partially (50%) correct the CF defect in Cl^- transport *in vivo* and do not correct the Na^+ transport defect at all. We investigated this discrepancy between the *in vivo* and *in vitro* transfer efficiency using CF mou

The Melanocortin Receptors: Agonists, Antagonists, and the Hormonal Control of Pigmentation

ROGER D. CONE,* DONGSI LU,* SANDHYA KOPPULA,* DAG INGE VAGE,† HELGE KLUNGLAND,† BRUCE BOSTON,* WENBIAO CHEN,* DAVID N. ORTH,‡ COLIN POUTON,§ AND ROBERT A. KESTERSON*

Vollum Institute for Advanced Biomedical Research, Oregon Health Sciences University, Portland, Oregon 97201; †Department of Animal Science, Agricultural University of Norway, Ås, Norway N-1432; ‡Department of Medicine, Vanderbilt University Medical Center, Nashville, Tennessee 37232–6306; §School of Pharmacy and Pharmacology, University of Bath, Bath, BA2 7AY United Kingdom

ABSTRACT

Molecular cloning experiments have led to the identification and characterization of a family of five receptors for the melanocortin (melanotropic and adrenocorticotropic) peptides. The first two members of the family cloned were the well-characterized melanocyte-stimulating hormone receptor (MSH-R) and adrenocorticotropin receptor (ACTH-R). The three new melanocortin receptors have been termed the MC3-R, MC4-R, and MC5-R, according to the order of their discovery, and little is known at this point concerning their function.

Agouti and *extension* are two genetic loci known to control the amounts of eumelanin (brown-black) and phaeomelanin (yellow-red) pigments. Chromosomal mapping demonstrated that the MSH-R, now termed MC1-R, mapped to *extension*. *Extension* was shown to encode the MC1-R, and mutations in the MC1-R are responsible for the different pigmentation phenotypes caused by this locus. Functional variants of the MC1-R, originally characterized in the mouse, have now also been identified in the guinea pig and cow. Dominant constitutive mutants of the MC1-R are responsible for causing dark black coat colors while recessive alleles result in yellow or red coat colors.

Agouti, a secreted 108 amino acid peptide produced within the hair follicle, acts on follicular melanocytes to inhibit α-MSH-induced eumelanin production. Experiments demonstrate that *agouti* is a high-affinity antagonist, acting at the MC1-R to block α-MSH stimulation of adenylyl cyclase, the effector through which α-MSH induces eumelanin synthesis. The MC1-R is thus a unique bifunctionally controlled receptor, activated by α-MSH and antagonized by *agouti*, both contributing to the variability seen in mammalian coat colors. The variable tan and black coat color patterns seen in the German Shepherd, for example, can now be understood on the molecular level as the interaction of a number of *extension* and *agouti* alleles encoding variably functioning receptors and a differentially expressed antagonist of the receptor, respectively.

I. Introduction

Pigmentation is not ordinarily classified as an endocrinological phenomenon. Nevertheless there are many fascinating and striking examples of hormonal control of hair and skin color, such as the seasonal control of pelage in the snowshoe

hare, *Leptus americanus* (Searle, 1968), or the arctic fox, *Alopex lagopus* (Nes *et al.*, 1988); adaptation to background color in reptiles; and the hyperpigmentation in humans from endocrine disorders such as Addison's disease that result in elevation of circulating adrenocorticotropin (ACTH) levels. One pathway for hormonal control of pigmentation has been elucidated recently with the molecular characterization of the melanocyte-stimulating hormone (MSH) receptor (Mountjoy *et al.*, 1992) and the antagonist of this receptor, known as the *agouti* signaling peptide (Bultman *et al.*, 1992; Lu *et al.*, 1994; Miller *et al.*, 1993). It has been known for many years that two genetic loci, *extension*, which encodes the MSH receptor, and *agouti* are commonly involved in controlling the regional distribution of brown-black (eumelanin) and yellow-red (phaeomelanin) pigments in the coat of an animal, as well as the distribution of these two pigments along each individual hair shaft (Searle, 1968). For example, the varying distribution of tan and black pigments in the German Shepherd dog results from the interaction of a number of alleles at *extension* and *agouti* (Little, 1957).

The principal pigment cells, melanocytes, elaborate a number of enzymes that act in concert to synthesize from tyrosine both eumelanin and phaeomelanin, the two major classses of melanin pigments. The rate-limiting enzyme in this process, tyrosinase (Hearing and Jimenez, 1987; Pawelek, 1976), is regulated both transcriptionally and post translationally by intracellular cAMP (Fuller *et al.*, 1987; Halaban *et al.*, 1984; Hoganson *et al.*, 1989; Wong and Pawelek, 1975). Phaeomelanin is the major default product of this biosynthetic pathway, with eumelanin synthesis resulting from increased tyrosinase activity. MSH, produced by the melanotroph cells of the intermediate lobe of the pituitary and also possibly in keratinocytes and hair follicle cells, is the primary hormonal regulator of pigmentation and acts by binding to its receptor and elevating intracellular cAMP, thus inducing tyrosinase activity. Similarly, *agouti* has been known for some time to be produced by the hair follicle and act in trans on the follicular melanocytes to inhibit eumelanin synthesis, thereby resulting in phaeomelanin production (Silvers, 1958; Silvers and Russel, 1955).

The molecular nature of different MSH receptor alleles and their interaction with the agonist MSH and the antagonist *agouti* to produce variation in mammalian coat color is the main subject of this review. The ability of the *agouti* peptide, when expressed outside of the hair follicle, to cause obesity will also be examined. To discuss either of these subjects it is necessary to first review the melanocortin peptides and their receptors.

II. The Melanocortin Peptides

The term "melanocortin" refers to peptides derived from the larger proopiomelanocortin (POMC) polypeptide precursor that possess melanotropic or adrenocorticotropic activity (Fig. 1A). These peptides are produced primarily in the anterior and intermediate lobes of the pituitary and in lower levels in the arcuate nucleus and nucleus of the solitary tract in the brain. POMC has also been

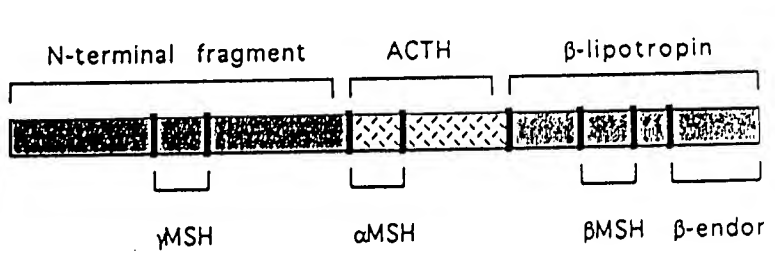

B

ACTH H2N-SYSMEHFRWGKPVGKKRRPVKVYPNGAEDESAEAFPLE
α-MSH AC-SYSMEHFRWGKPV-NH2
β-MSH H2N-AEKKDEGPYRMEHFRWGSPPKD-OH
γ-MSH H2N-YVMGHFRWDRFG-OH
NDP-MSH AC-SYSXEHZRWGKPV-NH2

FIG. 1. The melanocortin peptides. (A) Structure of the proopiomelanocortin (POM cursor. Major melanocortin peptides are indicated by brackets and basic dipeptide proteolytic c sites are indicated by the heavy bars. (B) Amino acid sequence of the major melanocortin p All peptides are derived from human POMC with the exception of Nle⁴, D-Phe⁷-α-MSH (NDP a potent synthetic analogue. The conserved H-F-R-W pharmacophore is underlined. In the se of NDP-MSH, X represents norleucine and Z represents D-phenylalanine. [Reprinted with per from *Ann. N.Y. Acad. Sci.* 680, 343, 1995.]

reported to be expressed in several other tissues, including keratinocytes ar follicle cells, which may be particularly relevant to pigmentation as disc below. These peptides are processed from three different regions of POMC of which contains a conserved sequence, -His-Phe-Arg-Trp-, that serves pharmacophore for melanocortin receptor recognition and activation (Fi (Eberle, 1988; Eberle *et al.*, 1984). Peptides from the amino terminus or minal POMC are called γ-MSH peptides and are found in a variety of ACTH and α-MSH are overlapping peptides cleaved from the middle portic consist of amino acids 1–39 and 1–13, respectively. β-MSH, β-LPH, and γ all derive from the carboxy-terminal portion of the POMC precursor. A de account of the tissue-specific cleavage and processing of these peptides ha reviewed elsewhere (Smith and Funder, 1988).

III. The Melanocortin Receptors

Prior to cloning, two melanocortin receptors, the MSH receptor (M and the ACTH receptor (ACTH-R) were known from classical physiologic pharmacological studies. The MSH receptor was specifically found on m

cytes and melanoma cells from a variety of vertebrate organisms, and was reported to respond to nanomolar concentrations of α-MSH by stimulating tyrosinase activity and melanogenesis subsequent to activation of adenylyl cyclase and elevation of intracellular cAMP (Pawelek, 1976). Cross-linking studies had demonstrated this receptor to be present as a molecular species of approximately 45 kd (Gerst *et al.*, 1988; Solca *et al.*, 1989). A high-affinity ACTH receptor had been demonstrated to be expressed in both adrenocortical cells as well as adipocytes, and like the MSH receptor, was found to couple to activation of adenylyl cyclase (Buckley and Ramachandran, 1981; Oelofsen and Ramachandran, 1983).

Two lines of evidence also suggested the presence of high-affinity melanocortin receptors outside of the melanocyte and adrenal cortex, particularly in the central nervous system. First, a large body of literature demonstrated a variety of activities for the melanocortin peptides in the brain (for review, see DeWied and Jolles, 1982). These included, for example, central effects on learning and memory (Garrud *et al.*, 1974; Sandman *et al.*, 1969), temperature regulation (Feng *et al.*, 1987), hypothalamic-pituitary-adrenal (H-P-A) axis control (Calogero *et al.*, 1988; Motta *et al.*, 1965; Suda *et al.*, 1986), and cardiovascular homeostasis (Calogero *et al.*, 1988; Gruber and Callahan, 1989; Motta *et al.*, 1965; Suda *et al.*, 1986). Peripheral effects on inflammation (Catania and Lipton, 1993), nerve regeneration (Bijlsma *et al.*, 1981; Strand and Kung, 1980; Strand *et al.*, 1991), and myoblast proliferation (De Angelis *et al.*, 1992) had also been reported.

Second, high-affinity MSH and ACTH binding sites were reported in the lacrimal gland, brain, and a variety of peripheral sites (Hnatowich *et al.*, 1989; Salomon *et al.*, 1993; Tatro, 1990; Tatro and Reichlin, 1987). Little pharmacological data accompanied these reports, so it was not possible to ascertain whether these were MSH-R, ACTH-R, or novel melanocortin receptor sites.

Our first cloning of melanocortin receptors resulted from attempts to isolate the MSH-R from a human melanoma sample known to express a high number of MSH binding sites (Mountjoy *et al.*, 1992). Degenerate oligonucleotides were designed to recognize all G protein-coupled receptor sequences known as of approximately 1991, and these were used in polymerase chain reaction (PCR) with first-strand cDNA from the melanoma tissue. A large number of resulting fragments were subcloned and sequenced, and one fragment was identified as a putative MSH receptor based on its ability to recognize a mRNA specifically expressed in melanocytes. This fragment was then used as a hybridization probe to clone a mouse MSH-R cDNA and a human genomic MSH-R sequence. The human MSH-R was independently cloned by Chhajlani and Wikberg (1992) using a similar method.

The amplification from human melanoma tissue also produced a sequence fragment that was clearly a unique G protein-coupled receptor highly related to the MSH-R. Northern hybridization analysis clearly demonstrated that this fragment recognized a mRNA specific to adrenal tissue and was thus a candidate ACTH-R. This probe was used to isolate a human genomic ACTH-R sequence

(Mountjoy *et al.*, 1992) as well as a bovine ACTH-R cDNA (Cone and Mour 1993).

PCR using degenerate oligonucleotide primers and low-stringency hy ization with existing MSH-R and ACTH-R sequences rapidly led to the disc of three additional members of the melanocortin receptor gene family (Bar *al.*, 1994; Chhajlani *et al.*, 1993; Desarnaud *et al.*, 1994; Fathi *et al.*, 1995; C *et al.*, 1993a,b, 1994a; Griffon *et al.*, 1994; Labbe *et al.*, 1994; Mountjoy 1994; Roselli-Rehfuss *et al.*, 1993). Since these receptors had not been ch terized previously using classical pharmacological or physiological methods have been called the melanocortin-3 , melanocortin-4, and melanocortin-5 r tors (MC3-R, MC4-R, and MC5-R), according to the order of their discover avoid confusion, many in the field now refer to the MSH-R and ACTH- MC1-R and MC2-R, respectively, and the corresponding loci in the mous human genome use this nomenclature as well.

As mentioned above, the MSH-R and ACTH-R appear to be restrict their expression primarily to melanocytes and adrenocortical cells. Norther bridization analysis has demonstrated MC3-R expression in brain and plac although reverse transcription-polymerase chain reaction (RT-PCR) has used to detect the mRNA in stomach, duodenum, and pancreas (Gantz 1993a). *In situ* hybridization has been used to map MC3-R mRNA to 30 diff rat brain nuclei primarily in hypothalamus and other limbic system struc (Roselli-Rehfuss *et al.*, 1993).

The MC4 receptor mRNA has been found by northern hybridization expressed only in the brain (Gantz *et al.*, 1993b). Detailed neuroanatomical ping by *in situ* hybridization demonstrated that this receptor mRNA is much widely expressed in the rat brain than the MC3-R, being found in 148 diff brain nuclei in virtually every brain region including cortex, thalamus, hypo amus and limbic system, brain stem, and spinal cord (Mountjoy *et al.*, 199-

More recently, the MC5-R was cloned from human (Chhajlani *et al.*, 1 mouse (Fathi *et al.*, 1995; Gantz *et al.*, 1994a; Labbe *et al.*, 1994), rat (Gr *et al.*, 1994), and sheep (Barret *et al.*, 1994). This receptor mRNA has a rem ably wide distribution of expression, being found in skin, muscle, thymus, sp ovary, testis, adrenal cortex, lung, brain, and pars tuberalis. The distributi all five receptors is summarized in Table I.

TABLE I

The Melanocortin Receptors

Receptor	Sites of expression	Functions
MC1 (MSH-R)	Melanocytes	Pigmentation
MC2 (ACTH-R)	Adrenal cortex, adipocytes	Steroidogene
MC3	Hypothalamus, limbic system, placenta, gut	Unknown
MC4	Hypothalamus, limbic system, cortex, brain stem	Unknown
MC5	Muscle, liver, spleen, lung, brain, adipocytes ...	Unknown

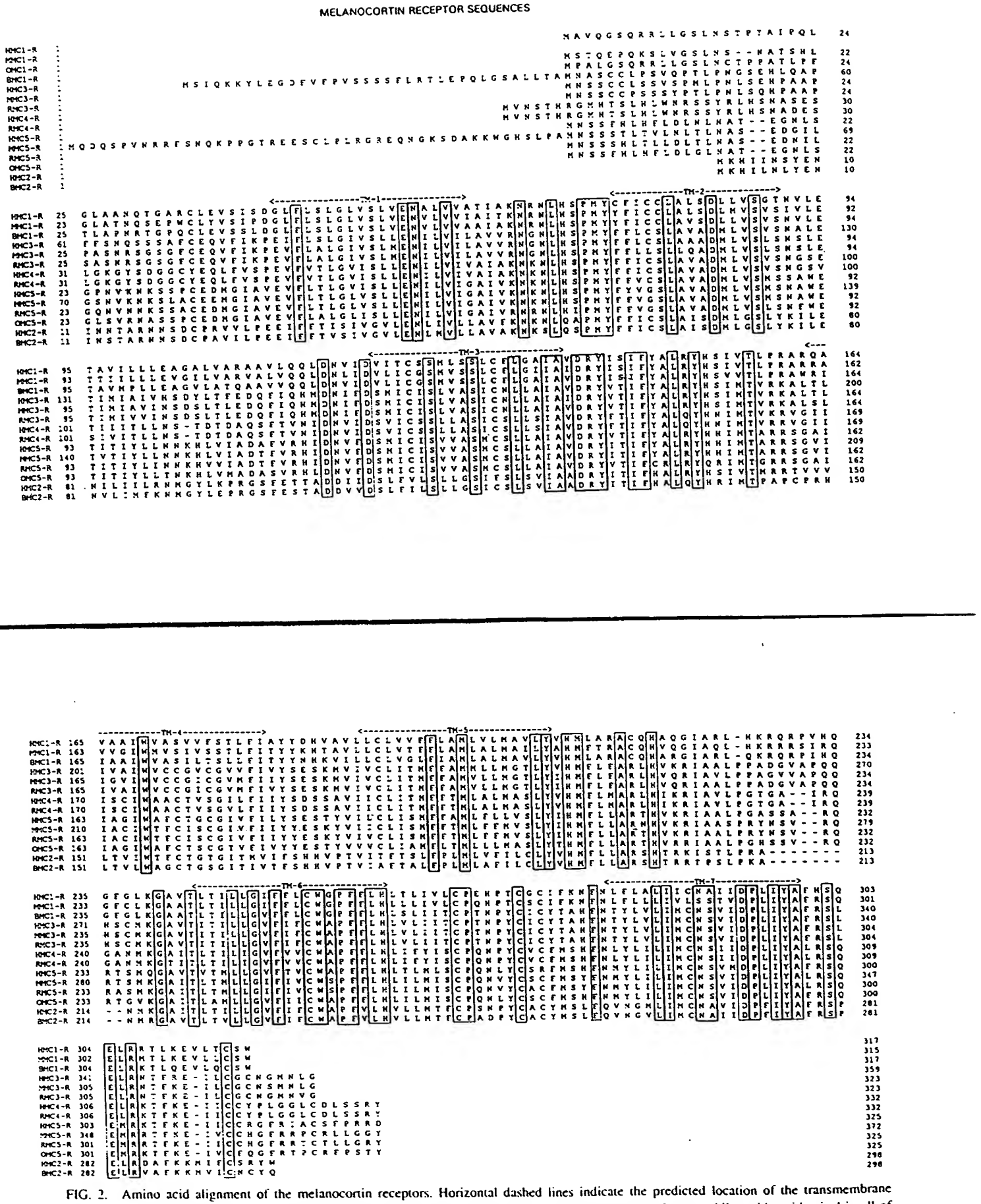

FIG. 2. Amino acid alignment of the melanocortin receptors. Horizontal dashed lines indicate the predicted location of the transmembrane domains. Amino acid residues conserved in many of the G protein-coupled receptors are indicated by heavy boxes, while residues identical in all of the known melanocortin receptors are indicated by the light boxes. Prefixes to each receptor indicate the species (H, human; M, mouse; R, rat; B,

The five melanocortin receptors are 39–61% identical to one another on the amino acid level, and all belong to the large superfamily of G protein-coupled receptors (Fig. 2). Interestingly, the MC3, MC4, and MC5 receptors appear more related to one another (55–61%) than to the MC1 and MC2 receptors (43–46%), and the MC1 and MC2 receptors are the most distantly related (39%).

Each of the melanocortin receptors couples to activation of adenylyl cyclase but displays a unique pharmacological profile for activation by the different melanocortin peptides (Fig. 3). One report suggests that the MC3-R may also couple to Gq, resulting in a modest activation of inositol 1,3,4-trisphosphate turnover as well (Konda *et al.*, 1994). In a sense, the MC1 and MC2 receptors are the most specialized in terms of ligand recognition. The MC2 receptor exhibits an absolute specificity for ACTH, requiring two peptide domains for recognition and activation, the core H-F-R-W sequence present in all the melanocortin peptides and a highly basic motif found only in the midportion of ACTH. This makes the ACTH receptor unique; the core H-F-R-W pharmacophore is a full agonist, albeit at low affinity, of the other four melanocortin receptors. Most mammalian MC1-Rs demonstrate a preference for α-MSH over ACTH. α-MSH is five-fold more

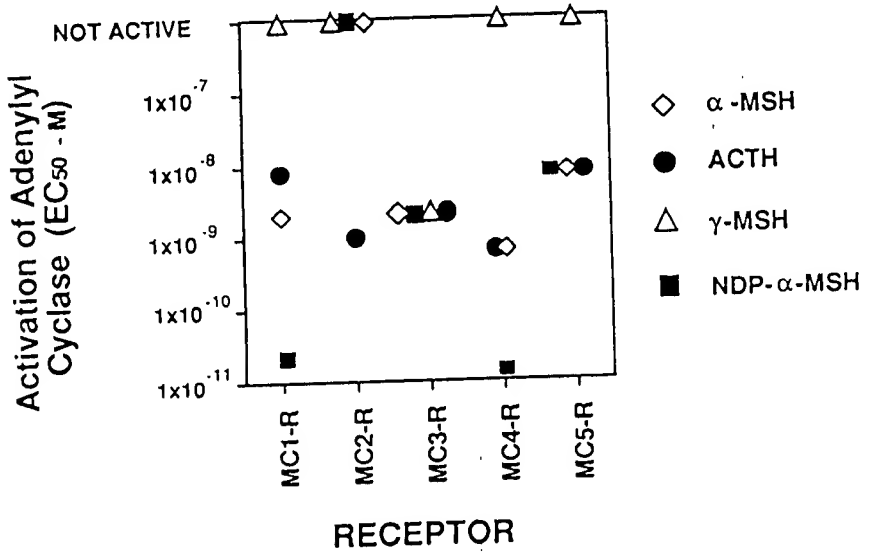

FIG. 3. Pharmacology of the melanocortin receptors. Data represent published EC_{50} values for activation of adenylyl cyclase for each receptor by the peptides indicated. Not active means an EC_{50} >> 10^{-7}M. In the case of the MC2-R, except for ACTH, no activity at all is seen at peptide concentrations up to μM. Data from Mountjoy *et al.*, 1992 (MC1-R), Buckley *et al.*, 1981 (MC2-R), Roselli-Rehfuss *et al.*, 1993 (MC3-R), Mountjoy *et al.*, 1994 (MC4-R), and W. Chen, unpublished data (MC5-R).

potent than ACTH at the murine receptor but may be as high as 1000-fold the MC1-R in *Rana pipiens* or *Anolis carolinenesis* (Eberle, 1988; Eberle *et* 1984). The human MC1-R is apparently unique in responding to ACTH at sim or even lower EC_{50} values than those for α-MSH (Abdel-Malek *et al.*, 1995; *et al.*, 1994; Mountjoy, 1994).

In contrast, the MC3-R, MC4-R, and MC5-R are less selective, being potently activated by α-MSH or ACTH. Furthermore, the MC3-R and MC are activated equally well by the predominant form of α-MSH found in the riphery (monoacetyl-α-MSH) as well as the brain (desacetyl-α-MSH) (Mou *et al.*, 1994). The peripheral MC1-R tends to be less potently activated by desacetyl form (Eberle, 1988; Mountjoy, 1994). Interestingly, only one of the receptors, MC3-R, binds γ-MSH with high affinity (Gantz *et al.*, 1993a; Ro Rehfuss *et al.*, 1993).

The chromosomal location of all five melanocortin receptors has been mined in humans by fluorescent *in situ* hybridization (Chowdhary *et al.*, Gantz *et al.*, 1993b, 1994b; Magenis *et al.*, 1994; Malas *et al.*, 1994; Vamv poulos *et al.*, 1993) (Table II). The chromosomal locations in the mouse MC1-R, MC2-R, MC3-R, and MC5-R have been determined using an inte specific mapping panel (Magenis *et al.*, 1994; R. Cone, unpublished data) surprisingly, the MC1-R was found to map to the distal end of chromosom the mouse, near a pigmentation locus known as *extension*. None of the receptors mapped to previously identified gene loci in humans or in the m However, a rare endocrine disorder, inherited ACTH resistance or familia cocorticoid deficiency, does map to the ACTH receptor locus in about half individuals with this disease . In these cases the disease appears to result mutations in the coding sequence of the ACTH-R (Clark *et al.*, 1993; Tsig *al.*, 1993). Difficulty in expression of the ACTH-R in heterologous cells, rep by a number of laboratories, has hampered the study of these ACTH-R al The recent report of a subclone of the mouse adrenocortical Y1 cell line that endogenous receptor expression may lead the way for further studies of

TABLE II

Human and Murine Map Locations of the Melanocortin Receptors

Receptor	Mouse chromosome	Human chrom
MSH-R	Distal end of Chr 8 identical with the *extension* locus	16q2
ACTH-R	Distal end of Chr18 near *Pdea*	18p11.2
MC3-R	Distal half of Chr 2 near *El-2*	20q13.2
MC4-R	RFLP not yet found	18q22
MC5-R	Distal end of Chr 18, near D18Mit9 and *sy*	18p11.

ACTH receptors (Schimmer *et al.*, 1995). Additionally, it has recently been reported that, in contrast to the human ACTH-R, the mouse ACTH-R is readily expressed in HeLa cells (Cammas *et al.*, 1995).

IV. Allelic Variants of the MC1 Receptor

The *extension* locus, characterized in a wide variety of mammalian species, was named for the extension of black pigmentation that results from the expression of dominant *extension* alleles (Fig. 4; Table III). Cloning of the MC1-R from mice containing different *extension* locus alleles (*e*, E^{Sa}, and E^{tob}) confirmed that the *extension* locus encoded the MC1 receptor, since 18 of 18 clones isolated from the homozygous recessive yellow *e/e* mouse had a frameshift mutation at amino acid position 183 of the receptor (Robbins *et al.*, 1993). At the time this

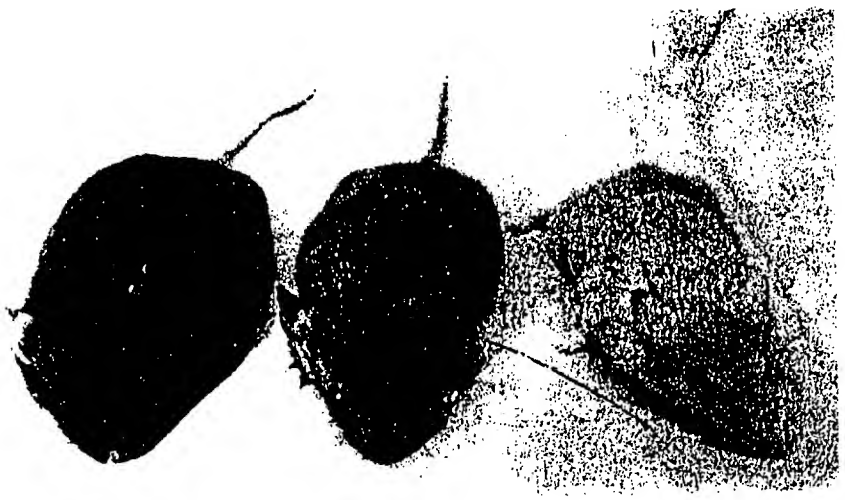

FIG. 4. Coat pigmentation in mice containing dominant, wild-type, and recessive alleles at the *extension* locus. The genotypes of the mice, from left to right, are $E^{Sa}E^{+}$, $E^{+}E^{+}$, and *ee*.

TABLE III
Examples of Mammalian Extension *Alleles*

Mice	Foxes	Cattle
E^{Sa}. . . . . dominant black	E^{A}. . . . dominant black	E^{d}. . . . dominant black
E^{tob}. . . . . dominant black		
E. . . . . normal extension of black	E. . . . . normal extension of black	E. . . . . normal extension of black
		e^{br}. . . . . brindled
e. . . . . non-extension of black		e. . . . . non-extension of black

was determined, no other naturally occuring functional variants in the G prot coupled receptors had been reported. Consequently, the existence of a large n ber of dominant alleles of this receptor across a wide number of species w very exciting prospect. A summary of all the mutations in the MC1-R ident to date is shown in Figure 5.

A. MOUSE

Initially we characterized two of the three dominant alleles found in mouse, E^{Sa-J} and E^{tob}. The tobacco allele, E^{tob}, is found in the darkly pigme wild tobacco mouse (*M. poschiavinus*) and results from a serine-to-leucine ch at position 69 in the first intracellular loop of the receptor. Pharmacologic when expressed in the heterologous 293 cell line, this receptor has a slig elevated basal activity but is also able to more significantly stimulate ader cyclase when compared directly to the wild-type receptor (Robbins *et al.*, 19 In contrast, the sombre allele E^{Sa-J}, which occurred spontaneously in the C J strain to produce a dark black mouse (Fig. 4), creates a receptor that is pote constitutively activated and not significantly stimulated even by treatment

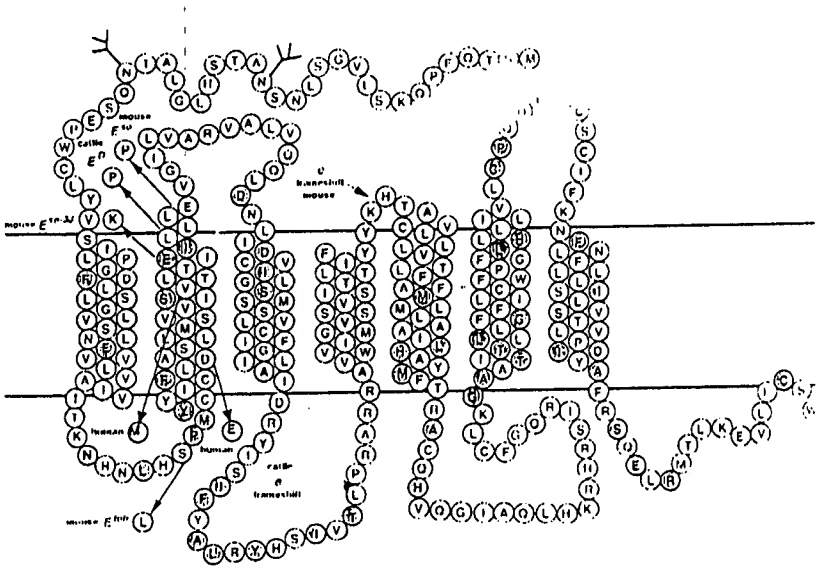

FIG. 5. Summary of mutations identified in the MC1-R. Graphic is a pseudostructural pl the MC1-R indicating putative transmembrane topology. Residues shaded gray are identical in melanocortin receptors. Mutations are described in more detail in Robbins *et al.*, 1993 (mouse). Klungland *et al.*, 1995 (cattle). [Reprinted with permission from *Cell* 72, 827–834. Copyright Cell Press.]

high concentrations of α-MSH (Fig. 6A). Preliminarily, we only examined the ability of α-MSH to stimulate this receptor. In subsequent experiments (Fig. 6B), we have discovered that the superpotent α-MSH analogue Nle^4, D-Phe^7-α-MSH (NDP-MSH) is capable of further activating the sombre receptor to maximal levels.

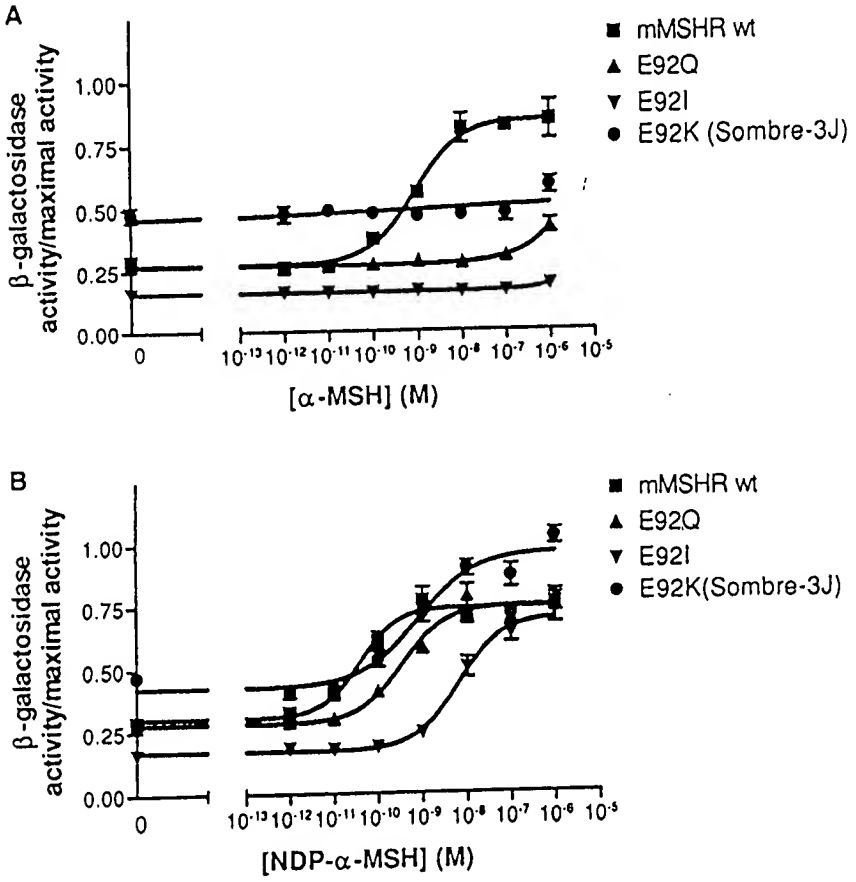

FIG. 6. Pharmacological properties of the mouse $E^{Som\text{-}3J}$ allele of the MC1-R. The wild-type MC1-R, $E^{Som\text{-}3J}$ allele containing the E92K mutation, and *in vitro*-generated E92Q and E92I mutants, cloned into the pcDNA Neo expression vector (Invitrogen), were transfected stably into the HEK 293 cell line. G418^r cell populations were selected and assayed for intracellular cAMP levels following hormone stimulation using a cAMP-dependent β-galactosidase reporter construct as described previously (Chen *et al.*, 1995). Data points are the average of triplicate determination with error bars indicating the standard deviation. Data is normalized to cell number and presented as % maximal activity (10 μM forskolin-stimulated) for each individual cell population. The forskolin-stimulated activities did not vary significantly among cell populations. Panels show data from stimulations with α-MSH (A) and NDP-MSH (B).

Pharmacological data from an independent occurence of the sombre a the mouse (E^{So}) has also been obtained recently. This allele results from a l to-proline change at position 98, and is pharmacologically very simila E92K allele ($E^{So\text{-}3J}$) (Fig. 7).

B. CATTLE

Recent data show that black coat color in Norwegian cattle is due to inant extension allele, E^D, resulting from a L99P mutation (Fig. 5) (Klun *al.*, 1995). This mutation is one amino acid carboxy-terminal to the mo mutation, and suggests that any disruption of the α-helix in this region mi be expected to constitutively activate the receptor, although this mutation yet been characterized pharmacologically. This group also demonstrated coat color in Norwegian cattle breeds is due to a frameshift in the MSH r (Fig. 5). Since the frameshift in the mouse results in a yellow coat col clear that modifier genes must exist that can control the range of phaeo pigment.

C. HUMANS

Tremendous polymorphism of skin, hair, and eye color is seen in h and it would be interesting to determine if any of this results from fu variants of the MC1 receptor. To approach this problem we have obtained s resulting from dermatologic procedures derived from patients characteriz

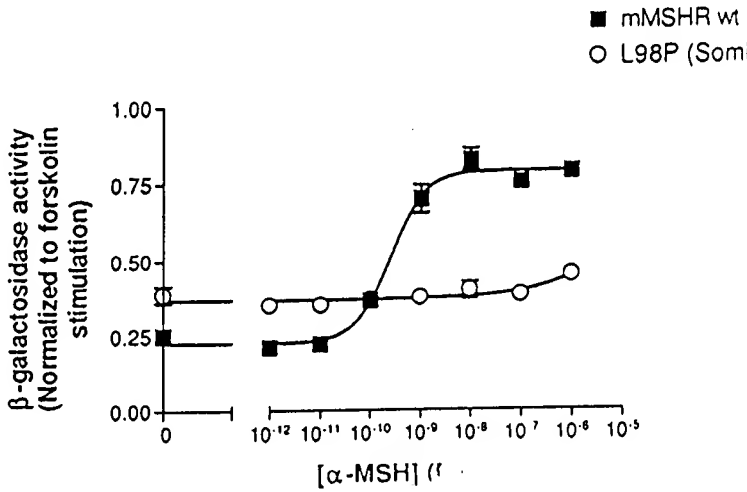

FIG. 7. Pharmacological properties of the mouse E^{So} allele of the MC1-R. The E^{So} the MC1-R, containing the L98P mutation, was characterized as described in Figure 6.

regard to hair and eye color and skin type. This latter characteristic was determined according to the method of Fitzpatrick (Pathak *et al.*, 1987) and is a general indicator of the degree of melanization of the skin. MC1 receptor coding fragments were isolated from these samples by PCR and sequenced following subcloning. After completing the sequence of the receptors from only a small number of individuals, two coding polymorphisms of the MC1-R were identified, V92M and D84E. Individuals were found that were both heterozygous and homozygous for V92M, and the one D84E allele was found in an individual that was a compound heterozygote, also containing the V92M allele (Table IV). Interestingly, the V92M allele does appear nonrandomly distributed across individuals categorized according to skin type, being present in type I individuals with an allele frequency of 0.11 and individuals with type II skin at a frequency of 0.02. In preliminary experiments we do not see any pharmacological consequences of these polymorphisms. Nevertheless, it is intriguing that these alterations cluster in TM2 along with other naturally occuring variants of the receptor found in other species (Fig. 5).

D. GUINEA PIG

Variegated pigment patterns (i.e. coats containing an irregular patchwork of two or more colors) have often been associated with heterozygosity of X-linked pigment genes in the female animal. A classic example is the orange locus (*O*) in the cat, resulting from X chromosome inactivation in the female as proposed by Lyon (1961). Males and homozygous females containing this allele are yellow-orange while heterozygous females (*+/O*) have the tortoise-shell or calico coat consisting of irregularly distributed patches of yellow and brown pigment. Yet variegated brindle and tortoise-shell coat color patterns map to the autosomal *extension* locus in a variety of mammals, including the rabbit, dog, cattle, pig, and guinea pig (Searle, 1968).

We were fascinated by this example of variegated gene function at the *extension* locus, and chose to begin a study of the problem in the guinea pig, in which an allele, e^{y}, produces the tortoise-shell coat pattern in homozygous male or female animals. Our initial hypothesis was that such a phenotype might result from variable MC1-R gene expression that could be easily detectable as a gene

TABLE IV
Characteristics of Individuals with MC1R Polymorphisms

Individuals	Skin type	Eye color	Hair color	Genotype
1	I	Blue	Blond	D84E/V92M
2	I	Blue	Blond	+/V92M
3	I	Green	Blond	V92M/V92M
4	II	Brown	Black	+/V92M

re-arrangement. Analysis of the MC1-R gene locus by Southern hybridizati not confirmed this (Fig. 8). Interestingly, however, after probing DNA fr black, tortoise-shell, and red guinea pig with a small coding sequence fra of the mouse MC1-R, we did observe a large deletion in this gene in t guinea pig. This confirms the observations in the mouse and in cattle that a of functional MC1 receptor does not affect melanocyte development or mi into the skin and hair follicle, but simply ablates exp ssion of eumelanin coat of the animal. Further work will be required to understand the mec of variegated function of the MC1-R in tortoise-shell and brindle animals

V. Structure/Function Studies of the MSH Receptor

We have taken information from three different lines of experimenta attempt to develop a model of the structure of the MC1-R. First, clonir sequence determination of all five melanocortin receptors has allowed us certain which residues are identical or conserved in all the receptors (Figs. 5). Second, this information was then used by one of us (C.W.P.) to cons three-dimensional computer model of the receptor (Fig. 9) using recent mation from a low-resolution model of rhodopsin (Schertler *et al.*, 1993) with the molecular model for rhodopsin proposed by Baldwin (1993). The pieces of information have suggested the presence, in particular, of five con residues in close proximity (Phe43, Phe278, Glu92, Asp119, and Asp 11 might form the basis of a binding pocket for the His-Phe-Arg-Trp pharmac of the melanocortins. The Phe and Trp residues might form stacking inter with the two receptor Phe residues, while the Arg and His residues in th macophore could form electrostatic interactions with the Glu92 and/or A 115 residues.

Finally, we have tried to use information from constitutively active r mutants to understand how the receptor can undergo a transition from a qu state to an active state, albeit in this case in the absence of ligand. Initia proposed a model for the sombre receptor similar to that proposed for mu that constitutively activate rhodopsin (Robinson *et al.*, 1992). In the case dopsin, a naturally occuring mutation in K296 resulted in a receptor that tutively activates transducin in the absence of light or 11-cis-retinal. Th mophore 11-cis retinal is covalently attached to the receptor via a Schi linkage involving the ε amino group of K296. Stabilization of the prot Schiff base is brought about through interaction with the negatively charg tamic acid at position 113. It is thought that light-induced isomerization chromophore moves the protonated Schiff base away from E113, and disr of the E113-K296 salt bridge results in deprotonation of the Schiff base ni known to be involved in formation of the active state of rhodopsin. Thus, been proposed that mutagenesis of either of these residues produces an

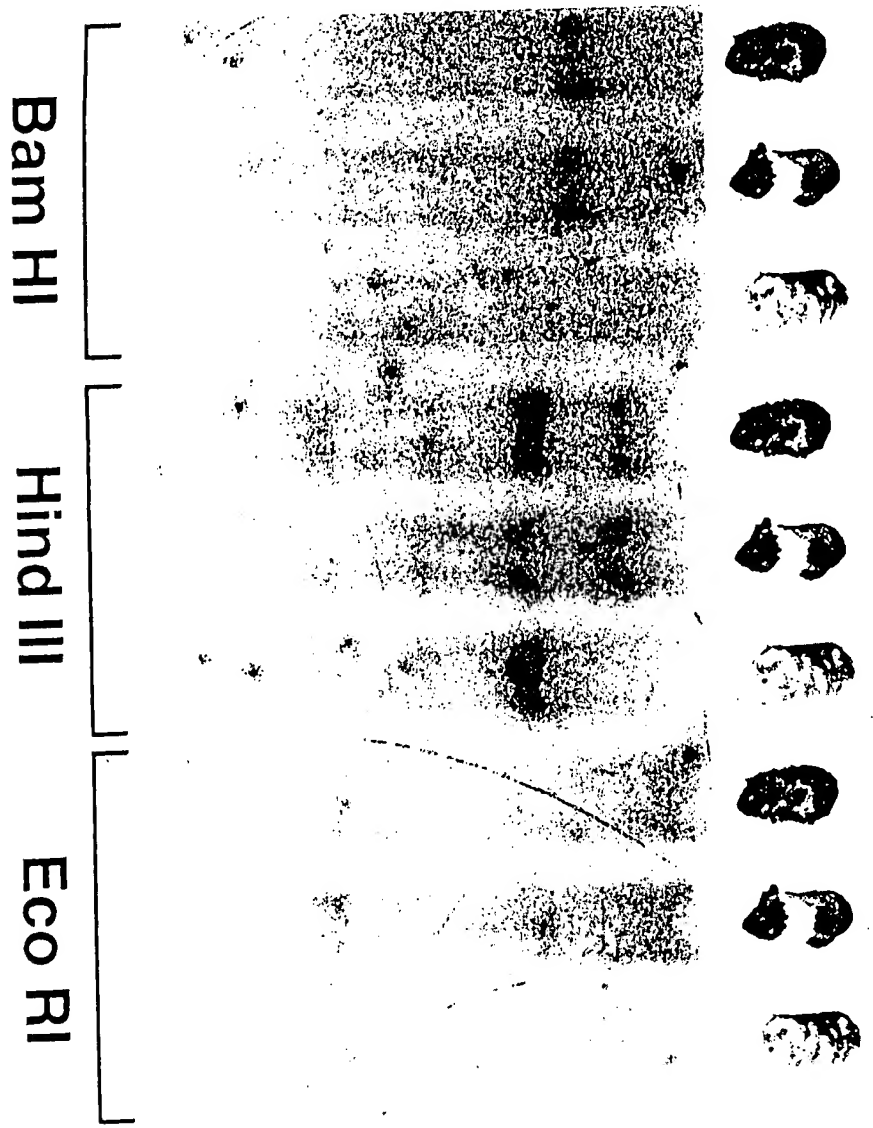

FIG. 8. Southern hybridization analysis of the guinea pig MC1-R locus. Whole blood from the black, tricolor, and red guinea pig was obtained from Pioneer Animal Supply (Mt. Vernon, OH). Genomic DNAs were prepared and treated with the restriction enzymes indicated. The order of samples in each panel are (from left to right) black, tricolor, and red. The radiolabelled probe was a ~ 1 kb fragment of MC1-R coding sequences from the mouse.

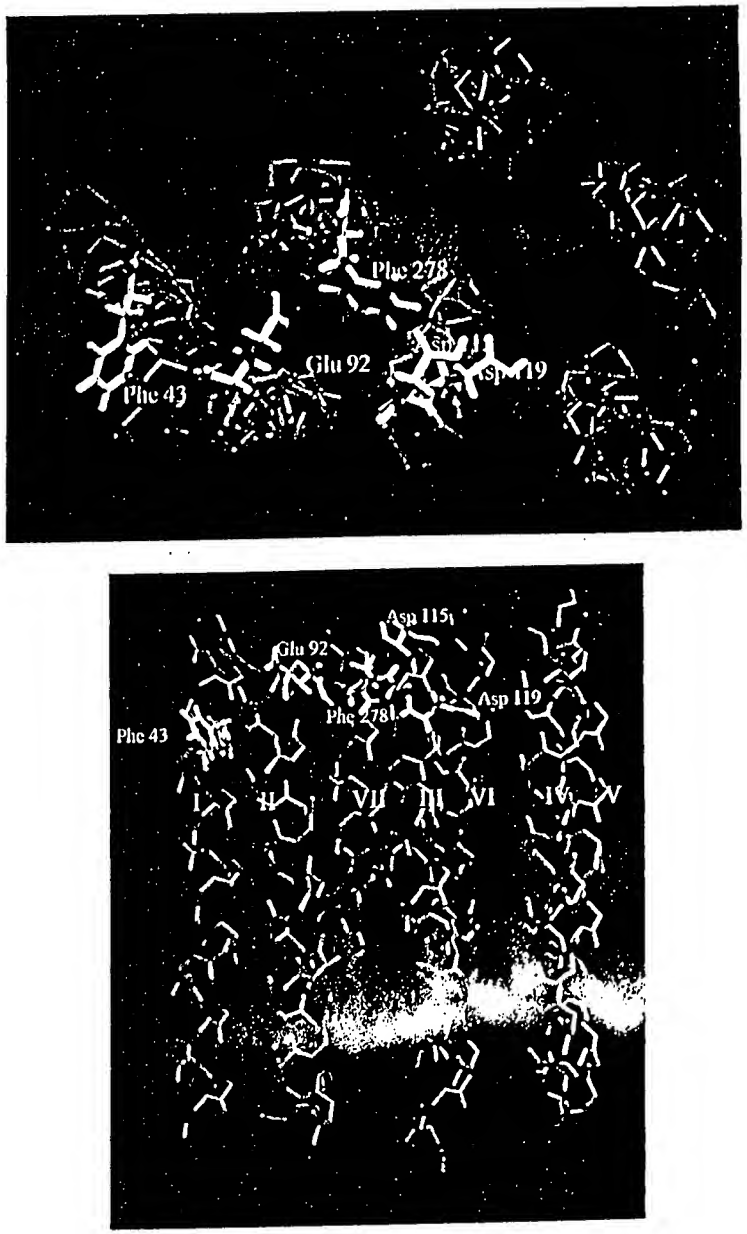

FIG. 9. Three-dimensional computer model of the mouse MC1-R. The peptide backb each helical transmembrane domain are shown in dark grey. Key residues thought to be invo ligand binding and activation are highlighted and include Phe 78 (TMI), Glu 92 (TMII), Asp Asp 119 (TM III), and Phe 278 (TMVII). Views are looking down at receptor from outside (A) and in the plane of the membrane (B). Models were derived using the projection struc bovine rhodopsin and the model of Baldwin, and do not utilize molecular dynamic or energy mization corrections.

receptor in a manner that is mechanistically similar to stimulation of the receptor by light (Cohen *et al.*, 1992).

We initially proposed that the E92 in TM2 of the MSH-R was likely to be stabililized via electrostatic interaction with a basic residue somewhere else in the receptor (Robbins *et al.*, 1993). Disruption of this interaction by the E92K mutation would break this internal constraint and produce a partial hormone-independent activation of this receptor. In rhodopsin, this model has been supported by two observations (Robinson *et al.*, 1992). First, a variety of mutations at position 296 constitutively activate the receptor, demonstrating that the absence of the lysine is critical for the activation. Second, disruption of the other member of the salt bridge, E113, produces a similar phenotype.

Subsequent experiments have discounted the salt-bridge model for constitutive activation of the MC1-R. The conserved basic residues in the transmembrane domains of the MC1-R have been altered by *in vitro* mutagenesis without any significant change in the basal functioning of the receptor (Lu and Cone, unpublished data). More importantly, we have been unable to constitutively activate the receptor unless we change E92 to a basic residue; alteration of the glutamic acid to an isoleucine or glutamine disrupts the affinity of the receptor for ligand but produces no constitutive activation (Fig. 6).

We are considering the possibility that E92K introduces a positive charge capable of an electrostatic interaction with one of the aspartic acid residues, and constitutively activates by indirectly disrupting the constraining bond(s) that these residues form. For example, E92K might pair electrostatically with D119, thus disrupting the ability of D119 to hydrogen bond with some other residue. This would be an example of a model by which the E92K change indirectly disrupts an internal constraint to activate the receptor. This model predicts that the residues involved directly in the constraint might also activate the receptor when mutagenized, and we have made a large number of mutations in the mouse MSH receptor to test this hypothesis (Lu and Cone, unpublished data).

To further understand the constitutively active MC1 receptors it would be valuable to also examine the affinity of the receptors for ligand. Unfortunately, it has been difficult to perform the necessary binding experiments with these mutants. Presumably as a consequence of a dramatic decrease in ligand affinity and/or a potent downregulation of the constitutively active receptors, we are unable to detect ligand binding to the E92K receptor at tracer concentrations expected to result in approximately 30% receptor occupancy (Fig. 10). The very high concentrations of NDP-MSH required to further activate these receptors fit the model that these receptors have greatly reduced affinity for ligand.

VI. Pharmacological Mechanisms of Agouti Action

Agouti is a pigmentation locus that, like *extension*, regulates the relative levels of eumelanin versus phaeomelanin, but generally acts in a diametrically

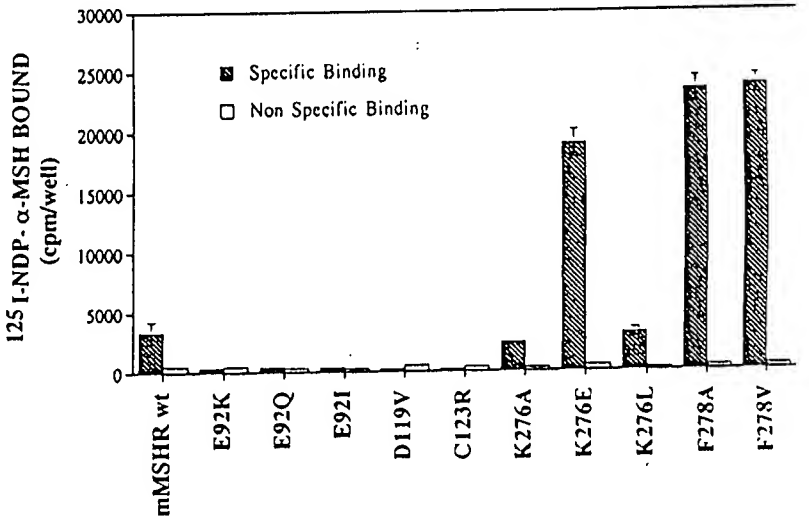

FIG. 10. Binding of ^{125}I-NDP-MSH to wild-type and mutant MC1 receptors. Cells (a mately 5 × 10^4) expressing the wild-type or mutant MC1 receptors indicated were incubat ^{125}I-NDP-MSH (100,000 CPM) for 1 hr at 37°C, washed twice, lysed, and counted in a γ-scin counter. Nonspecific binding was that remaining in the presence of 10 $^{-6}$M unlabelled NDI Tracer concentrations used were calculated, in the case of the wild-type receptor, to result in imately 30% receptor occupancy.

opposed manner. That is, dominant *agouti* alleles produce animals with y or red coat colors (e.g. the red fox or yellow A^y mouse), while homoz recessive animals have dark black coat colors (Searle, 1968; Siracusa, 199 wild-type allele results in the subterminal band of phaeomelanin in the hai seen in the coats of many animals, and named after the prominent pattern South American rodent, the agouti. Melanocyte transplantation exper clearly demonstrated that an animal's *agouti* phenotype did not transplar the melanocyte, but rather was produced by the hair follicle and acted o to inhibit the MSH-induced synthesis of eumelanin in the transplanted m cytes (Silvers, 1958; Silvers and Russel, 1955).

Cloning of *agouti* in the mouse demonstrated that this locus encoded tative secreted protein of 108 amino acid residues (Bultman *et al.*, 1992; *et al.*, 1993). Naturally, this led to the hypothesis that *agouti* is an antago the MC1 receptor, elaborated by follicle cells to act in a paracrine fashion MC1-R during the phase of the hair growth cycle when the subterminal b yellow pigment is laid down in the growing hair shaft (Jackson, 1993) examples of endogenous peptide antagonists of a G protein-coupled recept previously been reported (Taminaga *et al.*, 1990; Zhu and Solomon, 1992) sequently, a counterhypothesis was also proposed that *agouti* might act own receptor to inhibit the induction of adenylyl cyclase downstream of

at the MC1 receptor (Conklin and Bourne, 1993). One piece of genetic evidence weighed heavily in favor of the former hypothesis, however. In the mouse, the sombre allele E^{Sm} is epistatic to even the most dominant *agouti* alleles, A^{y}, A^{w}, and A^{vy}, that is, when a dominant black (E^{Sm}) animal is crossed to a dominant yellow (Bateman, 1961; Wolff *et al.*, 1978) animal, a black animal results. This suggests that *agouti* can only act upstream of the MC1-R and cannot independently modify adenylyl cyclase levels.

At this point, evidence strongly supports the former hypothesis (Fig. 11). The murine *agouti* peptide has been demonstrated to be a potent antagonist of the MC1 receptor in an heterologous cell expression system, and also blocks the binding of melanotropic peptides to the receptor (Ki = 6×10^{-10}M), an action suggesting competitive antagonism (Lu *et al.*, 1994).

Much remains to be learned about this fascinating peptide, however. For example, there are at least three known gene loci that are required for *agouti* function, *mahogany*, *mahoganoid*, and *umbrous* (Silvers, 1979). When these loci are crossed into a dominant yellow animal, *agouti* action is blocked and an eumelanized animal results (e.g. Lane and Green, 1960).

Second, recent evidence has suggested that *agouti* might also increase intra-

FIG. 11. Murine *agouti* is an antagonist of the MC1-R. (A) *Agouti* inhibits activation of the mMC1-R by α-MSH in stably transfected 293 cells as monitored by stimulation of adenylyl cyclase activity. *Agouti* (0.7nM) increased the EC_{50} for activation of adenylyl cyclase from $1.5 \pm 1.1 \times 10^{-9}$ M to $2.2 \pm 1.2 \times 10^{-8}$ M. Cells were stimulated with varying concentrations of α-MSH in the presence or absence of 0.7nM *agouti* for 40 min. Medium was aspirated and 2.5% perchloric acid containing 0.1 mM cAMP was used to stop the incubation. Adenylyl cyclase activity was calculated by determining the percent conversion of [^{3}H]-adenine to [^{3}H]-cAMP as described (Johnson and Salomon, 1991). Data represent means and standard deviations from triplicate data points. (B) *Agouti* inhibits the binding of $ACTH_{1-39}$ to the mMC1-R. Competition binding studies demonstrated *agouti* protein blocked [^{125}I]-$ACTH_{1-39}$ binding to the mMC1-R with an IC50 value of $6.6 \pm 3.8 \times 10^{-10}$ M. As a control, baculovirus supernatants from SF9 cells infected with a virus containing an unrelated gene insert were purified in parallel with *agouti* protein and used for competition binding studies at the same range of protein concentrations as that used for *agouti*. Values are displayed in protein concentrations in order to directly compare *agouti* with control post-cation column protein. Data represent means and standard errors from triplicate data points. EC_{50} values were calculated using GraphPad InPlot version 4.0. The methods used for competition binding with radiolabelled ACTH were essentially those of Rainey *et al.* (1989). Cells (5×10^5) were incubated in binding medium contained 200,000 cpm of [^{125}I]-$ACTH_{1-39}$ (Amersham). [^{125}I]-$ACTH_{1-39}$ and varying concentrations of *agouti* protein, post-cation control protein, or cold ACTH were added to the cell culture dish and incubated at room temperature for 2 hours. Cells were then washed 3 times with ice-cold binding medium and lysed. Bound radioactivity was then determined using a γ-scintillation counter, and data were analyzed using the Kaleidagraph software package. Nonspecific binding, determined as the amount of radioactivity bound in the presence of 10^{-5} M unlabeled ACTH, was 10% of the total counts bound. [Reprinted with permission from *Nature* 371, 801. Copyright 1994, Macmillan Magazines Limited.]

cellular Ca^{2+} concentrations in cells via a mechanism that may not involve tagonism of the melanocortin receptors (Zemel *et al.*, 1995). Interestingly, spacing of cysteines in the *agouti* peptide is nearly identical to that found conotoxins and plectotoxins of snails and spiders, respectively (Manne *et* 1995). These peptide toxins are agonists and antagonists of a variety of ion cl

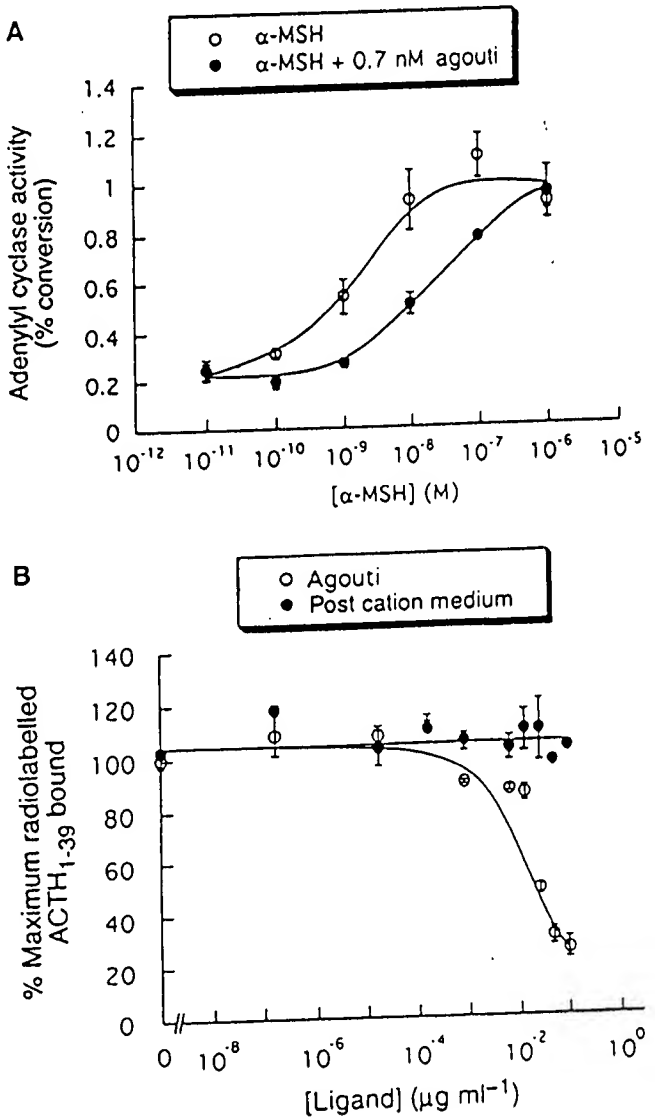

nels including Ca^{2+} channels, thus perhaps *agouti* also binds and stimulates activation of Ca^{2+} channels.

Finally, the most intriguing question concerns how some dominant *agouti* alleles in the mouse cause obesity. It has been known for many years that several dominant *agouti* alleles in the mouse, notably A^{y} and A^{vy}, cause hyperinsulinemia, obesity, and increased somatic growth (for reviews see Siracusa, 1994; Yen *et al.*, 1994). Recent molecular biological experiments have demonstrated that, for each these alleles, promoter re-arrangements have resulted in the expression of high levels of *agouti* mRNA throughout the animal, in contrast to the normally tightly regulated expression of the gene only in the hair follicle during a brief period of the hair cycle (Bultman *et al.*, 1992; Michaud *et al.*, 1994; Miller *et al.*, 1993; Vrieling *et al.*, 1994). Furthermore, ectopic expression of *agouti* in a transgenic animal in which the β-actin promoter drives *agouti* expression also leads to obesity (Klebig *et al.*, 1995; Perry *et al.*, 1995).

How might *agouti* cause obesity? We have observed that mouse *agouti* protein not only is an antagonist of the MC1-R in melanocytes, but is also a potent antagonist of the neural MC4 receptor (Fig. 12) (Lu *et al.*, 1994). This has led us to propose the "melanocortin hypothesis" for the induction of obesity by *agouti*: aberrant ectopic expression of *agouti* leads to obesity as a consequence of pathogenic antagonism of one or more of the melanocortin receptors. This hypothesis has led us to carefully examine the expression of melanocortin receptors in tissues involved in weight homeostasis. Since adrenalectomized A^{y} animals still become obese, the adrenocortical MC2-R can be ruled out as the critical site of *agouti* action (Jackson *et al.*, 1976). Two potential sites of *agouti* action are adipocytes and brain regions involved in feeding behavior and weight homeostasis (Fig. 13). It has been known for some time that adipocytes express a high-affinity ACTH binding site, and that ACTH induces lipolysis (Oelofsen and Ramachandran, 1983). We have recently characterized these sites as resulting from the expression of the MC2-R in all adipose tissues tested and MC5-R in a subset of those (Fig. 13A). Perhaps more intriguing is the expression of both the MC3 and MC4 receptors in different regions of the hypothalamus (Fig. 13B) (Mountjoy *et al.*, 1994; Roselli-Rehfuss *et al.*, 1993). This brain region has long been known, from lesioning studies, to be important in the regulation of feeding behavior. Furthermore, both of the neural melanocortin receptors are expressed throughout regions of the brain regulating autonomic outflow, and thus may impact weight homeostasis by other mechanisms in addition to alteration of feeding.

VII. Development of Melanocortin Receptor Antagonists

While many significant advances have been made in the peptide chemistry of the melanocortins (for review, see Eberle, 1988), surprisingly no high-affinity antagonists of the melanocortin receptors have ever been identified. To better understand the structure and function of these receptors, we set out to remedy

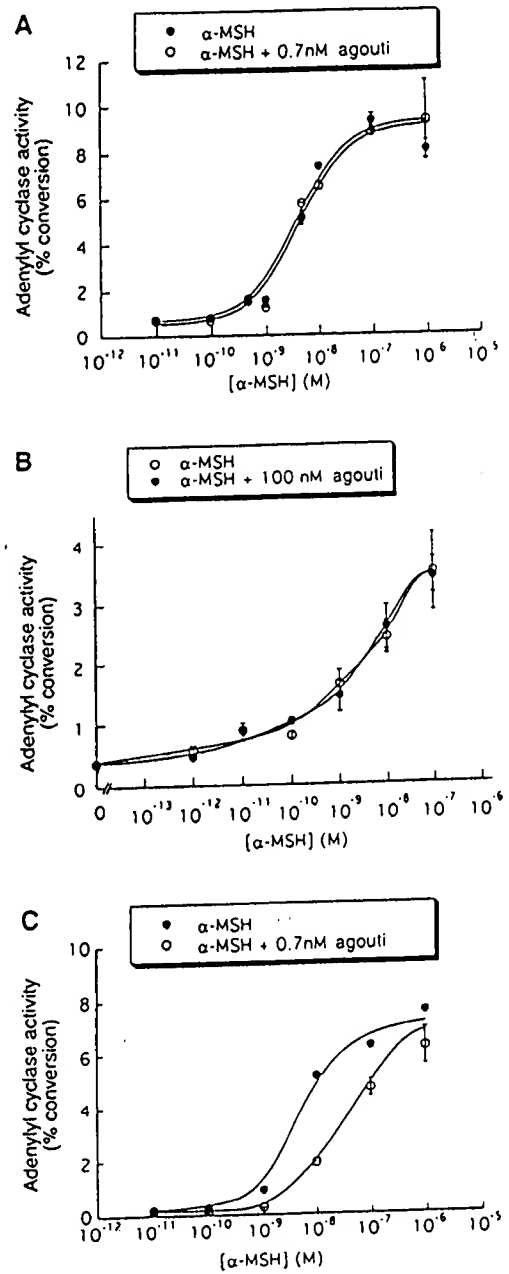

FIG. 12. Murine *agouti* is an antagonist of the MC4-R. The ability of murine *agouti* to onize the rMC3-R (A), hMC5-R (B), and mMC4-R (C) was examined as described in Fig [Reprinted with permission from *Nature* 371, 801. Copyright 1994, Macmillan Magazines Li

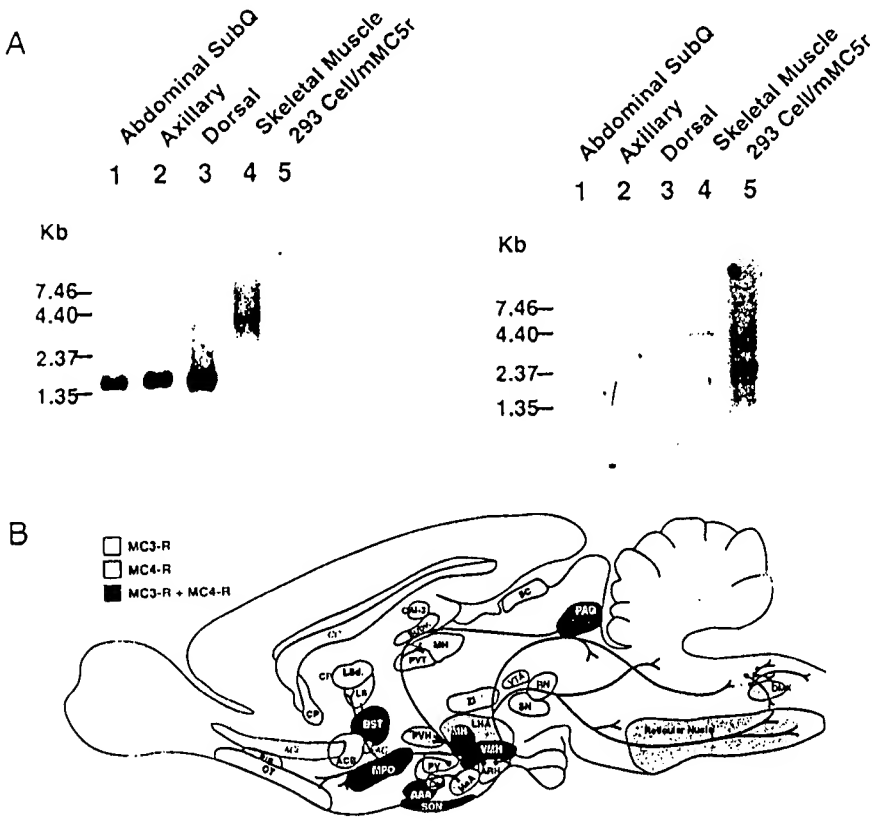

FIG. 13. Expression of melanocortin receptors in putative target tissues of *agouti* action. (A) Melanocortin receptor mRNA expression in adipocytes. Murine adipocytes from the fat pads indicated were used for the preparation of RNA. Poly A+ mRNA (2 μg) was electrophoresed on a formaldehyde agarose gel and transferred to a nylon membrane. The membrane was then hybridized to a mouse MC2-R probe (left panel) or mouse MC5-R probe (right panel). [Reprinted with permission from Boston, B., and Cone, R.D., Characterization of melanocortin receptor subtype expression in murine adipose tissues and in the 3T3-L1 cell line. *Endocrinology*, in press, 1996. © The Endocrine Society]. (B) Melanocortin receptor mRNA expression in the rat brain. The distribution of MC3-R and MC4-R mRNA in the rat brain was examined by *in situ* hybridization. Detailed accounts of the distributions are published elsewhere (Mountjoy *et al.*, 1994; Roselli-Rehfuss *et al.*, 1993). A schematic representation of brain regions containing the MC3 receptor mRNA (light gray), MC4 receptor mRNA (medium gray), or both (dark grey) is shown here.

this situation. We began by first developing a high-throughput screening method for measuring agonism and antagonism of these receptors (Chen *et al.*, 1995). The melanocortin receptors couple to adenylyl cyclase, but conventional cyclase or cAMP assays are expensive and time consuming, requiring large numbers of cells and the use of radionuclides. First, all five melanocortin receptors were

transfected into the human 293 cell line, and clonal lines expressing each were isolated. Next, a β-galactosidase gene fused to a cAMP-responsive p containing five repeats of the CRE element was obtained. Finally, conditi determined such that following transient transfection of the fusion gene cells and hormone treatment, adenylyl cyclase activity could be determ function of β-galactosidase activity using a rapid colorimetric assay in a plate format (Chen *et al.*, 1995). This rapid assay allows us to screen mately 1000 compounds per day, in contrast to the 100 assays per day be performed by cAMP radioimmunoassay or by one of the more wid adenylyl cyclase assays (Salomon, 1991).

We began by first screening existing melanocortin peptide analog viously examined using the classic frog skin bioassay for activity at the

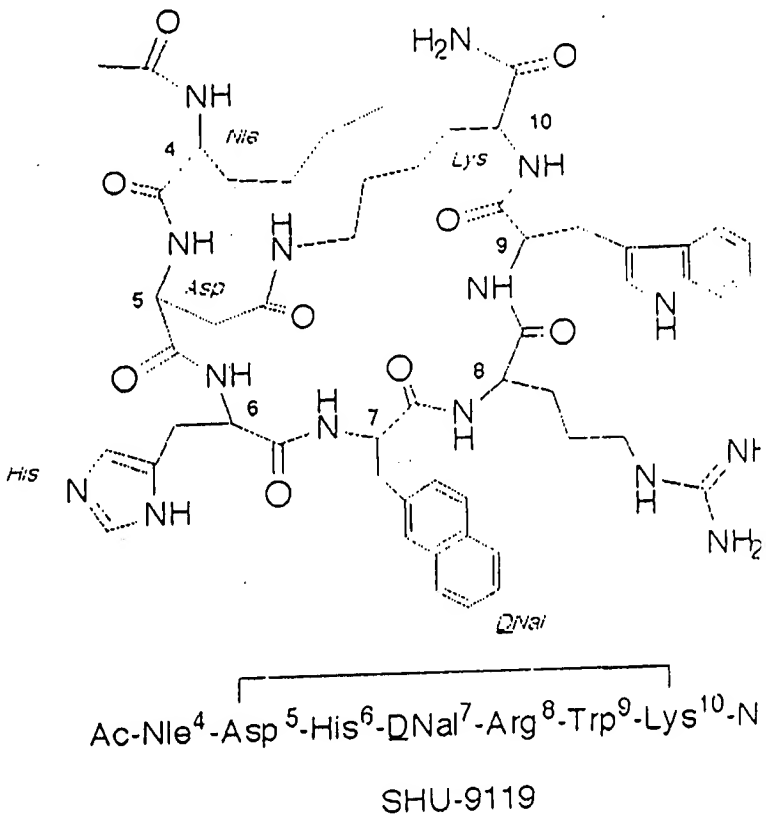

FIG. 14. Structure of SHU9119 (Ac-Nle⁴-c[Asp⁵, D-Nal (2)⁷, Lys¹⁰)] α-MSH(4- cyclic lactam derivative of α-MSH that is a potent antagonist of the MC3 and MC4 n receptors.

(Shizume *et al.*, 1954), and rapidly identified a series of analogues with potent antagonist properties, the most potent of which can be seen in Figure 14 (for a detailed description, see Hruby *et al.*, 1995). This series of compounds is based upon the potent cyclic lactam analogue of α-MSH (Al-Obeidi *et al.*, 1989a,b). Like NDP-MSH, this compound is a potent agonist of the MC1, MC3, MC4, and MC5 receptors. Interestingly, it appears that replacement of the Phe in the His-Phe-Arg-Trp pharmacophore region with D-naphthylalanine (SHU9119) or para-iodophenylalanine (SHU8914) results in the production of potent and specific antagonists of the MC3 and MC4 receptors (Table V). These compounds are high-affinity competitive antagonists of the MC3 and MC4 receptors, but surprisingly are both full agonists of the MC1 and MC5 receptors (Fig. 15). SHU8914 retains significant partial agonist activity at the MC3-R and MC4-R while SHU9119 does not.

Recently, other groups have reported the identification of melanocortin antagonists. Adan *et al.* (1994) examined analogues of the linear $ACTH_{4-10}$ with modifications at positions 6–10. pA2 values the range of 6–8.6 were reported, with ($Pro^{8,10}$, Gly^{9})-$ACTH_{4-10}$ being the most potent with a pA2 value of 8.6 at the MC4-R. Interestingly, a linear $ACTH_{4-10}$ with a L-paraiodophenylalanine at position 7 was reported to have antagonist activity at the MC3, MC4, and MC5 receptors (pA2 = 7.4–8.4). Combinatorial peptide library approaches have been used to identify a melanocortin analogue (Met-Pro-D-Phe-Arg-D-Trp-Phe-Lys-Pro-Val-NH2) that can antagonize the *Xenopus* MC1-R with an IC_{50} of 11 nM (Jayawickreme *et al.*, 1994). Larger random combinatorial libraries were then used to identify a peptide, D-Trp-Arg-Leu-NH_2, that antagonized the human MC1-R with an IC_{50} of 0.6 μM (Quillan *et al.*, 1995).

TABLE V

EC_{50} (pM) and pA_2 Values for Phe^7-Substituted Ac-Nle^4-c[Asp^5, D-Phe^7, Lys^{10}]α-MSH(4-10)-NH_2 Compounds

	hMC1R	hMC3R	hMC4R	mMC5R
α-MSH	91 ± 69	669 ± 355	210 ± 57	807 ± 125
NDP-α-MSH	23 ± 7	132 ± 31	17 ± 18	not done
SHU9128	16 ± 3	191 ± 9	19 ± 14	1360 ± 549
"(*p*-F1)Phe^7 SHU9203	5 ± 4	63 ± 26	18 ± 14	117 ± 70
"(*p*-C1)Phe^7 SHU8914	55 ± 31	1134 ± 197 partial agonist $pA_2 = 8.3$	573 ± 357 partial agonist $pA_2 = 9.7$	684 ± 227 partial agonist
"(*p*-1)Ph^7 SHU9119 "(D-Nal)	36 ± 12	2813 ± 575 partial agonist $pA_2 = 8.3$	no activity $pA_2 = 9.3$	434 ± 260

[a] Indicates the halogen substitution at the *para* position of Phe^7.

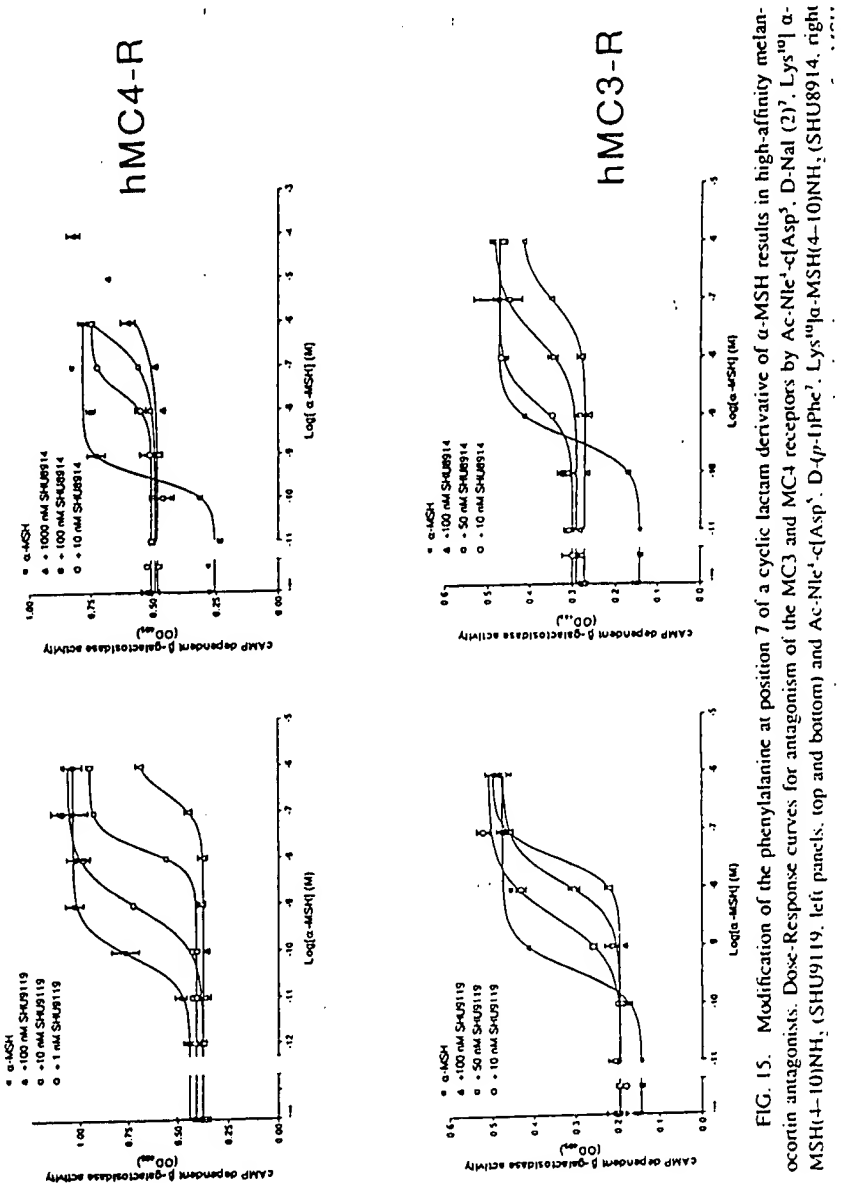

FIG. 15. Modification of the phenylalanine at position 7 of a cyclic lactam derivative of α-MSH results in high-affinity melanocortin antagonists. Dose-Response curves for antagonism of the MC3 and MC4 receptors by Ac-Nle^4-c[Asp^5, D-Nal (2)^7, Lys^{10}]α-MSH(4–10)NH_2 (SHU9119, left panels, top and bottom) and Ac-Nle^4-c[Asp^5, D-(*p*-I)Phe^7, Lys^{10}]α-MSH(4–10)NH_2 (SHU8914, right

Preliminary data show that these compounds will be very useful for the analysis of melanocortin receptor function *in vivo*. Experiments are currently underway to determine if centrally administered SHU9119 can affect feeding behavior or weight homeostasis, to test the hypothesis that antagonism of the MC4-R by *agouti* is the mechanism of induction of obesity by this peptide. While potent antagonists have not yet been found for the MC1 or MC5 receptors, substitution of Phe7 with bulky amino acid residues that retain aromatic character may be a way to eventually derive antagonists of these receptors as well.

VIII. Conclusions

Many mysteries concerning melanocortin action remain unsolved. For example, peripherally administered α-MSH induces eumelanin synthesis in skin and hair, yet hypophysectomized mice retain a darkly pigmented coat. How is eumelanin production by follicular melanocytes maintained in the absence of circulating α-MSH? Is it regulated by locally produced POMC peptides or perhaps via basal MC1-R activity? The products of at least three genes, *mahogany*, *mahoganoid*, and *umbrous*, are required for *agouti* action in pigmentation, and possibly obesity as well. What are these products and what are their roles?

Yet, progress has been made. The majority of the melanocortin receptors, perhaps all of them, have been cloned and characterized, and several groups are busily developing specific antagonists. Gene knockout experiments are also underway for the MC3-R, MC4-R, and MC5-R. Two biological activities have been demonstrated for the *agouti* peptide, antagonism of the MC1 and MC4 melanocortin receptors and elevation of intracellular Ca^{2+}, and readily testable hypotheses have been proposed for the mechanism of action of this peptide in pigmentation and obesity. The data reviewed here should convince the reader that some very useful tools have been developed in recent years for unraveling many of these remaining mysteries.

Note added in press: Valverde *et al.* (1995) have now reported the identification of nine coding polymorphisms in the human MC1-R, inclusive of the V92M and D84E changes reported here, that appear to be associated with light skin and red hair color in a study of British and Irish individuals. The new coding variants include D294H, A64S, T95M, V97I, F76Y, A103V, and L106Q.

ACKNOWLEDGMENTS

This work was supprted with funds to R.D.C. from the National Institutes of Health (AR42415, HD30236) and from the Lucille P. Markey Charitable Trust.

REFERENCES

Abdel-Malek, Z., Swope, V.B., Suzuki, I., Akcali, C., Harriger, M.D., Boyce, S.T., Urabe, K., and Hearing, V.J. (1995). *Proc. Natl. Acad. Sci. USA* 92, 1789–1793.

Adan, R.A.H., Oosterom, J., Ludvigsdotter, G., Brakkee, J.H., Burbach, J.P.H., and Gispen, W.H. (1994). *Eur. J. Pharm.* 269, 331–337.

Al-Obeidi, F., Castrucci, A.M.d.L., Hadley, M.E., and Hruby, V.J. (1989a). *J. Med. Chem.* 32, 2561.

Al-Obeidi, F., Hadley, M.E., Pettitt, B.-M., and Hruby, V.J. (1989b). *J. Am. Chem. Soc.* 111, 3416.

Baldwin, J. (1993). *EMBO J.* 12, 1693–1703.

Barret, P., MacDonald, A., Helliwell, R., Davidson, G., and Morgan, P. (1994). *J. Mol. Endo* 12, 203–213.

Bateman, N. (1961). *J. Hered.* 52, 186–189.

Bijlsma, W.A., Jennekens, F.G.I., Schotman, P., and Gispen, W.H. (1981). *Euro. J. Pharmac* 73.

Boston, B.A., and Cone, R.D. (1996). *Endocrinology*, in press.

Buckley, D.I., and Ramachandran, J. (1981). *Proc. Natl. Acad. Sci. USA* 78, 7431–7435.

Bultman, S.J., Michaud, E.J., and Woychik, R.P. (1992). *Cell* 71, 1195–1204.

Calogero, A.E., Gallucci, W.T., Gold, P.W., and Chrousos, G.P. (1988). *J. Clin. Invest.* 82, 76

Cammas, F.M., Kapas, S., Barker, S., and Clark, A.J.L. (1995). *Biochem. Biophys. Res. Co* 212, 912–918.

Catania, A., and Lipton, J.M. (1993). *Endocr. Rev.* 14, 564–576.

Chen, W., Shields, T.S., Stork, P.J.S., and Cone, R.D. (1995). *Analyt. Biochem.* 226, 349–35

Chhajlani, V., Muceniece, R., and Wikberg, J.E.S. (1993). *Biochem. Biophys. Res. Comm.* 195 873.

Chhajlani, V., and Wikberg, J.E.S. (1992). *FEBS Lett.* 309, 417–420.

Chowdhary, B.P., Gustavsson, I., Wikberg, J.E., and Chhajlani, V. (1995). *Cytogenet. Cell* 68, 79–81.

Clark, A.J.L., McLoughlin, L., and Grossman, A. (1993). *Lancet* 341, 461–462.

Cohen, G.B., Oprian, D.D., and Robinson, P.R. (1992). *Biochemistry* 31, 12592–12601.

Cone, R.D., and Mountjoy, K.G. (1993). *Trends in Endocrinol. Metab.* 4, 242–247.

Conklin, B.R., and Bourne, H.R. (1993). *Nature* 364, 110.

De Angelis, L., Cusella-De Angelis, M.G., Bouche, M., Vivarelli, E., Boitani, C., Molinaro, M Cossu, G. (1992). *Devel. Biol.* 151, 446–458.

Desarnaud, F., Labbe, O., Eggerickx, D., Vassart, G., and Parmentier, M. (1994). *Biochem.* 367–373.

DeWied, D., and Jolles, J. (1982). *Physiol. Rev.* 62, 977–1059.

Eberle, A.N. (1988). "The Melanotropins, Chemistry, Physiology and Mechanisms of Actio Karger Publishers, Basel, Switzerland.

Eberle, A.N., de Graan, P.N.E., Baumann, J.B., Girard, J., van Hees, G., and van de Veerdonk, (1984). *Yale J. Biol. Med.* 57, 353–354.

Fathi, Z., Iben, L.G., and Parker, E.M. (1995). *Neurochem. Res.* 20, 107–113.

Feng, J.D., Dao, T., and Lipton, J.M. (1987). *Brain Res.* 18, 473–477.

Fuller, B.B., Lunsford, J.B., and Iman, D.S. (1987). *J. Biol. Chem.* 262, 4024–4033.

Gantz, I., Shimoto, Y., Konda, Y., Miwa, H., Dickinson, C.J., and Yamada, T. (1994a). *Bi Biophys. Res. Comm.* 200, 1214–1220.

Gantz, I., Yamada, T., Tashiro, T., Konda, Y., Shimoto, Y., Miwa, H., and Trent, J.M. (1 *Genomics* 19, 394–395.

Gantz, I., Konda, Y., Tashiro, T., Shimoto, Y., Miwa, H., Munzert, G., Watson, S.J., DelVa and Yamada, T. (1993a). *J. Biol. Chem.* 268, 8246–8250.

Gantz, I., Miwa, H., Konda, Y., Shimoto, Y., Tashiro, T., Watson, S.J., DelValle, J., and Y T. (1993b). *J. Biol. Chem.* 268, 15174–15179.

Garrud, P., Gray, J.A., and DeWied, D. (1974). *Physiol. Psychol.* 112, 109–119.

Gerst, J.E., Sole, J., Hazum, E., and Salomon, Y. (1988). *Endocrinology* 123, 1792–1797.

Griffon, N., Mignon, V., Facchinetti, P., Diaz, J., Schwartz, J.-C., and Sokoloff, P. (1994). *Biochem. Biophys. Res. Comm.* **200**, 1007–1014.
Gruber, K.A., and Callahan, M.F. (1989). *Am. J. Phys.* **257**, R681-R694.
Halaban, R., Pomerantz, S.H., Marshall, S., and Lerner, A.B. (1984). *Arch. Biochem. Biophys.* **230**, 383–387.
Hearing, V.J., and Jimenez, M. (1987). *Int. J. Biochem.* **19**, 1141–1147.
Hnatowich, M.R., Queen, G., Stein, D., and LaBella, F.S. (1989). *Can. J. Physiol. Pharmacol.* **67**, 568–576.
Hoganson, G.E., Ledwitz-Rigby, F., Davidson, R.L., and Fuller, B.B. (1989). *Som. Cell. Mol. Genet.* **15**, 255–263.
Hruby, V.J., Lu, D., Sharma, S.D., Castrucci, A.L., Kesterson, R.A., Al-Obeidi, F.A., Hadley, M.E., and Cone, R.D. (1995). *J. Med. Chem.* **38**, 3454–3461.
Hunt, G., Todd, C., Kyne, S., and Thody, A.J. (1994). *J. Endocrinol.* **140**, R1-R3.
Jackson, E.J., Stolz, D., and Martin, R. (1976). *Horm. Metab. Res.* **8**, 452–455.
Jackson, I.J. (1993). *Nature* **362**, 587–588.
Jayawickreme, C.K., Quillan, J.M., Graminski, G.F., and Lerner, M.R. (1994). *J. Biol. Chem.* **269**, 29846–29854.
Johnson, R.A., and Salomon, Y. (1991). *Meth. in Enzymol.* **195**, 3–21.
Klebig, M.L., Wilkinson, J.E., Geisler, J.G., and Woychik, R.P. (1995). *Proc. Natl. Acad. Sci. USA* **92**, 4728–4732.
Klungland, H., Vage, D.I., Gomez-Raya, L., Adelsteinsson, S., and Lien, S. (1995). *Mamm. Genome* **6**, 636–639.
Konda, Y., Gantz, I., DelValle, J., Y., S., Miwa, H., and Yamada, T. (1994). *J. Biol. Chem.* **269**, 13162–13166.
Labbe, O., Desarnaud, F., Eggerickx, D., Vassart, G., and Parmentier, M. (1994). *Biochemistry* **33**, 4543–4549.
Lane, P.W., and Green, M.C. (1960). *J. Hered.* **51**, 228–230.
Little, C.C. (1957). "The Inheritance of Coat Colors in Dogs." Macmillan Publishing Company, New York.
Lu, D., Willard, D., Patel, I.R., Kadwell, S., Overton, L., Kost, T., Luther, M., Chen, W., Woychik, R.P., Wilkison, W.O., and Cone, R.D. (1994). *Nature* **371**, 799–802.
Lyon, M.F. (1961). *Nature* **190**, 372–373.
Magenis, R.E., Smith, L., Nadeau, J.H., Johnson, K.R., Mountjoy, K.G., and Cone, R.D. (1994). *Mamm. Genome* **5**, 503–508.
Malas, S., Peters, J., and Abbot, C. (1994). *Mammalian Genome* **5**, 577–579.
Manne, J., Argeson, A.C., and Siracusa, L.D. (1995). *Proc. Natl. Acad. Sci. USA* **92**, 4721–4724.
Michaud, E.J., Vugt, M.J.v., Bultman, S.J., Sweet, H.O., Davisson, M.T., and Woychik, R.P. (1994). *Genes & Devel.* **8**, 1463–1472.
Miller, M.W., Duhl, D.M.J., Vrieling, H., Cordes, S.P., Ollmann, M.M., Winkes, B.M., and Barsh, G.S. (1993). *Genes & Devel.* **7**, 454–467.
Motta, M., Mangili, G., and Martini, L. (1965). *Endocrinology* **77**, 392–395.
Mountjoy, K.G. (1994). *Mol. Cell. Endocrinol.* **102**, R7-R11.
Mountjoy, K.G., Mortrud, M.T., Low, M.J., Simerly, R.B., and Cone, R.D. (1994). *Mol. Endocrinol.* **8**, 1298–1308.
Mountjoy, K.G., Robbins, L.S., Mortrud, M.T., and Cone, R.C. (1992). *Science* **257**, 543–546.
Nes, N., Einarsson, E.J., Lohi, O., Jarosz, S., and Scheelje, R. (1988). "Beautiful Fur Animals and Their Colour Genetics." Scientifur, Glostrup, Denmark.
Oelofsen, W., and Ramachandran, J. (1983). *Arch. Biochem. Biophys.* **225**, 414–421.
Pathak, M.A., Fitzpatrick, T.B., Greiter, F., and Kraus, E.W. (1987). Preventive treatment of sunburn, dermatoheliosis, and skin cancer with sun-protective agents. In "Dermatology in General

Medicine" (T.B. Fitzpatrick, A.Z. Eizen, K. Wolff, I.M. Freeberg, and K. F. Auste 1507. McGraw-Hill, New York.
Pawelek, J. (1976). *J. Invest. Dermatol.* **66**, 201–209.
Perry, W.L., Hustad, C.M., Swing, D.A., Jenkins, N.A., and Copeland, N.G. (1995). *Ge* 267–274.
Quillan, J.M., Jayawickreme, C.K., and Lerner, M.R. (1995). *Proc. Natl. Acad. Sci. USA* 2898.
Robbins, L.S., Nadeau, J.H., Johnson, K.R., Kelly, M.A., Roselli-Rehfuss, L., Baack, E., K.G., and Cone, R.D. (1993). *Cell* **72**, 827–834.
Robinson, P.R., Cohen, G.B., Zhukovsky, E.A., and Oprian, D.D. (1992). *Neuron* **9**, 719–
Roselli-Rehfuss, L., Mountjoy, K.G., Robbins, L.S., Mortrud, M.T., Low, M.J., Tatro, J.B., M.L., Simerly, R., and Cone, R.D. (1993). *Proc. Natl. Acad. Sci. USA* **90**, 8856–8.
Salomon, Y. (1991). *Meth. Enzymology* **195**, 22–28.
Salomon, Y., Zohar, M., Dejordy, J.O., Eshel, Y., Shafir, I., Leiba, H., Garty, N.B., Schmi Azrad, A., Shai, E., and Deganis, H. (1993). *Ann. N.Y. Acad. Sci.* **680** 364–377.
Sandman, C.A., Kastin, A.J., and Schaally, A.V. (1969). *Experientia* **25**, 1001–1002.
Schertler, G.F.X., Villa, C. and Henderson, R. (1993). *Nature* **362**, 770–772.
Schimmer, B.P., Kwan, W.K., Tsoa, J., and Qui, R. (1995). *J. Cell. Physiol.* **163**, 164–17
Searle, A.G. (1968). "Comparative Genetics of Coat Colors in Mammals." Logos Pres London.
Shizume, K., Lerner, A.B., and Fitzpatrick, T.B. (1954). *Endocrinology* **54**, 533–560.
Silvers, W.K. (1979). "The Coat Colors of Mice: A Model for Mammalian Gene Action action." Springer-Verlag, New York.
Silvers, W.K. (1958). *J. Exp. Zool.* **137**, 189–196.
Silvers, W.K., and Russel, E.S. (1955). *J. Exp. Zool.* **130**, 199–220.
Siracusa, L.D. (1994). *Trends in Genet.* **10**, 423–428.
Smith, A.I., and Funder, J.W. (1988). *Endocr. Rev.* **9**, 159–179.
Solca, F., Siegrist, W., Drozdz, R., Girard, J., and Eberle, A.N. (1989). *J. Biol. Chem.* **26** 14280.
Strand, F.L., and Kung, T.T. (1980). *Peptides* **1**, 135–138.
Strand, F.L., Rose, K.J., Zuccarelli, L.A., Kume, J., Alves, S.E., Antonawich, F.J., and Ga (1991). *Physiol. Rev.* **71**, 1017–1046.
Suda, T., Yajima, F., Tomori, N., Sumitomo, T., Nakagami, Y., Ushiyama, T., Demur Shizume, K. (1986). *Endocrinology* **118**, 459–461.
Taminaga, T., Fukata, J., Naito, Y., Funakoski, S., Fujii, N., and Imura, H. (1990). *J. E.* **125**, 287–292.
Tatro, J.B. (1990). *Brain Res.* **536**, 124–132.
Tatro, J.B., and Reichlin, S. (1987). *Endocrinology* **121**, 1900–1907.
Tsigos, C., Arai, K., Hung, W., and Chrousos, G.P. (1993). *J. Clin. Invest.* **92**, 2458–2461
Valverde, P., Healy, E., Jackson, I., Rees, J.L., and Thody, A.J. (1995). *Nature Genet.* **11**.
Vamvakopoulos, N.C., Rojas, K., Overhauser, J., Durkin, A.S., Nierman, A.C., and Chro (1993). *Genomics* **18**, 454–455.
Vrieling, H., Duhl, D.M.J., Millar, S.E., Miller, K.A., and Barsh, G.S. (1994). *Proc. Natl. USA* **91**, 5667–5671.
Wolff, G.L., Galbraith, D.B., Domon, O.E., and Row, J.M. (1978). *J. Hered.* **69**, 295–298
Wong, G., and Pawelek, J. (1975). *Nature* **255**, 644–646.
Yen, T.T., Gill, A.M., Frigeri, L.G., Barsh, G.S., and Wolff, G.L. (1994). *FASEB J.* **8**, 47
Zemel, M.B., Kim, J.H., Woychik, R.P., Michaud, E.J., Kadwell, S.H., Patel, I.R., and W.O. (1995). *Proc. Natl. Acad. Sci. USA* **92**, 4733–4737.
Zhu, Q., and Solomon, S. (1992). *Endocrinology* **130**, 1413–1423.

DISCUSSION

Fred Stormshak: Some wild fur-bearing species undergo a coat color change in response to changes in photoperiod; i.e., from brown or black in spring or summer to white in fall and winter. Is this change in coat color from dark to white due to a block of the melanocortin receptor, reduction in melanocortin production, or some other mechanism?

Roger Cone: The seasonal coat color change seen in animals like the snowshoe rabbit, *Leptus americanus*, is unlikely to involve the MC1 receptor or agouti peptide. These molecules are regulators of the relative levels of phaeomelanin (red-yellow) versus eumelanin (brown-black) pigments. Thus for example, animals lacking functional MSH receptor, such as the red guinea pig, still have plenty of melanin in hair and skin. Animals that turn white in the winter must have a complete absence of melanins, possibly as a result of a total inhibition of tyrosinase. While I am unaware of the mechanism by which melanin synthesis is blocked, data in the rabbit points to gonadotropic hormone as the triggering factor.

Thomas Means: What are the mechanisms by which some of these receptors become constitutively active in the genetic models?

Roger Cone: We do not yet have a detailed molecular model for constitutive activation of the MSH receptor in the mouse, cow, or fox. The data we have collected at this point, however, do not support the original model that we proposed in which E92 maintains the receptor in a constrained state via an electrostatic interaction (Robbins *et al.*, 1992). First, the model would predict that substitution of any residue for the glutamic acid, with the possible exception of aspartic acid, would constitutively activate the receptor. This is not the case, suggesting that the insertion of a basic residue at position 92 is required for constitutive activation. Secondly, we have been unable to find any basic residues in the receptor that, when altered also, constitutively activate the receptor.

Larry Davis: Are there ever circulating levels of α-MSH in humans that are great enough to contribute melanocyte activity and pigmentation?

Roger Cone: Unlike other mammals examined, circulating levels of α-MSH are not generally detectable in man. Interestingly, the human MC1 receptor is one to two logs more sensitive to ACTH than is the mouse receptor, suggesting that ACTH is the melanotropic peptide in man. Of course, while pathophysiologically elevated levels of ACTH can produce hyperpigmentation in man, the role of normal pituitary-derived melanotropins in basal pigmentation is unclear. Hair pigmentation remains unchanged in the absence of pituitary function, suggesting that either basal MC1 receptor function or locally produced melanocortin peptides are responsible for the normal production, by follicular melanocytes, of eumelanin in the hair.

Larry Davis: Are there known variations in α-MSH levels?

Roger Cone: Abdel-Malek has recently shown that human melanocytes in culture do proliferate in response to α-MSH, which raises the important question that you have asked. One could imagine that constitutively active MC1 receptors might be involved in some stage of melanoma induction, just as activated TSH receptors are found in thyroid tumors. To my knowledge, a thorough examination of melanoma samples for MC1 receptor mutations has not been done. One observation, however, that may be relevant to the question is that no enhanced incidence of melanoma has been reported for any of the darker-pigmented animals, such as the Sombre mouse, that already express constitutively active MC1 receptors.

1: *Nat Med* 1995 Dec;1(12):1311-4 Related Articles, Books

Leptin levels reflect body lipid content in mice: evidence for di induced resistance to leptin action.

Frederich RC, Hamann A, Anderson S, Lollmann B, Lowell BB, Flier

Division of Endocrinology, Beth Israel Hospital (Research North), Boston, Massachusetts 02215, USA.

The regulation of body weight and composition involves input from genes environment, demonstrated, for example, by the variable susceptibility of i strains of mice to obesity when offered a high-fat diet. The identification o gene responsible for obesity in the ob/ob mouse provides a new approach t defining links between diet and genetics in the regulation of body weight. gene protein product, leptin, is an adipocyte-derived circulating protein. Administration of recombinant leptin reduces food intake and increases en expenditure in ob/ob mice, suggesting that it signals to the brain the magni fat stores. Information on the regulation of this protein is limited. In severa models of obesity including db/db, fa/fa, yellow (Ay/a) VMH-lesioned, an induced by gold thioglucose, monosodium glutamate, and transgenic ablati brown adipose tissue, leptin mRNA expression and the level of circulating are increased, suggesting resistance to one or more of its actions. We have assessed the impact of increased dietary fat on circulating leptin levels in n FVB mice and FVB mice with transgene-induced ablation of brown adipos tissue. We find that high-fat diet evokes a sustained increase in circulating in both normal and transgenic mice, with leptin levels accurately reflecting amount of body lipid across a broad range of body fat. However, despite in leptin levels, animals fed a high-fat diet became obese without decreasing t caloric intake, suggesting that a high content of dietary fat changes the 'set for body weight, at least in part by limiting the action of leptin.

PMID: 7489415, UI: 96083634

1: *Diabetes* 1997 Sep;46(9):1516-20 Related Articles, Books

Published erratum appears in Diabetes 1997 Nov;46(11):1920

Low plasma leptin in response to dietary fat in diabetes- and obesity-prone mice.

Surwit RS, Petro AE, Parekh P, Collins S

Department of Psychiatry and Behavioral Sciences, Duke University Medi Center, Durham, North Carolina 27710, USA. surwi001@mc.duke.edu

Despite the fact that mutations resulting in the absence of leptin or its rece have been associated with severe obesity and diabetes, such mutations do n appear to be responsible for most human obesity. Indeed, diet-induced obe animals and humans has been characterized by hyperleptinemia. This has b interpreted as evidence for leptin resistance. However, no careful longitudi studies evaluating the role of leptin in the development of obesity exist. W a series of studies in A/J and C57BL/6J (B/6) mice that demonstrate a dire relationship between the ability to increase plasma leptin levels in response high-fat diet and resistance to the subsequent development of obesity and diabetes. While leptin levels are similar in lean, low-fat-fed A/J and B/6 mi effects of a high-fat diet on plasma leptin differ dramatically between the t strains. After 4 weeks of high-fat feeding, leptin levels in A/J mice increas fold, and this elevated level was maintained independent of weight gain throughout a 14-week feeding period. However, in B/6 mice, leptin levels remained at least twofold lower and only rose very gradually along with a significant increase in adiposity, hyperglycemia, and hyperinsulinemia. Th differences in the response of leptin to diet are independent of food intake plasma insulin levels during the 1st month of feeding. Further, we demonst that leptin administration did not influence the expression of the novel unc protein UCP2, which also responds to dietary fat. From these results, we su that the response of leptin to fat feeding may be an important predictor of t development of subsequent obesity.

PMID: 9287057, UI: 97431552

1: *Am J Physiol Endocrinol Metab* 2000 Apr;278 (4):E677-83

Related Article

Effects of fructose and glucose on plasma leptin, insulin, and i resistance in lean and VMH-lesioned obese rats.

Suga A, Hirano T, Kageyama H, Osaka T, Namba Y, Tsuji M, Miura Adachi M, Inoue S

First Department of Internal Medicine, Showa University School of Medic Shinagawa-ku, Tokyo 142-8666, Japan.

To determine the influence of dietary fructose and glucose on circulating le levels in lean and obese rats, plasma leptin concentrations were measured i ventromedial hypothalamic (VMH)-lesioned obese and sham-operated lean fed either normal chow or fructose- or glucose-enriched diets (60% by calo for 2 wk. Insulin resistance was evaluated by the steady-state plasma gluco method and intravenous glucose tolerance test. In lean rats, glucose-enrich significantly increased plasma leptin with enlarged parametrial fat pad, wh neither leptin nor fat-pad weight was altered by fructose. Two weeks after t lesions, the rats fed normal chow had marked greater body weight gain, enl fat pads, and higher insulin and leptin compared with sham-operated rats. a marked adiposity and hyperinsulinemia, insulin resistance was not increa VMH-lesioned rats. Fructose brought about substantial insulin resistance a hyperinsulinemia in both lean and obese rats, whereas glucose led to rather enhanced insulin sensitivity. Leptin, body weight, and fat pad were not significantly altered by either fructose or glucose in the obese rats. These r suggest that dietary glucose stimulates leptin production by increasing adip tissue or stimulating glucose metabolism in lean rats. Hyperleptinemia in lesioned rats is associated with both increased adiposity and hyperinsuline not with insulin resistance. Dietary fructose does not alter leptin levels, alt this sugar brings about hyperinsulinemia and insulin resistance, suggesting hyperinsulinemia compensated for insulin resistance does not stimulate lep production.

PMID: 10751202, UI: 20215239

1: *Biochem Biophys Res Commun* 2000 Oct 14;277 (1):20-6

Related Article

IDEAL

Leptin resistance of adipocytes in obesity: role of suppressors cytokine signaling.

Wang Z, Zhou YT, Kakuma T, Lee Y, Kalra SP, Kalra PS, Pan W, Un RH

Gifford Laboratories, Touchstone Center for Diabetes Research, Departme Internal Medicine, University of Texas Southwestern Medical Center, 532 Hines Boulevard, Dallas, Texas, 75390, USA.

[Medline record in process]

Liver-derived hyperleptinemia induced in normal rats by adenovirus-induc transfer causes rapid disappearance of body fat, whereas the endogenous adipocyte-derived hyperleptinemia of obesity does not. Here we induce liv derived hyperleptinemia in rats with adipocyte-derived hyperleptinemia of acquired obesity caused by ventromedial hypothalamus lesioning (VMH ra by feeding 60% fat (DIO rats). Liver-derived hyperleptinemia in obese rats only a 5-7% loss of body weight, compared to a 13% loss in normoleptine lean animals; but in actual grams of weight lost there was no significant dif between obese and lean groups, suggesting that a subset of cells remain lep sensitive in obesity. mRNA and protein of a putative leptin-resistance facto suppressor of cytokine signaling (SOCS)-1 or -3, were both increased in w adipose tissues (WAT) of VMH and DIO rats. Since transgenic overexpres SOCS-3 in islets reduced the lipopenic effect of leptin by 75%, we conclud the increased expression of SOCS-1 and -3 in WAT of rats with acquired o could have blocked leptin's lipopenic action in the leptin-resistant WAT population.

PMID: 11027633, UI: 20483672

1: *Proc Natl Acad Sci U S A* 1999 Aug 31;96 (18):10373-8

Related Article

FREE full text article at www.pnas.org PubMed Central - FREE full text

Comparing the hypothalamic and extrahypothalamic actions endogenous hyperleptinemia.

Wang ZW, Zhou YT, Kakuma T, Lee Y, Higa M, Kalra SP, Dube MG PS, Unger RH

Gifford Laboratories, Center for Diabetes Research, Department of Interna Medicine, University of Texas Southwestern Medical Center, Dallas, TX 7 USA.

To determine whether the depletion of body fat caused by adenovirus-indu hyperleptinemia is mediated via the hypothalamus, we used as a "bioassay hypothalamic leptin activity the hypothalamic expression of a leptin-regula peptide, cocaine- and amphetamine-regulated transcript (CART). The valid of this strategy was supported by the demonstration that CART mRNA wa profoundly reduced in obese rats with impaired leptin action, whether beca ablation of the ventromedial hypothalamus (VMH) or a loss-of-function m in the leptin receptor, as in Zucker diabetic fatty rats. We compared leptin in normal rats made hyperleptinemic by adenovirus-leptin treatment (43 +/ ng/ml, cerebrospinal fluid leptin 100 pg/ml) with normal rats made hyperleptinemic by a 60% fat intake (19 +/- 4 ng/ml, cerebrospinal fluid le +/- 22 pg/ml). CART was increased 5-fold in the former and 2-fold in the l yet in adenovirus-induced hyperleptinemia, body fat had disappeared, wher high-fat-fed rats, body fat was abundant. Treatment of the high-fat-fed rats adenovirus-leptin further increased their hyperleptinemia to 56 +/- 6 ng/ml without changing CART mRNA or food intake, indicating that leptin actio hypothalamus had not been increased. Nevertheless, their body fat decline suggesting that an extrahypothalamic mechanism was responsible. We con that in diet-induced obesity body-fat depletion by leptin requires supraphys plasma concentrations that exceed the leptin-transport capacity across the b brain barrier.

PMID: 10468615, UI: 99398715